Carbon and Root System Architecture: Key Regulators of Nitrate Uptake in *Lolium perenne* L. and *Brassica napus* L.

A thesis submitted in partial fulfilment of the requirements for

the Degree of

Doctor of Philosophy in Plant Biology

at the University of Canterbury

by

Qianqian Guo

University of Canterbury

2017

Statement of originality

The work presented in this thesis is, to the best of my knowledge and belief, original. The material has not been submitted, either in whole or in part, for a degree at this or any other university.

Qianqian Guo

January 12, 2017

Acknowledgements

I offer my greatest thanks to my supervisors, Professor Matthew Turnbull and Professor Paula Jameson, who secured the initial funding, conceived my study and helped me with my scientific writing, and to my co-supervisor, Professor Jiancheng Song, who guided me through the primer design and gene expression analysis.

I offer my greatest thanks to my co-supervisor, Dr Jonathan Love, who guided me through the entire research process. Jonathan was always available to provide feedback, advice and insights for my experiment design. His support and encouragement kept me enthusiastic and enjoyable in my PhD research. The patience, time and effort Jonathan devoted to my academic development kept me going through some of the hard times. Also I am grateful for the feedback, advice and assistance from my group member and friend Jessica Roche.

I gratefully acknowledge the technical help I have received from Thomas Evans, Dave Condor, Nick Etheridge, Jackie Healy, Marta Gallart, Minhuang Wang, Anish Malde and Sonal Satish Kanpariya.

I gratefully acknowledge Ballance AgriNutrients for the principle financial support for the research presented in this thesis and for a scholarship.

Contents

List of tables

List of Figures

List of Abbreviations

BA	6-benzylaminopurine
HATS	High-affinity transport system
HMW	High molecular weight
HN	High nitrogen level
cZ	*cis*-zeatin
iP	N^6-(Δ^2-isopentenyl)adenine
tZ	*trans*-zeatin
LATS	Low-affinity transport system
LMW	Low molecular weight
LN	Low nitrogen level
LR	Lateral root
LRD	Lateral root branching density
NRT	Nitrate transporter
NR	Nitrate reductase
NiR	Nitrite reductase
PR	Primary root
PI-55	6-(2-hydroxy-3-methylbenzylamino) purine
RSA	Root system architecture
WSC	Water soluble carbohydrate

Deputy Vice-Chancellor's Office
Postgraduate Office

UNIVERSITY OF CANTERBURY
Te Whare Wānanga o Waitaha
CHRISTCHURCH NEW ZEALAND

Co-Authorship Form

This form is to accompany the submission of any thesis that contains research reported in co-authored work that has been published, accepted for publication, or submitted for publication. A copy of this form should be included for each co-authored work that is included in the thesis. Completed forms should be included at the front (after the thesis abstract) of each copy of the thesis submitted for examination and library deposit.

Please indicate the chapter/section/pages of this thesis that are extracted from co-authored work and provide details of the publication or submission from the extract comes:

Chapter 2 has been submitted to *Journal of Experimental Botany* as a research article entitled "*Depletion of carbohydrate reserves limits nitrate uptake during early regrowth in L. perenne*" (Guo et al. 2017 doi: 10.1093/jxb/erx056)

Please detail the nature and extent (%) of contribution by the candidate:

Qianqian Guo (80%) and Dr. Jonathan Love (20%) designed the experiments, carried out the experiments and analysed the data. Jessica Roche assisted with the experiments (<5%).

Qianqian Guo wrote the manuscript (85%) with comments and edits from Dr. Jonathan Love, Prof. Paula Jameson and Prof. Matthew Turnbull (15%).

Jana Späth provided the fructan analysis (95%) on samples prepared by Dr. Jonathan Love and

Qianqian Guo (5%).

Qianqian Guo searched homologous sequences in NCBI database (5%), Prof. Jiancheng Song analysed the transcriptome and designed primers (95%).

Qianqian Guo performed the gene expression work (95%) with advice from Prof. Jiancheng Song (5%).

Dr. Ondřej Novák provided the cytokinin analysis (95%) on samples prepared by Qianian Guo (5%) at the University of Canterbury.

Certification by Co-authors:

If there is more than one co-author then a single co-author can sign on behalf of all

The undersigned certifys that:

- The above statement correctly reflects the nature and extent of the PhD candidate's contribution to this co-authored work
- In cases where the candidate was the lead author of the co-authored work he or she wrote the text

Paula Jameson
10/1/2017

Deputy Vice-Chancellor's Office
Postgraduate Office

UNIVERSITY OF CANTERBURY
Te Whare Wānanga o Waitaha
CHRISTCHURCH NEW ZEALAND

Co-Authorship Form

This form is to accompany the submission of any thesis that contains research reported in co-authored work that has been published, accepted for publication, or submitted for publication. A copy of this form should be included for each co-authored work that is included in the thesis. Completed forms should be included at the front (after the thesis abstract) of each copy of the thesis submitted for examination and library deposit.

Please indicate the chapter/section/pages of this thesis that are extracted from co-authored work and provide details of the publication or submission from the extract comes:

Chapter 3 has been submitted to the specific journal *Plant Growth Regulation* as a research article entitled "*A comprehensive analysis of root morphological changes in Brassica napus in response to different nitrogen sources"*

Please detail the nature and extent (%) of contribution by the candidate:

Qianqian Guo (90%) designed the experiments, carried out the experiments and analysed the data with advice from Dr. Jonathan Love (10%).

Qianqian Guo wrote the manuscript (85%) with comments and edits from Prof. Paula Jameson and Prof. Matthew Turnbull (15%).

Certification by Co-authors:

If there is more than one co-author then a single co-author can sign on behalf of all

The undersigned certifys that:

- The above statement correctly reflects the nature and extent of the PhD candidate's contribution to this co-authored work
- In cases where the candidate was the lead author of the co-authored work he or she wrote the text

Paula Jameson 10/1/2017

Deputy Vice-Chancellor's Office
Postgraduate Office

UNIVERSITY OF CANTERBURY
Te Whare Wānanga o Waitaha
CHRISTCHURCH NEW ZEALAND

Co-Authorship Form

This form is to accompany the submission of any thesis that contains research reported in co-authored work that has been published, accepted for publication, or submitted for publication. A copy of this form should be included for each co-authored work that is included in the thesis. Completed forms should be included at the front (after the thesis abstract) of each copy of the thesis submitted for examination and library deposit.

Please indicate the chapter/section/pages of this thesis that are extracted from co-authored work and provide details of the publication or submission from the extract comes:

Chapter 4 has been submitted to the specific journal *Functional Plant Biology* as a research article entitled "*Insights into the functional relationship between cytokinin-induced root system phenotypes and nitrate uptake in Brassica napus"*

Please detail the nature and extent (%) of contribution by the candidate:

Qianqian Guo (80%) and Dr. Jonathan Love (15%) designed the experiments, carried out the experiments and analysed the data. Jessica Roche (5-10%) assisted with experiments.

Qianqian Guo wrote the manuscript (85%) with comments and edits from Prof. Paula Jameson, Prof. Matthew Turnbull and Dr. Jonathan Love (15%).

Qianqian Guo searched homologous sequences in NCBI database (5%), Prof. Jiancheng Song analysed the transcriptome and designed primers (95%).

Certification by Co-authors:

If there is more than one co-author then a single co-author can sign on behalf of all

The undersigned certifys that:

- The above statement correctly reflects the nature and extent of the PhD candidate's contribution to this co-authored work
- In cases where the candidate was the lead author of the co-authored work he or she wrote the text

Paula Jameson
10/1/2017

Abstract

Nitrogen (N) is an essential macronutrient that limits plant yield and productivity. In order to increase crop yield, considerable amounts of nitrogenous fertilizers are applied to agriculture systems each year. However, about 25-70% of the applied fertilizer in ecosystem has been leached and released to the environment, in the form of NO, N_2O and NH_3, aggravating environmental pollution. Therefore, increasing nitrogen use efficiency in agriculture systems is essential to maintain the food production while alleviating the deleterious environmental effects of applied N.

The mechanisms linking C/N balance to N uptake and assimilation are central to plant responses to changing soil nutrient levels. Defoliation and subsequent regrowth of pasture grasses both impact C partitioning, thereby creating a significant point of interaction with soil N availability. Using defoliation as an experimental treatment, the dynamic relationships between plant carbohydrate status and NO_3^--responsive uptake systems, transporter gene expression and N assimilation were investigated in *Lolium perenne*. High- and low-affinity NO_3^- uptake were reduced in an N-dependent manner in response to a rapid and large shift in carbohydrate remobilization triggered by defoliation. This reduction in NO_3^- uptake was rescued by an exogenous 1% glucose supplement, confirming the carbohydrate-dependence of NO_3^- uptake. The regulation of NO_3^- uptake in response to the perturbation of plant C/N was associated with changes in expression of the nitrate high-affinity transporter *LpNRT2.1b*. Furthermore, NO_3^- assimilation appears to be regulated by the C/N balance, implying a mechanism that signals the availability of C metabolites for NO_3^- uptake and assimilation at the whole-plant level. This study also shows that cytokinins are involved in the regulation of nitrogen acquisition and assimilation in response to the changing C/N ratio.

Root architecture is also a crucial component that impacts the capacity of plants to access nutrients and water. By using the recently developed package RootNav, comprehensive morphological changes in root system architecture in response to different N sources were investigated in *Brassica napus*. In order to avoid a light-induced morphological and physiological responses affecting whole plant growth, an existing solid agar vertical-plate system was modified so that to allow roots to be shielded from light without sucrose addition and the emerging shoot to be grown without direct contact with the medium, thereby mimicking more closely the environmental conditions in nature. The results of 10-days-old *B.*

napus seedlings showed that total root length, LR density and root exploration area decreased with increasing external NO_3^- concentrations from 0.5 mM to 10 mM. The application of 0.5 mM NO_3^- induced more branching in the root system relative to the treatments with higher N concentrations (5 mM and 10 mM). The proportion of biomass allocation occupied by roots was greater in the low NO_3^- treatment relative to the high NO_3^- treatments, reflecting the fact that plants invested more resources in their roots when nutrient uptake from the environment was limited. In treatments of increasing NH_4^+ concentration from 0.5 mM to 10 mM, primary root length, total root length, LR branching zone, LR density and root exploration area were reduced. These results indicated that NH_4^+ toxicity usually leads to a stunted root system in *B. napus*, whereas a low concentration of NH_4^+ is an optimal nitrogen resource for plant growth. Increasing L-glutamate concentration from 0.01 mM to 0.1 mM suppressed primary root length, whilst the LR branching zone did not change in the different L-glutamate treatments, suggesting that L-glutamate even at micromolar level could arrest primary root growth and LR branching in *B. napus*.

By using *in situ* ^{15}N isotope labelling, morphological and molecular phenotypes generated pharmacologically were employed to investigate whether the impacts of contrasting root traits are of functional interest in relation to N acquisition. *Brassica napus* L. were grown in solid medium containing 1 mM KNO_3 and treated with cytokinin, 6-benzylaminopurine, the cytokinin antagonist (PI-55), or both in combination. The contrasting root traits induced by PI-55 and 6-benzylaminopurine were strongly related to ^{15}N uptake rate. Large root proliferation led to greater ^{15}N cumulative uptake rather than greater ^{15}N uptake efficiency per unit root length. This relationship was associated with changes in C and N resource distribution between the shoot and root, and in expression of *BnNRT2.1*. The root/shoot biomass ratio was positively correlated with ^{15}N cumulative uptake, suggesting the functional utility of root investment for nutrient acquisition. These results demonstrate that root proliferation in response to external N is a behaviour which integrates local N availability and systemic N status in the plant.

In conclusion, using two major economic forage species, *L. perenne* and *B. napus*, this thesis illuminates the impacts of carbon and root system architecture on N uptake. This work contributes to our understanding of the mechanisms regulating N uptake and will help further in efforts to improve nitrogen use efficiency.

Chapter 1-Introduction and Overview: the physiological and molecular mechanisms underpinning nitrogen uptake, allocation and sensing in plants

1.1 BACKGROUND

Nitrogen (N) is one of the major mineral nutrients required throughout plant growth. Along with water, N is generally considered to limit plant growth and development most frequently (Miller and Cramer 2005). Given that N is a key element for crop productivity, it is not surprising that large amounts of N fertiliser are applied to the field as a means to increase crop or forage yields. There is no question that the increased application to the soil of synthetic nitrogenous fertilisers applied to soil in the past decades has had positive effects on global food production (Good *et al.* 2004; Götz *et al.* 2007). During the past 50 years, cereal production has tripled, and is associated with the sharp rise from 12 to 104 Tg of synthetic N fertilizers applied to the field annually (Mulvaney *et al.* 2009). However, only about 40% of N fertiliser in the soil is taken up by the plant, indicating a significant proportion of the applied N leached to the environment, resulting in high N-loading of rivers and oceans and substantial loss of freshwater and marine life and diversity (Vitousek *et al.* 2009). In addition, it has been reported that excessive N fertiliser application causes a significant increase in nitrous oxide (N_2O) emitted from agricultural production systems. N_2O is a cause of stratospheric ozone depletion and global warming (Wuebbles 2009). In this context, investigating the N economy of plants could be a strategy with significant environmental benefits and economic value.

Major efforts to increase the nitrogen use efficiency (NUE) of crops are underway. NUE in its broadest sense is defined as the crop yield per given amount of N fertiliser applied. While traditional breeding strategies to improve crop yield have been successful, selections have generally been made in N-rich environments without a consideration of NUE (Fischer *et al.* 2009). Current research has now begun turning attention to NUE and considering the input side of productivity, investigating new solutions that draw upon an understanding of plant physiology and developmental biology (Tsay *et al.* 2011; Xu *et al.* 2012). The objective of this field of research is to increase yield while maintaining, or preferably reducing, N application. To this end, key questions framing this research are 1) how do plants take up and assimilate N from the soil?, 2) what are the key regulators that determine nitrogen transport, distribution and storage?, and 3) what is the nature and mechanism of signalling pathways that regulate these processes?

Previous studies have conveyed information that plants have a complex mechanism to sense the available N in the soil and their internal N status. These studies indicate a cross-talk with plant hormones so that the plant adapts to fluctuating nitrogen concentrations by modulating

key transporter expression, enzyme activities and components of N metabolism. Together, these provide an efficient system to maintain C/N homeostasis in the plant (Sakakibara *et al.* 2006). In this context, investigating the way in which plants can sense N availability and its regulation by plant hormones is a key step for improving NUE by plants. In this review, the N sensory transduction and regulatory network by hormones is outlined – this forms the basis of an attempt to find a possible strategy for efficient use and assimilation of N in the context of physiological and developmental biology.

1.2 PRIMARY N METABOLISM

1.2.1. Nitrogen uptake and transport from the soil

Non-leguminous plants acquire nitrogen from the soil. Generally, nitrogen is available to plants in either an inorganic form, such as NO_3^- or NH_4^+, or an organic form including urea, amino acids, peptides and proteins. NO_3^- is a major form of N resource for plant growth and development (Schmidt *et al.* 2013). However, organic N forms are increasingly being recognised as an ecologically significant source of N (Schmidt *et al.* 2013). Notwithstanding this, nitrate, via the mineralisation of applied urea fertilisers, serves as the dominant source of N in agricultural systems. Interestingly, the nitrate molecule itself has the capacity to elicit a signal that has important effects on plant development and growth, sensing internal N and balancing of N in shoot and root (Ho *et al.* 2009b). The NO_3^- uptake by roots is determined by many factors, including nitrate itself, N-metabolites (e.g. ammonium and amino acids), and carbon products from photosynthesis.

Soil N distribution is heterogeneous. Spatial-temporal variation of soil nitrogen availability and form is due to environmental factors in the soil such as soil type, pH, temperature, moisture content and the activities of microorganisms. In this context, being immobile organisms, plants have evolved sophisticated systems that enable them to change their phenotype, thereby adapting to fluctuating environments. These modifications include regulation of N uptake capacity (Kiba *et al.* 2011), plasticity of root architecture (Ruffel *et al*, 2011) and adjustment of the shoot/root ratio (Hermans *et al*. 2006). This phenotypic plasticity is coordinated in concert with other abiotic stress responses including scarcity of potassium and phosphorus (Forde 2002a).

Nitrate is taken up by membrane-bound transporters localized in epidermal and cortical cells (Wang *et al.* 2012b). NO_3^- levels in the soil can fluctuate by more than four orders of magnitude. Consequently, plants have evolved two types of transport systems to cope with the fluctuations of nitrate in the soil, one involving a high-affinity transport system (HATS), and the other involving a low-affinity transport system (LATS). The HATS operate at low external nitrate concentrations (<250 μM), whereas the LAT systems operate at high external nitrate concentrations (>1 mM). The LATS systems of nitrate uptake are composed of inducible (iLATS) and constitutive components (cLATS) (Tsay *et al.* 1993; Huang *et al.* 1999a). Likewise, both inducible HATS (iHATS) and constitutive HATS (cHATS) have been found to be present at low nitrate concentrations in *Arabidopsis* and barley (Siddiqi *et al.* 1990). Genes that encode each family of transporters have been identified and characterized to constitute two large gene families: *NRT1* and *NRT2*. In *Arabidopsis*, nine of 53 members in the NRT1 family have been identified as NO_3^- transporters and AtNRT1.1 (CHL1) was the first identified nitrate transporter *in planta* (Tsay *et al.* 1993; Chen *et al.* 2012; Wang *et al.* 2012b). Two root-localized *NRT1* transporters (*NRT1.1*/*CHL1*) and *NRT1.2*, and three root-localized *NRT2* transporters (*NRT2.1*, *NRT2.2* and *NRT2.4*) have been identified as molecular components of nitrate uptake in roots (Tsay *et al.* 1993; Huang *et al.* 1999a; Kiba *et al.* 2012; Wang *et al.* 2012b). AtNRT1.1 and the MtNRT1.3 from *Medicago sativa* have been determined as dual-affinity nitrate transporters (Liu *et al.* 1999a; Morère-Le Paven *et al.* 2011). AtNRT1.1 is a NO_3^--inducible membrane transporter (Huang *et al.* 1999b). It has been found that AtNRT1.1 is also involved in nitrate inducible signalling (Remans *et al.* 2006; Ho *et al.* 2009b).

As a dual-affinity transporter, CHL1 (AtNRT1.1) modulates its affinity for nitrate by way of phosphorylation/dephosphorylation of threonine 101 (CHL1T101) by the CBL-interacting protein kinase CIPK23 (Liu and Tsay 2003). As a nitrate sensor, the phosphorylation switch of CHL1 is also responsible for sensing a wide range of external nitrate concentration, thus triggering various levels of the primary nitrate response (Ho *et al.* 2009b). Interestingly, nitrate binding, but not nitrate uptake, is required for triggering signals (Ho *et al.* 2009b). Under low NO_3^- availability, NO_3^- tends to bind to the high-affinity site, thus activating or recruiting CIPK23 to phosphorylate CHL1 at T101. As a consequence, the phosphorylated CHL1 inhibits a high nitrate primary response. In contrast, when exposed to high nitrate conditions, nitrate can bind to a low-affinity site. This low-affinity binding then prevents the phosphorylation of CHL1 at T101, which then induces a high nitrate primary response (Ho *et*

al. 2009b). Whether the switch of nitrate binding between high and low-affinity sites is related to conformation of CHL1 protein or other mechanisms is yet to be elucidated. Nonetheless, the proposed model indicates how CHL1 might functions as a sensor in plants in addition to its dual affinity transport function.

In the NRT2 family, several NRT2 members have been proposed to function in high-affinity nitrate uptake (Cerezo *et al.* 2001; Li *et al.* 2007; Kiba *et al.* 2012). It has been established that NRT2.1 is predominantly responsible for regulation of high-affinity transport of nitrate. Null mutants for NRT2.1 have been reported to lose partial HAT activity, with the residual HAT activity probably due to the existence of constitutive HAT transporters (Cerezo *et al.* 2001; Filleur *et al.* 2001; Li *et al.* 2007). As a consequence, the mutants cannot grow normally in nitrate-deprived conditions (e.g. <1 mM), confirming an important role of NRT2.1 in high-affinity NO_3^- transport (Orsel *et al.* 2006). Among these seven NRT2 members, only the transcript level of NRT2.1 showed a correlation with the regulation of the HATS and NRT2.1 is up-regulated by nitrate deficiency (Okamoto *et al.* 2003) and down-regulated by high N supply and by N metabolites, such as ammonium and amino acids (Lejay *et al.* 1999; Zhuo *et al.* 1999). Although the mechanism of NAR2.1 function is still unknown, it has been proposed that the active form of the transporter is in fact a NRT2.1/NAR2.1 hetero oligomer (Yong *et al.* 2010) and that the posttranscriptional control of both genes plays an essential role in regulation of HATS (Laugier *et al.* 2012).

1.2.2. Transportation of nitrate root-to-shoot

Because nitrate assimilation is energy intensive, herbaceous plants attempt to address this problem through transporting nitrate to leaves, where nitrate assimilation processes can directly access energy derived from photosynthesis (Canvin and Atkins 1974; Andrews 1986). The proportion of nitrate transported from root to shoot is dependent not only on intrinsic factors that differ between plant species but also on environmental factors, such as temperature, light levels, and nitrate availability of nitrate in the soil (Smirnoff and Stewart 1985). Under sufficient light conditions, nitrate assimilation in leaves is more energy efficient than that in roots (Smirnoff and Stewart 1985). In contrast, under low light intensity, leaf assimilation loses the advantage of lower energy cost because nitrate and CO_2 compete for ATP and reductants (Canvin and Atkins 1974). Consequently, a relatively greater portion of nitrate assimilation occurs in roots rather than leaves under stressful conditions (Deane-Drummond *et al.* 1980; Clarkson and Deane-Drummond 1983; Smirnoff and Stewart 1985).

For the long-distance transport of NO_3^-, xylem loading is required. In *Arabidopsis*, it is likely that *AtNRT1.5*, a low-affinity transporter, is involved in the root-to-shoot transport of nitrate. *AtNRT1.5* is localized in the plasma membrane of the xylem-pole pericycle. *AtNRT1.5* knockout mutations resulted in decreasing root-to-shoot transport of nitrate, confirming the role of *AtNRT1.5* in loading nitrate into root xylem (Lin *et al.* 2008b). However, the root-to-shoot transport of nitrate is not completely eliminated in the absence of NRT1.5, suggesting that in addition to NRT1.5, another xylem loading transporter or mechanism is also involved in xylem loading of nitrate (Lin *et al.* 2008b). Interestingly, Chen and co-workers found that NRT1.5 is also involved in stress tolerance (Chen *et al.* 2012).

So far, *AtNRT1.8* and *AtNRT1.9* have been identified to regulate the root-to-shoot transport of nitrate (Wang *et al.* 2012b). *AtNRT1.8*, an inducible low-affinity transporter, is mainly expressed in the plasma membrane of xylem parenchyma cells in *Arabidopsis* roots. The T-DNA insertion mutant *nrt1.8* shows a significant increase of nitrate accumulation on xylem sap relative to wild type, suggesting that AtNRT1.8 functions in xylem unloading to remove NO_3^- from xylem vessels. Similarly, the mutant *nrt1.9* shows increased root-to-shoot transport of nitrate and decreased nitrate concentration in root phloem exudates, suggesting that AtNRT1.9, located on the plasma membrane of the companion cells of the root phloem, facilitates phloem loading of nitrate (Wang and Tsay 2011a). It is likely that NRT1.8 and NRT1.9 are involved in retrieving nitrate from the xylem sap, whereas NRT1.5 imports nitrate into root xylem.

It seems that plants employ NRT1.5, NRT1.8 and NRT1.9 to co-ordinate and fine-tune long-distance transport of nitrate from root to shoot to regulate the distribution of nitrate in roots and shoots, thus optimising nitrate assimilation efficiency under variable external environmental conditions.

1.2.3. Nitrate remobilisation in the shoot

In addition to the root-to-shoot transport pathway of nitrate, there are other transport pathways in shoot tissue that regulate the remobilisation of nitrate. These pathways contribute to the allocation of nitrate within the whole plant in a co-ordinated manner. It is well known that remobilisation of nitrogen in plants is also a key factor in improving N use efficiency (Masclaux-Daubresse *et al.* 2010). NRT1.4, a low-affinity transporter which is mainly expressed in the leaf petiole, plays a critical role in mediating leaf NO_3^- balance and leaf development (Chiu *et al.* 2004). In the *nrt1.4* mutant, reduced nitrate amounts in the petiole

and increased amounts in the leaf lamina were observed. Given that AtNRT1.4 regulates the distribution of nitrate between petiole and lamina, it is likely that a lamina-derived signal sent to the petiole activates the remobilisation of nitrate stored in the petiole (Wang *et al.* 2012b). However, a mechanism for this remains unclear.

AtNRT1.7, a low-affinity transporter and localised in phloem tissue of older leaves, plays a role in source-to-sink remobilisation of NO_3^- (Fan *et al.* 2009). Relative to wild-type, a greater amount of nitrate is measured in the older leaves of the *nrt1.7* mutant and less in the phloem exudates of older leaves, suggesting that NRT1.7 participates in phloem loading of NO_3^- in the source leaf. Furthermore, less $^{15}NO_3^-$ in old leaves was remobilised into younger leaves indicating that NRT1.7 functions in transporting NO_3^- out of older leaves and into younger tissues with high N demand (Fan *et al.* 2009).

1.2.4 Nitrogen assimilation

The fraction of nitrogen taken up from the soil as nitrate is integrated into organic compounds via a number of enzymatic-catalysed steps. Once nitrate enters the cell, its reduction into NO_2^- is catalysed in the cytosol by NR, suggesting that NR has potential as a candidate for improving N uptake efficiency (Lejay *et al.* 1999). NR is a homodimer, each monomer having three components: flavin adenine dinucleotide (FAD), a heme and a molybdenum cofactor (Campbell 1999). After reduction of NO_3^- into NO_2^-, nitrite is translocated to the chloroplast and reduced to ammonium by the NiR. Ammonium, either originating from NO_3^- reduction or directly from soil, is mainly assimilated in the plastid/chloroplast by the GS/GOGAT cycle (Lea and Miflin 1974; Lea and Forde 1994). In this process, the glutamine synthetase (GS) fixes ammonium to a glutamate (Glu) molecule to form glutamine (Gln). Glutamine then reacts with 2-oxoglutarate to form two molecules of glutamate, this step being catalysed by the glutamine 2-oxoglutarate amino transferase (or glutamate synthase, GOGAT). In plants, there are two different forms of GOGAT: Fd-GOGAT which is mainly located in leaf chloroplasts, and NADH-GOGAT which is predominantly localized in plastids of non-photosynthetic tissues like seeds and roots (Suzuki and Knaff 2005).

Glutamate dehydrogenase (GDH) is also involved in ammonium assimilation, catalyzing a reversible enzymatic reaction involving the assimilation of ammonium into Glu and the deamination of Glu into 2-oxoglutarate (2OG) and ammonium (Lancien *et al.* 2000). The two types of GDH depend on either NAD(H) or NADP(H) located in the mitochondria and chloroplasts, respectively (Lancien *et al.* 2000).

1.3. CARBON AND HORMONAL REGULATION OF NO_3^- SIGNALLING COMPONENTS

As reviewed above, plants are able to sense changes in N availability in the soil, and regulate their own metabolism and development to adapt to these changes through integrating signalling of nitrogen availability at the intracellular, intercellular and inter-organ level. Recent studies have shown that carbon and some hormonal signal pathways are integrated signals of nitrogen deficiency/satiety.

1.3.1. Carbon

The regulation of root nitrate uptake by C metabolites from photosynthesis has previously been demonstrated by diurnal stimulation of NO_3^- uptake. Sugars transported from shoots to roots play an important role in this diurnal stimulatory effect (Rideout and Raper Jr 1994; Delhon *et al.* 1996; Lejay *et al.* 1999). Several nitrate transporter genes - *NRT2.1*, *NRT1.1* and *NRT2.4* - are not only responsive to N availability, but also C treatments (Lejay *et al.* 2003; Kiba *et al.* 2012). The expression of *NRT2.1* and *NRT1.1* has been shown to be stimulated by sugars. However, the signalling mechanism involved this regulation is still unclear. Several studies reported that the oxidative pentose phosphate pathway (OPPP) is required for the induction of *NRT2.1* and *NRT1.1* transcript accumulation by C, but also for the regulation of nitrate assimilatory genes in roots by C treatments. This suggests that OPPP could be one component that integrates N signalling with C metabolism (Lejay *et al.* 2008; Bussell *et al.* 2013; De Jong *et al.* 2014). Other evidence of regulation of root NO_3^- uptake by photosynthesis is the impact of CO_2 on root N uptake. The long-term treatment with a high concentration of CO_2 may lead to a decline of N status in plants, which is the opposite of what is observed in sugar treatments (Taub and Wang 2008; Leakey *et al.* 2009). These discrepancies reflect the fact that cross-talk between C and N in plants remains unclear.

Nitrate that is taken up by root cells, is translocated into shoots for assimilation, or directly assimilated in roots depending on plant species and environmental conditions. Nitrogen assimilation is an energy-dependent process, and also requires C skeletons. In leaves, inorganic N assimilation rates are considerable greater when the plant is exposed to light compared with in dark, due to the efficient provision of ATP and reducing power by the products of photosynthesis (Matt *et al.* 2001). N assimilates are integrated into photosynthesis, photorespiration and respiration. These reflect an extremely close

relationship between nitrogen and carbon in plants. Microarray analysis of *Arabidopsis* transiently exposed to a matrix of C and N treatments has indicated that a large proportion of genes responded to a C/N interaction, suggesting C and/or N, or a metabolic product of C and N assimilation (e.g. an amino acid), might act as a signal in the regulation of gene expression (Gutiérrez *et al.* 2007). It has been known that plants employ an intricate regulatory network that integrates nutrient availability, the ability of N assimilation and C metabolism, environmental conditions with plant growth and development (Nunes-Nesi *et al.* 2010).

1.3.2. Cytokinin

Cytokinins (CK) can regulate plant development and growth, and modify metabolism and morphogenesis in response to environmental fluctuations (Mok and Mok 2001; Sakakibara *et al.* 2006; Choi and Hwang 2007). Recently, cytokinin has been identified as mediator in nitrogen signalling pathways (Ruffel *et al.* 2008; Ruffel *et al.* 2011). In addition to nitrate, plants appear to recruit other molecules to communicate N availability between roots and shoots. It has been reported that cytokinins within the xylem and phloem, might be involved in the communication of the N status between roots and shoots. The isoprenoid cytokinins are biosynthesied via adenosine phosphate-isopentenyltransferase (IPT). The first formed cytokinins are the nucleotides. The riboside forms are regarded as the main translocated forms, and the free bases the biologically active forms detected by receptors (Sakakibara 2006). The signalling pathway in *Arabidopsis* involves a multi-step signalling network linking between the receptors and the response regulators (RRs) (Hwang *et al.* 2012). The *cis*-forms of the cytokinins derive from the turnover of specific tRNA moities. Cytokinin homeostasis is determined by the rate of ctyokinin degradation which is catalysed by cytokinin oxidase/dehydrogenase (CKX) and by conjugation. For a general overview of the cytokinins see Jameson (2017).

Many studies have investigated so far in the mechanisms of CK biosynthesis. The rate-limiting step of CK biosynthesis is the transfer of an isopentenyl moiety from dimethylallyl diposphate (DMAPP) to the N^6 position of ATP/ADP. This key step is catalysed by the enzyme adenosine phosphates-isopentenyltransferase (IPT) (Kakimoto 2001; Takei *et al.* 2001a; Sakakibara *et al.* 2006). *AtIPT1* and the homologs *AtIPT3-AtIPT8* have been characterized as CK biosynthesis genes in *Arabidopsis* (Takei *et al.* 2001a). Research using the model plant species *Arabidopsis* has provided an insight into nitrogen-mediated regulation of CK biosynthesis.

The expression of *AtIPT* gene family members is tissue-specific, suggesting that CKs are produced in both shoots and roots (Miyawaki *et al.* 2004; Hirose *et al.* 2008). Among seven *IPT* gene family members in *Arabidopsis*, the expression of *AtIPT3* is induced by application of nitrogen to deficient plants and is followed by an accumulation of CKs, whereas *AtIPT5* is affected by supplementing with nitrate and ammonium in long-term treatments (Miyawaki *et al.* 2004). Additionally, the DS transposon-insertion mutant of *AtIPT3*, showed a diminished nitrate-dependent accumulation of CKs. This indicates that *AtIPT3*, rather than *AtIPT5* is involved in the response of CK biosynthesis to rapid changes in nitrogen supply (Takei *et al.* 2004a).

Cytokinins are involve in regulating NO_3^- uptake systems in response to fluctuations in N availability (Krouk *et al.* 2011). It has been shown that *trans* zeatin (*t*Z)-type cytokinin is the major form in xylem sap, while isopentenyl adenine (iP-type) and *cis* Z-type cytokinins are predominantly presented in phloem sap (Takei *et al.* 2004b; Hirose *et al.* 2008). In *Arabidopsis*, iP-type cytokinins are translocated from the shoot to the root. The *atipt1:3:5:7* mutant, grafted with the wild-type shoot, showed normal growth and a restored level of iP-type cytokinins, suggesting that iP-type cytokinins translocated from the shoot to the root have biological function (Matsumoto-Kitano *et al.* 2008). It has been proposed that cytokinins could be involved in local and systemic signals to coordinate responses at the whole plant level, and to communicate N status between multiple organs (Takei *et al.* 2001b; Sakakibara *et al.* 2006; Matsumoto-Kitano *et al.* 2008; Kudo *et al.* 2010). A split-root experiment in *Arabidopsis* has demonstrated that NITRATE TRANSPORTER *NRT2.1* and *NAR2.1* regulation, driven by shoot-root systemic N signalling, is mediated by cytokinin biosynthesis under the control of *AtIPT3* and/or *AtIPT5*, and/or *AtIPT7* gene (Ruffel *et al.* 2011). Further, genome-wide analyses for cytokinin responsive genes in *Arabidopsis* have indicated that cytokinin can down-regulate root localized transporters including *AtNRT1.1*, *AtNRT2.1*, *AtNRT2.2*, and *AtNRT1.5* (Brenner *et al.* 2005; Li *et al.* 2007). These gene families have been functionally identified as major components of the NO_3^- uptake and xylem loading system (Liu *et al.* 1999b; Lin *et al.* 2008a). In contrast, cytokinin up-regulates shoot localized *AtNRT* genes under both high- and low-nitrogen conditions (Kiba *et al.* 2011).

Given that shoot-expression of *AtNRT* genes correlate well with nitrogen translocation and distribution, it is conceivable that CKs can induce shoot-type *AtNRT* genes to enhance nitrogen translocation and distribution.

1.3.3. Auxin

Auxin is an important hormone that can regulate plant morphology and development. Lateral root (LR) formation is a particularly well studied system (Fukaki and Tasaka 2009). Although auxin can be locally synthesised in the root, the majority of auxin is transported from the shoot by the phloem (Ljung *et al.* 2005). Given that auxin is transported basipetally and promotes LR branching, it is plausible to consider auxin as a candidate for mediating nitrogen shoot-to–root signals. In maize, the reduced root growth in response to high NO_3^- concentration is accompanied by low levels of auxin content in the phloem and can be restored by exogenous NAA and IAA, consistent with the suggestion that auxin plays a role in nitrate-dependent root elongation (Tian *et al.* 2008). Conversely, *Arabidopsis* roots with low N supply contain higher levels of auxin compared with seedlings with high N supply (Kiba *et al.* 2011).

Important advances in our mechanistic understanding of how nitrogen signalling regulates auxin signalling have been observed. It has been shown that the LR outgrowth in response to nitrogen is mediated via microRNA167a (miR167a) which represses the transcriptional level of a nitrogen-inducible *Auxin Response Factor* (*ARF8*) (Gifford *et al.* 2008). The link between microRNA regulation of other macro-nutrient responses has also been observed for phosphate and sulphate uptake (Bari *et al.* 2006). *ARF8* is a documented target of miR167 and is expressed in pericycle cells (Wu *et al.* 2006). Under nitrogen treatment (glutamine or some nitrate metabolites rather than nitrate itself), the levels of miR167a was down-regulated, the *ARF8* transcripts accumulate and an increase the ratio of initiating/emerging lateral roots was observed (Gifford *et al.* 2008). Interestingly, it has been observed that *AtNRT1.1* not only facilitates the transport of NO_3^-, but also auxin (Krouk *et al.* 2010). Under low NO_3^- conditions, *AtNRT1.1* preferentially carries auxin, thereby transporting auxin out of LRs and repressing LR growth. Conversely, NO_3^- competes with auxin in terms of transportation by *AtNRT1.1* under high NO_3^- condition, resulting in auxin accumulation in LR tips and thus stimulating their growth (Krouk *et al.* 2010).

1.4. ROOT DEVELOPMENT IN RESPONSE TO NITROGEN

1.4.1. Localised stimulation of lateral root growth in response to NO_3^-

Plants reveal considerable developmental plasticity in response to fluctuating environmental factors. Root development in response to varied N supply is an example of such plasticity. An

increase in localised nitrate stimulates proliferation of LRs, thereby allowing the plant to forage and better exploit NO_3^--rich soil zones (Zhang and Forde 2000). Several components are involved in the regulatory mechanism underlying the adaptive development of the LRs. The nitrate-induced MADS box transcription factor *ARABIDOPSIS NITRATE REGULATED 1* (*ANR1*) has been characterised as promoting LR elongation in response to NO_3^- (Zhang and Forde 1998). Plants with down-regulated *ANR1* no longer respond to localised nitrate supply by proliferating LRs, suggesting that *ANR1* is a key component in the developmental plasticity response to localised stimulus of nitrate. The identification of *ANR1* was an important step in determining a specific signalling pathway for the localised nitrate stimulatory response (Zhang *et al.* 2007). In addition, NRT1.1 is linked to the *ANR1*-dependent signalling pathway. The NRT1.1-deficient mutants display reduced LR growth. Interestingly, this reduced LR growth was independent of both reduced nitrate uptake and a decrease in N metabolite accumulation, because in NRT1.1-deficient mutants the specific NO_3^- uptake was increased and an alternative N source could not rescue the LR growth phenotype. In fact, perturbed sensitivity to a localised NO_3^- stimulus was accompanied by reduced *ANR1* expression and a similar phenotype to the *ANR1*-deficient mutants, indicating that NRT1.1 may act upstream of *ANR1* and regulate the abundance of *ANR1* transcript (Remans *et al.* 2006).

1.4.2. Systemic inhibition of lateral root development in response to NO_3^-

In addition to the local stimulatory effects on LR growth, NO_3^- also can repress LR development (Zhang and Forde 1998; Zhang *et al.* 1999; Zhang and Forde 2000). LR development is inhibited in *Arabidopsis* seedlings grown at high NO_3^- concentration. The inhibition of LR outgrowth occurs immediately after the emergence from the primary root, whereas stimulatory effects act on mature LRs. Further evidence of an inhibitory effect on LRs is due to an accumulation of NO_3^- itself inside the plant, rather than being due to downstream NO_3^- metabolite assimilation, as the nitrate reductase-deficient mutants showed enhanced inhibitory effects on LR development (Zhang *et al.* 1999). In this context, a long-distance signal generated from shoots has been proposed to regulate LR development (Zhang *et al.* 1999).

Although, the precise mechanism of this long-distance signal is unknown, several candidates have been identified. The first candidate that may contribute to this signal pathway is auxin, as it is transported basipetally from the shoot and acropetally in the root, and shoot-derived indole-3-acetic acid (IAA) is necessary for the initiation of lateral root primordia (LRP)

(Zhang *et al.* 1999; Bhalerao *et al.* 2002). Higher IAA concentrations have been observed in roots of *Arabidopsis* seedlings transferred to LN nitrate (1 mM) from HN nitrate (50 mM) compared with those still grown in HN condition (50 mM) (Walch-Liu *et al.* 2006a). This phenomenon seems to support the hypothesis that NO_3^- accumulation in the shoot may be responsible for inhibition of auxin transport to the root and thus lead to failure of LRs through the auxin-requiring threshold in LR development (Forde 2002a).

1.5. CONCLUSION

The integration of root architecture modulation, uptake-activity regulation and transcriptional responses provides an efficient system enabling plants to adapt to a variety of nitrogen conditions and avoid the accumulation of abundant or toxic levels of nitrogen metabolites. Over recent decades, investigations have improved our understanding of N signal transduction and several key components involved in this process have been characterization. Based on the current framework, it is clear that some components participate in multiple signalling responses and some seem to play a role in different nutrient signalling (Xu *et al.* 2006; Ho *et al.* 2009b). Therefore, a challenge for future research is to extend the current framework into comprehensive networks. In this case, the question on how these components exerts specific effects on each of these responses, and whether different nutrient signalling mechanisms overlap at some points, need to be addressed. However, the ultimate challenge will be to apply the knowledge and molecular tools obtained from the research to improve N use efficiency, thus decreasing the level of fertiliser application and reducing costs and environmental pollution.

1.6. RESEARCH QUESTIONS

In New Zealand's animal production system, *Lolium perenne*, a cool-season grass species, provides the main nutrients for grazing cows and sheep during spring and early summer, whereas forage brassica (*Brassica napus*) is grown as a supplement and alternative to pastures from early summer through to late winter due to severe drought and/or low temperature (de Ruiter *et al.* 2009; Hampton *et al.* 2012). In order to increase the yield of dry matter, a range from 250 to 325 kg N ha^{-1} N fertilizer is applied annually in New Zealand (Rossi *et al.* 2014). However, about 25-70% of applied N fertilizers in agricultural systems is leached and released to the environment, in the form of NO_3^-, NO, N_2O and NH_3, causing severe environmental issues (Davidson *et al.* 2011; Sutton *et al.* 2011; De Vries *et al.* 2013; Qiao *et al.* 2015). Improving N utilization efficiency is a priority to maintain food production while alleviating the deleterious environmental effects of N.

Current knowledge indicates that carbon and nitrogen metabolism is coordinated via sensing the C/N balance, and that this is regulated by the expression of genes involved in photosynthesis, metabolic pathways, protein degradation and N assimilation (Stitt and Krapp 1999; Coruzzi and Zhou 2001; Palenchar *et al.* 2004; Gutiérrez *et al.* 2007). Despite several studies proposing possible mechanisms underlying C and N signalling in *Arabidopsis*, a definitive mechanistic understanding remains elusive. In this context, the dramatic shift in C/N balance resulting from defoliation and regrowth in forage grasses such as *Lolium perenne* has the potential to reveal insights into the comprehensive understanding of C/N interactions in plants that are otherwise not possible to observe in dicotyledonous species. From this, a number of research questions can be posed:

(1) What is the dynamic relationship between carbohydrate reserves and N uptake rate?

(2) How does the plant sense the internal C/N balance?

(3) How does the plant cope with perturbation of the C/N balance?

Under field conditions, plant roots are major sites which directly interact with soil and absorb soil nitrogen. Given that root foraging is a behaviour which integrates intrinsic genetics with nutrient availability and demand for plant growth and development, a number of further questions are raised:

(1) How do plants respond to different N forms? Is there a common mechanism underpinning these responses to N resources?

(2) What is the functional significance of root system architecture?

(3) Does root foraging behaviour matter in nitrogen use efficiency?

1.7. HYPOTHESISES AND OVERVIEW OF THESIS

In this study, the first hypothesis that was tested was associated with the fact that there is a C-cost associated with inorganic N uptake and assimilation: the hypothesis was that N uptake is repressed in the days after defoliation due to the competing requirement of C to sustain regrowth in *L. perenne*. In the study of root system architecture, phenotypes with contrasting root traits were developed using pharmacological treatments to test the hypothesis that

differences in root system architecture would lead to functional differences in relation to N acquisition.

As described in Fig. 1.1, this thesis is divided into three experimental sections addressing the following topics:

Chapter 2

The aim of Chapter 2 was to assess the mechanisms linking C/N balance to N uptake and assimilation in *L. perenne*. *Lolium* was chosen specifically because of its importance as a pasture fodder species, and because its carbohydrate status can be manipulated by simulated grazing, from which it readily regrows from multiple growing points. Using defoliation in this way as an experimental treatment, perennial ryegrass plants were manipulated to have contrasting internal carbohydrate reserves. By using these plants possessing contrasting carbon and nitrogen status, $^{15}NO_3^-$ isotope experiments were used to investigate the dynamic relationship between carbohydrate reserves and nitrate uptake. Using primers designed based on transcriptome data, the expression of the high-and low-affinity transporter genes and nitrate assimilation genes were profiled. With collaboration with research groups in Sweden and the Czech Republic, the oligosaccharide and cytokinin metabolites in samples were profiled, respectively.

The results from this chapter are published in *Journal of Experimental Botany* (Guo et al. 2017 doi: 10.1093/jxb/erx056).

Chapter 3

This aim of this chapter was to develop the high-throughput 2-D root system architecture phenotyping platform. Initial investigations were conducted with both *Lolium perenne* and *Brassica napus* because of their contrasting growth forms and root systems. Due to technical issues, the vertical-plate culture system was not successful for root cultivation in *Lolium perenne*, so the study of RSA presented here focused on the dicot species *Brassica napus*. In order to capture the morphological response of root system architecture conveniently and effectively, the traditional vertical-plate culture system was improved by shielding plant roots from light. Coupling with RootNav software for root analysis, the root morphological

changes were investigated in *B. napus* in response to different N forms over a wide range of concentrations.

This piece of work provides a foundation for next investigation of the functional significance of root system architecture described in Chapter 4.

Chapter 4

In *Brassica napus*, using *in situ* ^{15}N isotope labelling, morphological and molecular phenotypes generated pharmacologically were employed to investigate that contrasting root traits are functionally related to nitrogen acquisition. Cytokinin (6-benzylaminopurine) and PI-55 (a cytokinin antagonist) were used to generate the phenotypes with contrasting root traits. By using transcriptome data of *B. napus* to develop primers, the nitrate transporter genes and root system architecture genes were profiled. Also, Michaelis-Menten kinetics were performed to investigate root V_{max} and K_m in these contrasting root phenotypes.

The results of this chapter have been submitted for publication in the journal *Functional Plant Biology*.

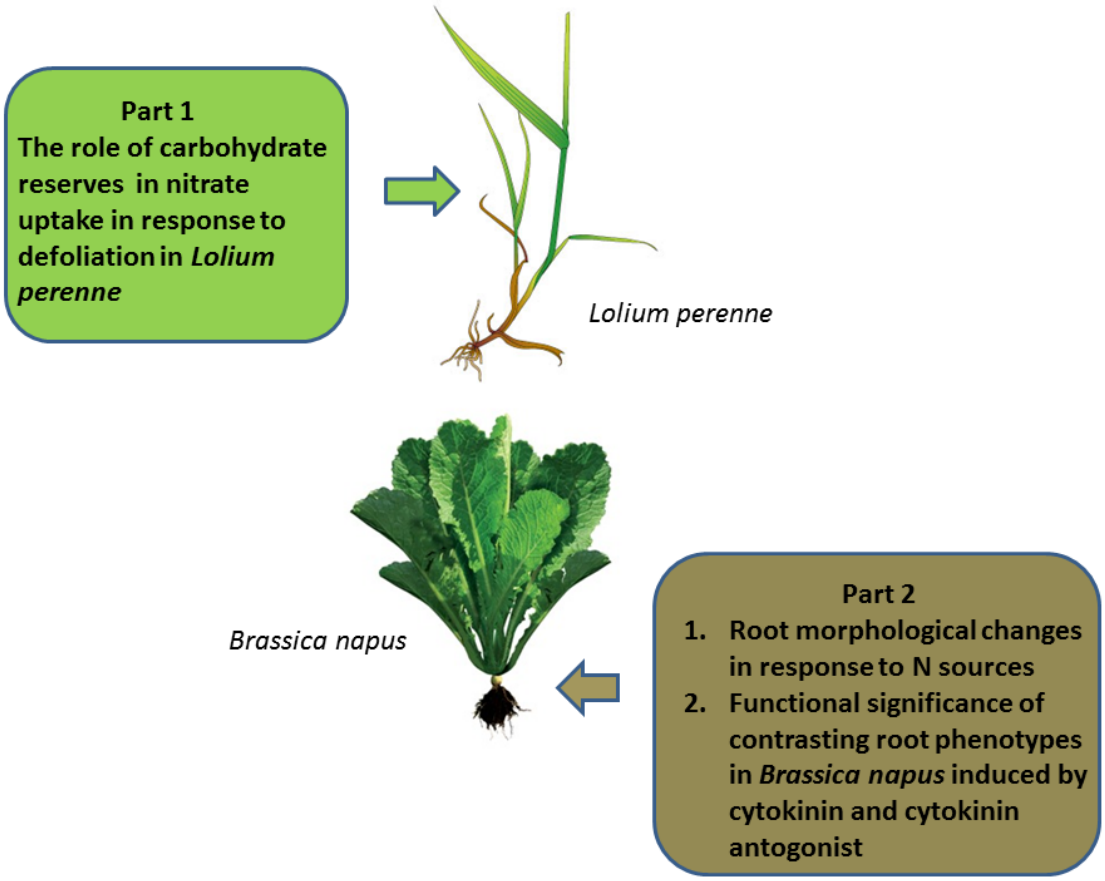

Fig 1. 1 The frame work of the research in the thesis.

Chapter 2-Depletion of carbohydrate reserve limits nitrate uptake during early regrowth in *Lolium perenne L.* via cytokinin-implicated regulation

2.1 INTRODUCTION

Grasses are well adapted to tolerate and recover from the severe and frequent defoliation associated with grazing (Lestienne *et al.* 2006). The most obvious developmental aspect of this is the physical protection of the meristem at the crown. Less overt, but no less critical, are the metabolic aspects of this tolerance. For instance, leaf regrowth and the re-establishment of photosynthesis in the leaf prior to its transition from sink to source is dependent upon the remobilization of stored nutrient resources, particularly carbon (C) and nitrogen (N) (Ourry *et al.* 1989; Lestienne *et al.* 2006). In the period immediately following defoliation, photosynthetic capacity is temporarily compromised, interrupting C assimilation and the capacity to assimilate newly acquired inorganic N into biomass, which is a process requiring reducing equivalents, ATP and C skeletons generated from respiration of sucrose derived from stored C (Dawar *et al.* 2010; Nunes-Nesi *et al.* 2010). Indeed, it has been established that root growth, inorganic N uptake, respiration and nitrate assimilation decline rapidly after defoliation (Boucaud and Bigot 1989; Ourry *et al.* 1989; Richards 1993; Louahlia *et al.* 2008).

Some evidence exists to suggest that carbon and nitrogen metabolism is coordinated via a sensing of plant C/N balance, and regulated by the expression of genes involved in photosynthesis, metabolic pathways, protein degradation and N assimilation (Stitt and Krapp 1999; Coruzzi and Zhou 2001; Palenchar *et al.* 2004; Gutiérrez *et al.* 2007). Microarray data from *Arabidopsis* transiently exposed to a matrix of C and N treatments has indicated that a large proportion of genes respond to a C/N interaction, suggesting C and/or N, or a metabolic product of C and N assimilation (e.g. an amino acid), might act as a signal in the regulation of gene expression (Gutiérrez *et al.* 2007). Despite several studies proposing possible mechanisms underlying C and N signalling in *Arabidopsis*, a definitive mechanistic understanding remains elusive. The dramatic shift in C/N metabolic partitioning resulting from defoliation and regrowth in forage grasses such as *Lolium perenne* L. has the potential to reveal insights into the integration of C/N assimilation in plants that are otherwise not possible to observe in dicotyledonous species.

Fructans, polymers of fructose that are based on sucrose, are the major storage carbohydrates in temperature forage grasses, such as *L. perenne* (Turner et al. 2006). Fructans from different sources display different degrees of polymerization (DP) and linkages between adjacent fructose residues (Sims *et al.* 1992). Fructan exohydrolases (FEHs), such as 1-FEHs and 6-FEHs, have been characterized as enzymes degrading fructans with β(2–1) and β(2–6) linkages, respectively (Van den Ende *et al.* 2004). *Lp1-FEH* has been functionally

characterized *in L. perenne* (Chalmers *et al.* 2005; Lothier *et al.* 2007). Previous research by our research group has confirmed that the fructan pool in *L. perenne* is degraded when NO_3^- is supplied to N-deficient plants (Roche et al. 2016), consistent with earlier work by Morvan-Betrand *et al.* (1999) and Louahlia *et al.* (2008). While it was observed that shoots initially contain a relatively larger pool of fructans than roots, and a greater relative proportion of fructan depletion was observed in shoots compared to roots, the root fructan pool appeared to be exhausted sooner than shoots, suggesting that both root and shoot fructan pools support nitrate uptake and assimilation (Roche et al. 2016). In response to defoliation, early shoot regrowth is also sustained by remobilization of the C stored as fructans in elongating leaf bases and mature leaf sheathes (Morvan-Bertrand *et al.* 1999; Morvan-Bertrand *et al.* 2001). Logically, the importance of root-derived C in supporting regrowth must also be considered in terms of the greater root biomass fraction that exists following defoliation. Thus, C and N remobilization under the new metabolic condition induced by defoliation must necessarily be coordinated at a whole plant level.

The cytokinins, in addition to multiple roles in plant growth and development, are well known to play a role in regulating NO_3^- uptake systems in response to fluctuations in N availability (Krouk *et al.* 2011). It has been shown that *trans* zeatin (*t*Z)-type cytokinins (which carry a hydroxyl on the isoprenoid side chain) are the major forms in xylem sap, while isopentenyl adenine (iP-type) and *cis* Z-type cytokinins are the predominant forms in phloem sap (Takei *et al.* 2004b; Hirose *et al.* 2008). Matsumoto-kitano *et al*. (2008) showed that iP-type cytokinins translocated from the shoot to the root in *Arabidopsis* were functional. It has been proposed that cytokinins could be involved in local and long-distance signalling to coordinate responses at the whole plant level, and to communicate N status between multiple organs (Takei *et al.* 2001b; Sakakibara *et al.* 2006; Turner *et al.* 2006; Matsumoto-Kitano *et al.* 2008; Kudo *et al.* 2010; Shtratnikova *et al.* 2015). A split-root experiment in *Arabidopsis* has demonstrated that NITRATE TRANSPORTER *NRT2.1* and *NAR2.1* regulation, driven by shoot-root systemic N signalling, is mediated by cytokinin biosynthesis (Ruffel *et al.* 2011). Further, genome-wide analyses for cytokinin responsive genes in *Arabidopsis* have indicated that exogenous cytokinin can down-regulate root localized transporters including *AtNRT1.1*, *AtNRT2.1*, *AtNRT2.2*, and *AtNRT1.5* (Brenner *et al.* 2005; Li *et al.* 2007). These gene families have been functionally identified as major components of the NO_3^- uptake and xylem loading system (Liu *et al.* 1999b; Lin *et al.* 2008a). In contrast, cytokinin also up-

regulates shoot localized *AtNRT* genes under both high- and low-nitrogen conditions (Kiba *et al.* 2011).

Crosstalk between sugar signalling and cytokinin signals has support from previous studies. Global gene profiling coupled with physiological analysis in *Arabidopsis* has indicated 74% of cytokinin-regulated genes may be significantly affected by glucose, either agonistically or antagonistically (Kushwah and Laxmi 2014). Among these genes, 98% of the agonistically regulated genes were influenced by glucose alone at the transcript level, while the majority of antagonistically regulated genes (58%) were affected non-transcriptionally in the presence of glucose alone. This suggests that interaction between glucose and cytokinin signalling may act via different mechanisms (Kushwah and Laxmi 2014). Additionally, up-regulation of *AtIPT3* and some Type A *ARABIDOPSIS RESPONSE REGULATORS* (*ARRs*) and *CYTOKININ RESPONSE FACTORS* (*CRFs*) by glucose suggests a potential role of glucose in modulating cytokinin signalling at various levels from biosynthesis to signalling (Kushwah and Laxmi 2014). It is thus plausible that cytokinins may play an active role in balancing the C/N status of the plant (Wang and Ruan 2016). Cytokinin deficiency, resulting from overexpression of *CYTOKININ OXIDASE/DEHYDROGENASE* (*CKX*), in *Arabidopsis* causes an increased root/shoot ratio, with inhibited shoot growth and a larger root system (Werner *et al.* 2003; Werner *et al.* 2008). This observation indicates that cytokinin deficiency may trigger a shift in C allocation from shoot to root, enhancing soil "foraging" capacity for nitrate under limited N availability (Ruffel *et al.* 2011). Once taken up, the increased NO_3^- induces cytokinin biosynthesis in a nitrate-dependent manner (Krouk *et al.* 2011). Consequently, cytokinins translocated to the shoot could regulate C allocation to keep a balanced shoot-to-root development (Wang and Ruan 2016).

With an ultimate goal of finding ways to better manage N input in grassland-based agricultural systems such as dairy farming, I investigated the nitrate uptake response to two independent but coinciding metabolic demands on fructan-defoliation and nitrate addition. I carried out a stable isotope N-uptake experiment, measured fructan content, and profiled cytokinin metabolites and relevant genes in *L. perenne* growing hydroponically. Of particular interest was the degree of metabolic constraint, if any, that the defoliation-regrowth cycle and associated fructan depletion has on inorganic N uptake efficiency. Given the C-cost associated with inorganic N uptake and assimilation (Roche et al. 2016), the hypothesis is that this metabolic demand is not adequately met in the days after defoliation due to the competing C allocation to sustain regrowth (Louahlia *et al.*, 2008). Then this study offers

insight into the underlying physiological and molecular regulation by profiling cytokinin levels together with expression of genes putatively involved in NO_3^- uptake, assimilation, fructan hydrolysis and cytokinin metabolism and signal transduction in response to defoliation and glucose supplement.

2.2 MATERIALS AND METHODS

2.2.1 Plant growth

Seeds of *Lolium perenne* L. cv. Grasslands Nui were germinated in 1.5 ml Eppendorf tubes filled with perlite (tube tips removed) and the tubes placed in unfertilized soil for 11 weeks at 20-24°C in a glasshouse located in University of Canterbury, Christchurch. The basic N-free Hoagland medium (pH 6.0; Bioworld, USA) was supplemented with 0.05 or 5 mM KNO_3 as a sole nitrogen source every week. Eight-week-old plants were defoliated at 4 cm above ground level. After 3-weeks regrowth, plant roots were washed and the plants transferred to a hydroponic system which contained basic N-free Hoagland medium supplemented with either 0.05 or 5 mM KNO_3, consistent with the previous growth conditions. The plants remained in the tube to avoid transplant damage and the tubes were slotted into the hydroponic channels (Fig. 2.1). Based on preliminary experiments, a one-week adaptation phase in liquid culture medium was required for plants to retain pre-transfer competence (as assessed by leaf gas exchange and stomatal conductance measurements). The pH of treatment solutions was maintained at 6.0. After the one-week adaptation half the plants were again defoliated. The time zero of the experiments is defined by the second defoliation of plants. Flow diagrams of the experimental processes are shown in Fig. 2.2.

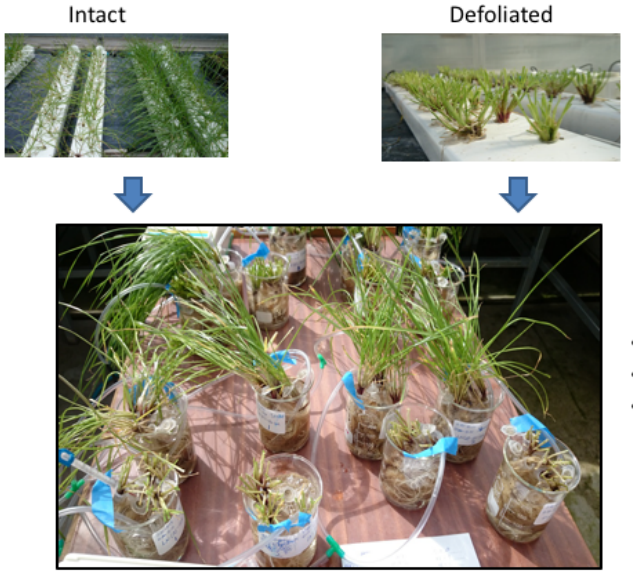

Fig 2. 1 Photographs of the intact and defoliated plants in the hydroponics system, and the experimental set up for the nitrate uptake experiments.

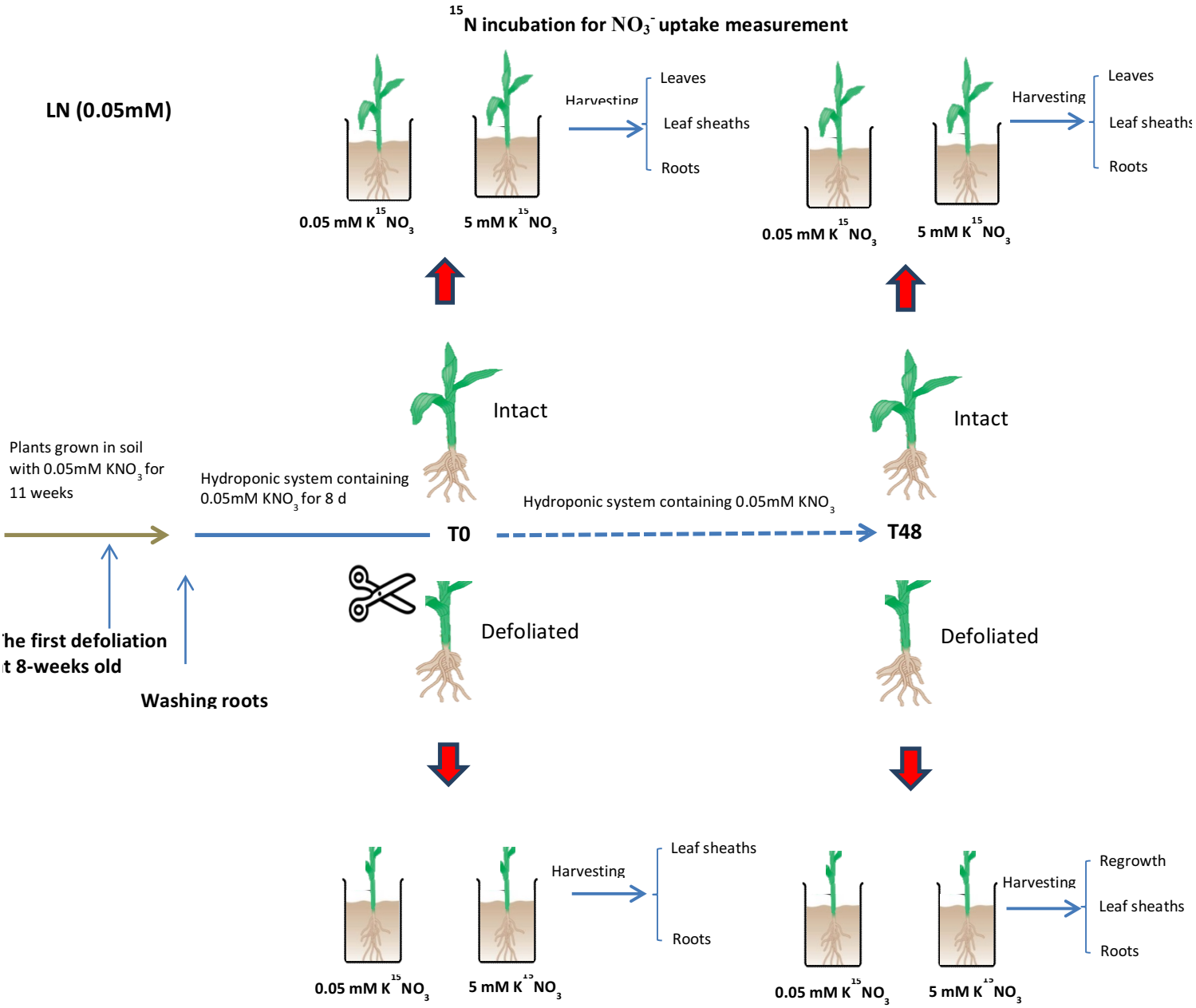
15N incubation for NO3- uptake measurement
LN (0.05mM)
Leaves
Leaf sheaths
Roots
Harvesting
0.05 mM K15NO3
5 mM K15NO3
Intact
Plants grown in soil with 0.05mM KNO3 for 11 weeks
Hydroponic system containing 0.05mM KNO3 for 8 d
Hydroponic system containing 0.05mM KNO3
T0
T48
Defoliated
he first defoliation
t 8-weeks old
Washing roots
Regrowth

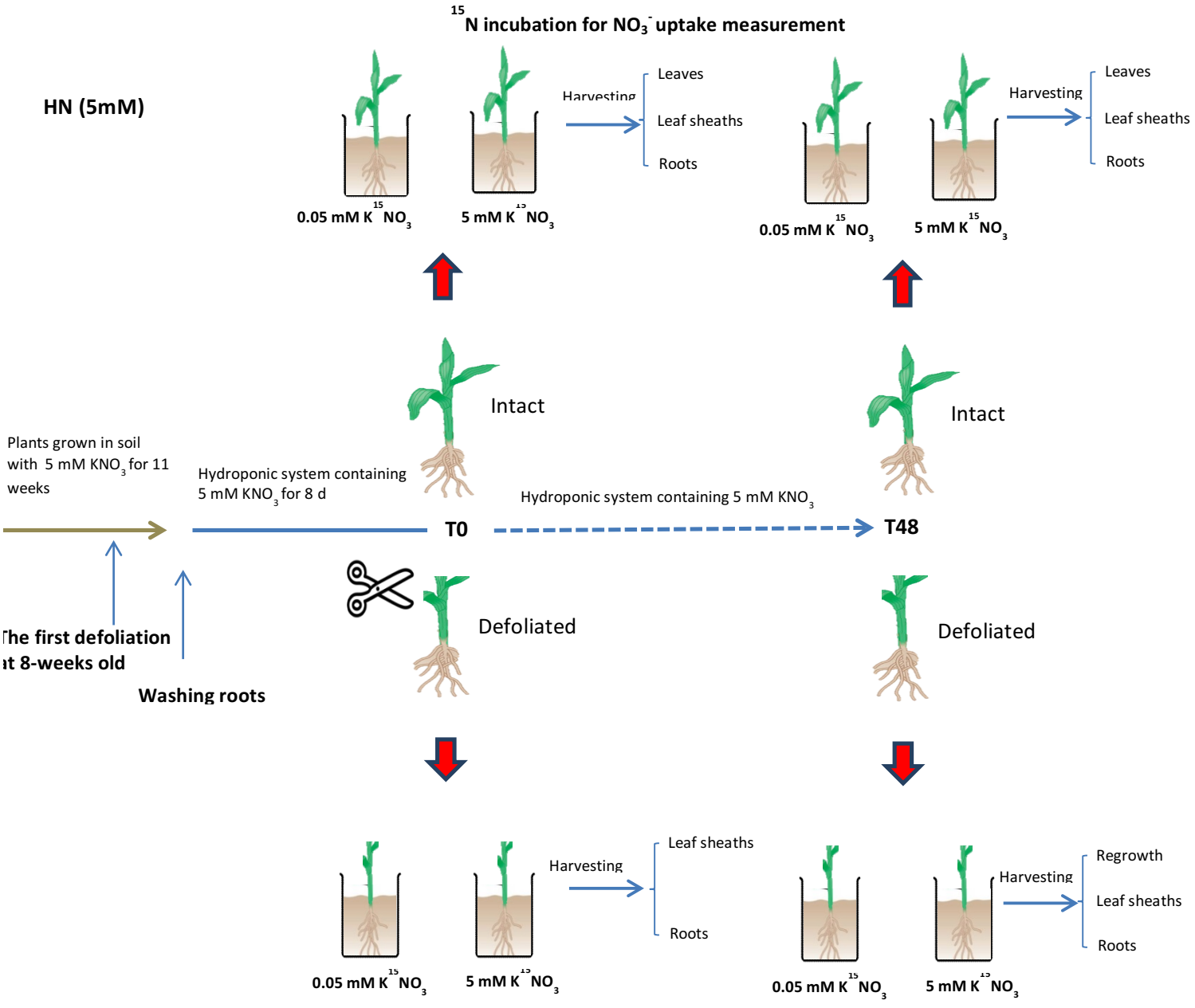

Fig 2. 2 Flow diagram of nitrate uptake experiments

2.2.2. $K^{15}NO_3$ uptake and isotope analysis

Nitrogen content was measured in roots and leaf sheaths of 12-week-old *L. perenne* plants 8 d after they were transferred from soil to a hydroponic solution and then defoliated to 40 mm above the crown. For the purpose of this study, the leaf sheath is defined as tissue from crown to 40 mm above, including elongating leaf bases and mature leaf sheaths, and this same part was harvested for the analysis in the intact plants. Root uptake of NO_3^- was determined by ^{15}N labelling. At 0 and 48 h after defoliation, plants were gently blotted on tissue paper and then immediately rinsed with 0.1 mM $CaSO_4$ for 1 min to remove any adsorbed compounds on the root surface, followed by 1 h of exposure to basic nitrogen-free Hoagland medium supplemented with either 0.05 or 5 mM ^{15}N-labelled KNO_3 (atom % ^{15}N: 10%). During the uptake experiments the incubation solutions were aerated by an aquarium pump. At the end of the incubation period, roots were immediately rinsed with 0.1 mM $CaSO_4$ for 1 min. Leaf sheaths and roots were separated, frozen in liquid nitrogen immediately and stored at -80 °C. For this study, five plants were pooled as one biological replicate and each treatment had five independent biological replicates. One gram of fresh samples was ground to a fine powder and freeze dried for 3 d. Total N and ^{15}N content in the samples were determined with an isotope ratio mass spectrometer (Waikato University, New Zealand).

2.2.3. Glucose treatment

After 42 h of regrowth as described above, 100 plants grown in solutions with 5 mM KNO_3 were then supplemented with either 0.1% or 1% (w/v) glucose (25 plants each) or with 0.1% or 1% (w/v) mannitol (25 plants each) as an osmotic control. After 6 h, $K^{15}NO_3$ uptake measurements were carried out by exposing roots to 5 mM ^{15}N-labelled KNO_3 (atom % ^{15}N: 10%) solutions as described above. A flow diagram of the experimental processes is shown in Fig. 2.3.

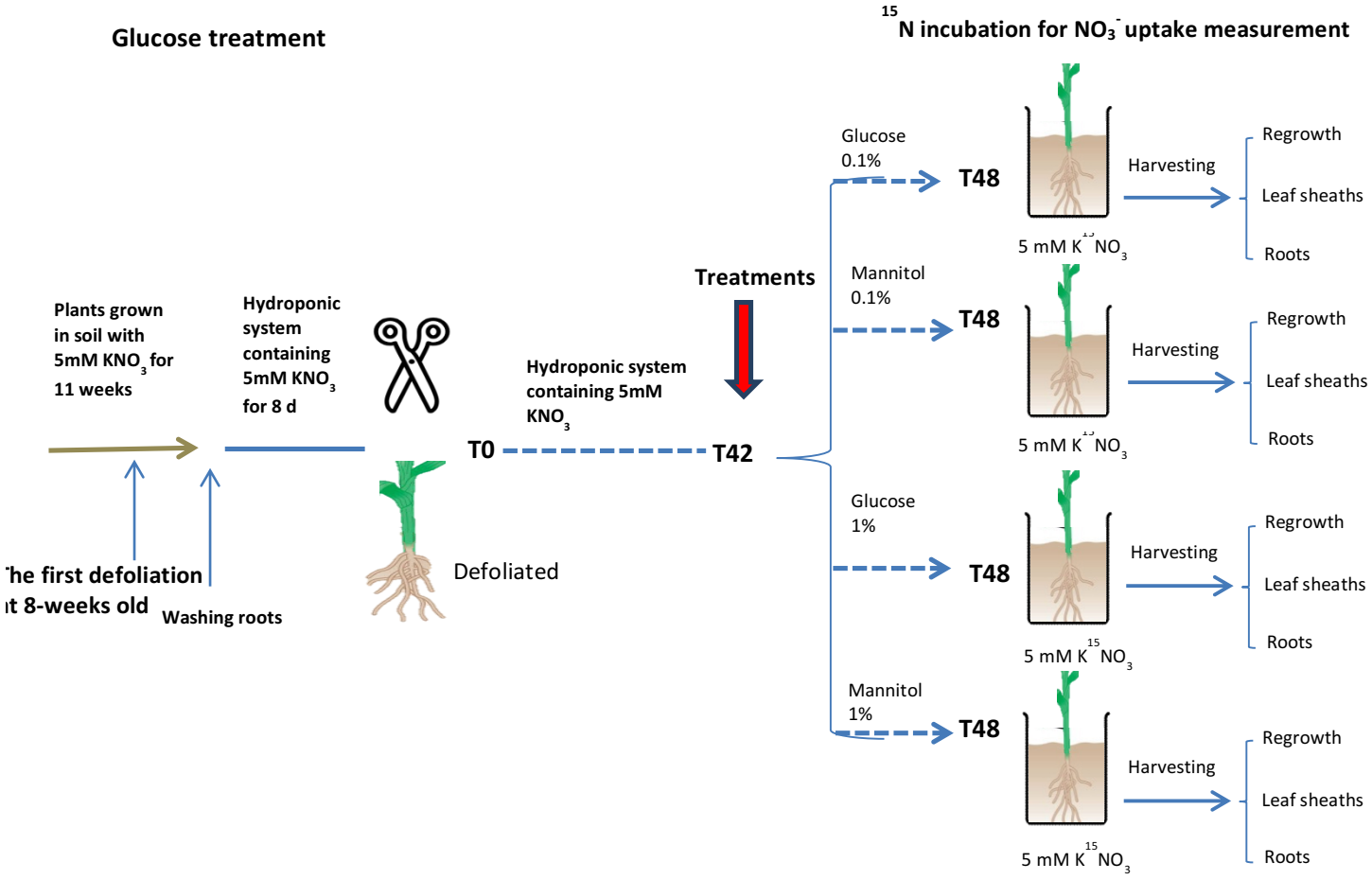

Fig 2. 3 Flow diagram of $K^{15}NO_3$ uptake measurement in glucose rescue experiment

A subset of HN plants as described in Fig. 2.1 above was subjected to glucose treatment at 42 h after defoliation. 100 plants grown in solutions with 5 mM KNO_3 were then supplemented with either 0.1% or 1% (w/v) glucose (25 plants each) or in 0.1% or 1% (w/v) mannitol (25 plants each) as control. After 6 h, the $K^{15}NO_3$ uptake measurement was carried out by exposing roots to 5 mM ^{15}N-labelled KNO_3 (atom % ^{15}N: 10%) solutions as described above.

2.2.4. Target gene sequence determination

Sequences of candidate target gene family members in perennial ryegrass were determined through BLAST searching the NCBI database and a RNA-Seq transcriptome database using prfect BLAST 2.0 software in the lab of Jiancheng Song at Yantai University. An Illumina HiSeq2000 genome analyzer and a pool of combined RNA samples extracted from multiple developmental stages of leaves, flower spikes and seeds of perennial ryegrass cv. Nui were used to generate the transcriptome database containing 169,862 assembled sequence contigs of 595 bp in average length. All available orthologue sequences of the target gene families in the GenBank database in perennial ryegrass and closely related species were used as local BLAST search query sequences. The putative sequences of interest were verified via BLAST searching the GenBank database and via multiple sequence alignment with representative orthologue sequences in closely related species. By using all of the annotated family members of *NRT* in *Brachypodium distachyon*, wheat, rice and maize species available in the GenBank database, most of the putative *NRT1*, *NRT2* and *NAR* orthologous sequences were identified in *L. perenne*.

Neighbor-joining (NJ) phylogenetic trees of the newly identified sequences of *LpNRT1*, *LpNRT2*, *LpNR*, *LpNiR*, *LpCKX* and *LpRR*, and their orthologues were created using Clustal X software with 1000 bootstrap replicates. The phylogenetic trees were visualized with TreeView software (Appendix Information Fig. S3). Each tree was rooted with an out group orthologue sequence from an unrelated species. The *LpRR* tree was shown in Roche *et al*. (2016). The GenBank accession numbers for the nucleotide sequences determined in this work will be listed in Table 1 of Appendix 1.

2.2.5. RNA isolation, primers design and quantitative RT-PCR

For gene expression analysis, total RNA was extracted from up to 100 mg of frozen samples using RNase Plant Mini Kit (Qiagen, Germany), following the manufacturer's protocols. Total RNA was then treated with DNase I Set (Qiagen) before checking integrity and quality by running on a 1% (w/v) agarose gel. The concentration and purity of the isolated RNA samples were assessed using a Nanodrop^{TM} spectrophotometer. Three independent tissue samples (each comprising tissues from five plants) for each treatment were used as biological

replicates. Up to 1 µg of extracted RNA was converted to cDNA using QuantiTect Reverse Transcription Kit according to the manufacturer's instructions (Qiagen).

Specific PCR primers were designed for each family member of the target genes, using Primer Premier 6.20. Whenever possible, primer pairs were designed to span at least one intron to avoid/detect genomic contamination. In most cases, four primer pair combinations were designed and the best one was chosen for gene expression analysis. Primer sequences for reference genes and target genes can be found in Appendix Information Table S1.

The relative expression levels of *LpNRT*, *LpNR*, *LpNiR*, *LpCKX* and *LpRR* gene family members were determined using RT-qPCR. A volume of 15 µL was used for all qPCR reactions containing 1 µL of 10-fold diluted cDNA, the relevant primers and home-made SYBR Green master mix (Song *et al.* 2012) in a Rotor-Gene Q real-time PCR machine (Qiagen, Germany). PCR products were Sanger-sequenced to confirm homology to genes which were already identified in NCBI gene databases. The expression levels of the target genes were normalized using two reference genes from *L. perenne*, *ELONGATION FACTOR* (*eEF-1α*) and *GAPDH*. The relative expression of each target gene was corrected and calculated using the $2^{-\Delta\Delta Ct}$ method as described in previous studies (Schmittgen and Livak 2008; Song *et al.* 2015).

2.2.6. Oligosaccharide profiling

WSC were measured in plants grown under high and low nitrate supply, 1 h and 48 h after defoliation. Samples were harvested and immediately flash frozen in liquid nitrogen. Ground and freeze-dried plant materials (25 mg) were weighed and placed into 2 mL Eppendorf tubes for fructan extraction using a protocol developed and conducted by Jana Späth at the Swedish Metabolomics Centre, Umea (See Appendix 2).

2.2.7. Endogenous cytokinin quantification

Extraction and qualification of cytokinins from around 3 mg DW samples were performed as described previously (Dobrev and Kamınek 2002; Antoniadi *et al.* 2015) using the LC-MS/MS system consisting of an ACQUITY UPLC ® System (Waters) and Xevo ® TQ-S (Waters) triple quadrupole mass spectrometer in the lab of Ondřej Novák at Palacký University (Svačinová *et al.* 2012).

2.2.8. Statistical analyses

For each treatment in the $K^{15}NO_3$ uptake experiment, values are the mean ± SE of five biological replicates, with each replicate comprising a pool of five plants. For gene expression analysis, three biological replicates, each comprising a pool of five plants, were tested and values are the mean ± SE. Means were tested for significance using a two-tailed t-test.

2.3 RESULTS

2.3.1 Regrowth 48 hours after defoliation

As expected, both leaf sheath and root N content was significantly greater (P<0.001) in plants grown under high NO_3^- (HN, 5 mM) conditions than in plants grown under low NO_3^- (LN, 0.05 mM) (Fig. 2.4a,b). During the early phase of recovery after defoliation, the regrowth rate in HN plants was more than 2-fold greater than in LN plants (Fig. 2.4c). Consequently, the regrowth biomass of HN plants was significantly greater than that of LN plants 48 h after defoliation (Fig. 2.4d).

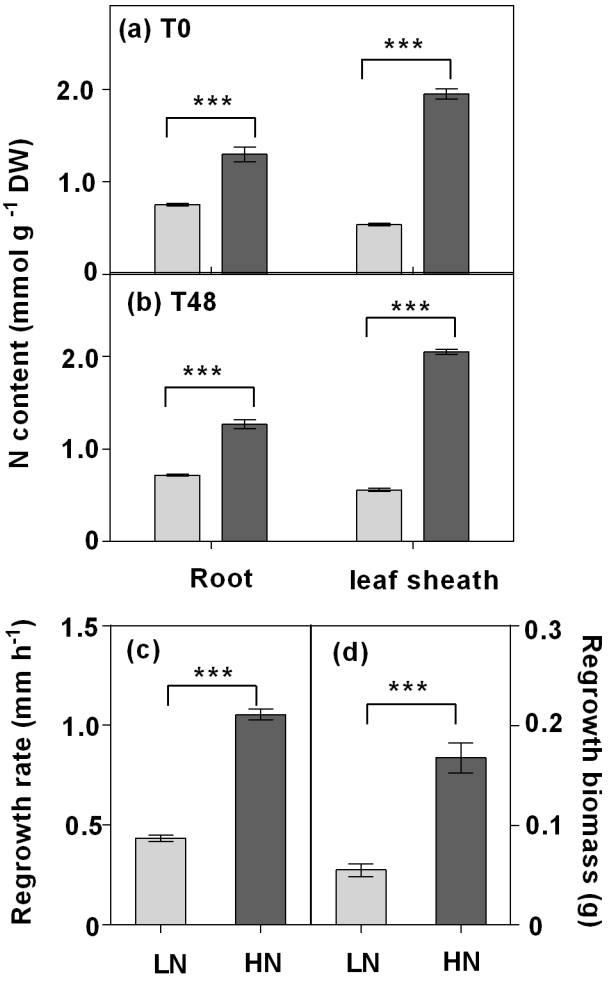

Fig 2. 4 Growth parameters 48 h after defoliation of *L. perenne* plants grown under low (0.05 mM) or high (5 mM) nitrate supply (LN vs HN).

(a, b) Nitrogen (N) content before and 48 h after defoliation; (c) regrowth rate; (d) dry biomass 48 h after defoliation. Values in (a), (b) and (d) are means ±SEM (n=5, pools of five plants each). Values in (c) are means ±SEM (n=36 plants). ***denotes significantly different means between LN plants (gray bars) and HN plants (black bars) at $P<0.001$.

2.3.2. Water-soluble carbohydrate and *Fructan exohydrolases gene* (*Lp1-FEH*) transcript level

In order to assess the dynamics of carbon metabolism during the first 48 h of regrowth, water soluble carbohydrates (WSC) were profiled. With the exception of disccharides, which showed similar relative abundance in LN plants and HN plants, fructans were found in greater relative abundance in LN roots and leaf sheaths compared to HN plants (Fig. 2.5). During the first hour after defoliation, the remobilization of fructans occurred only in roots of HN plants, while no difference was observed in either roots or leaf sheaths of LN plants relative to intact plants (Fig. 2.5a,b). In comparison to the intact plants, the total concentration of WSCs was significantly reduced 48 h after defoliation in both roots and leaf sheaths of HN plants, whereas in LN plants depletion of the fructan pool was only observed in roots, implying that the nature of defoliation-induced remobilization of the fructan pool after 48 h was tissue-specific (Fig. 2.5c,d). In roots, the extent of exhaustion of the fructan pool of HN plants was more severe compared to that in LN plants (Fig 2.5b,d). *Lp1-FEH* transcription broadly showed a trend of induction in response to defoliation, significantly so in LN roots and leaf sheaths after 48 h, where the fructan content was highest (Fig. 2.6).

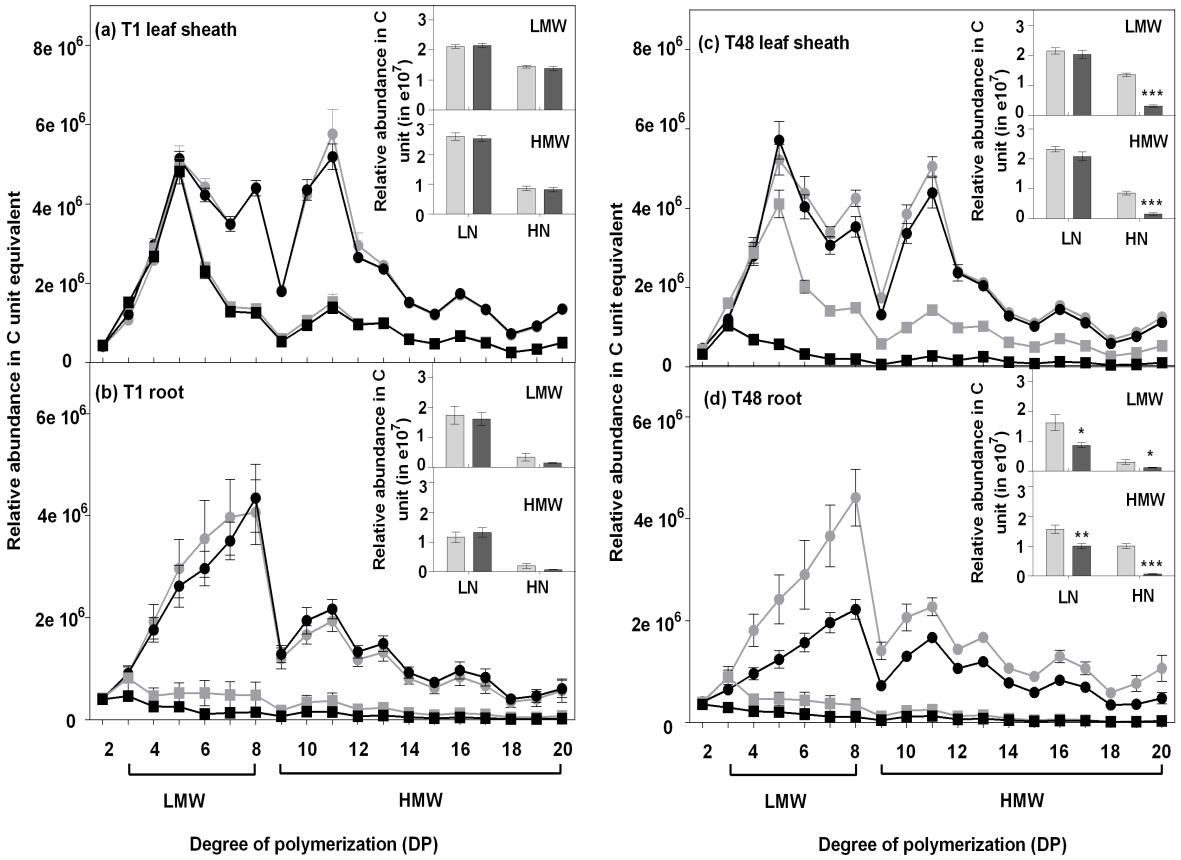

Fig 2. 5 Relative abundance in carbon (C) units of water-soluble carbohydrates (WSC) in *L. perenne*.

WSC were measured in plants grown under high (HN, squares) and low nitrate (LN, circles) supply, 1 h and 48 h after defoliation. Relative abundance in C units was calculated by multiplying peak intensity by degree of polymerization (DP). WSC profile in (a) leaf sheaths and (b) roots after 1 h; (c) leaf sheaths and (d) roots after 48 h. WSCs with degree of polymerization (DP) from three to eight are referred to here as low molecular weight (LMW) WSCs, and DP9 to DP20 are referred to as high molecular weight (HMW) WSCs. The total concentrations of LMW and HMW WSCs are shown in the inserted bar graphs. Values are means ±SEM (n=5 pools of five plants each). *denotes significantly different means between intact plants (gray) and defoliated plants (black) (* $P<0.05$, ** $P<0.01$, *** $P<0.001$).

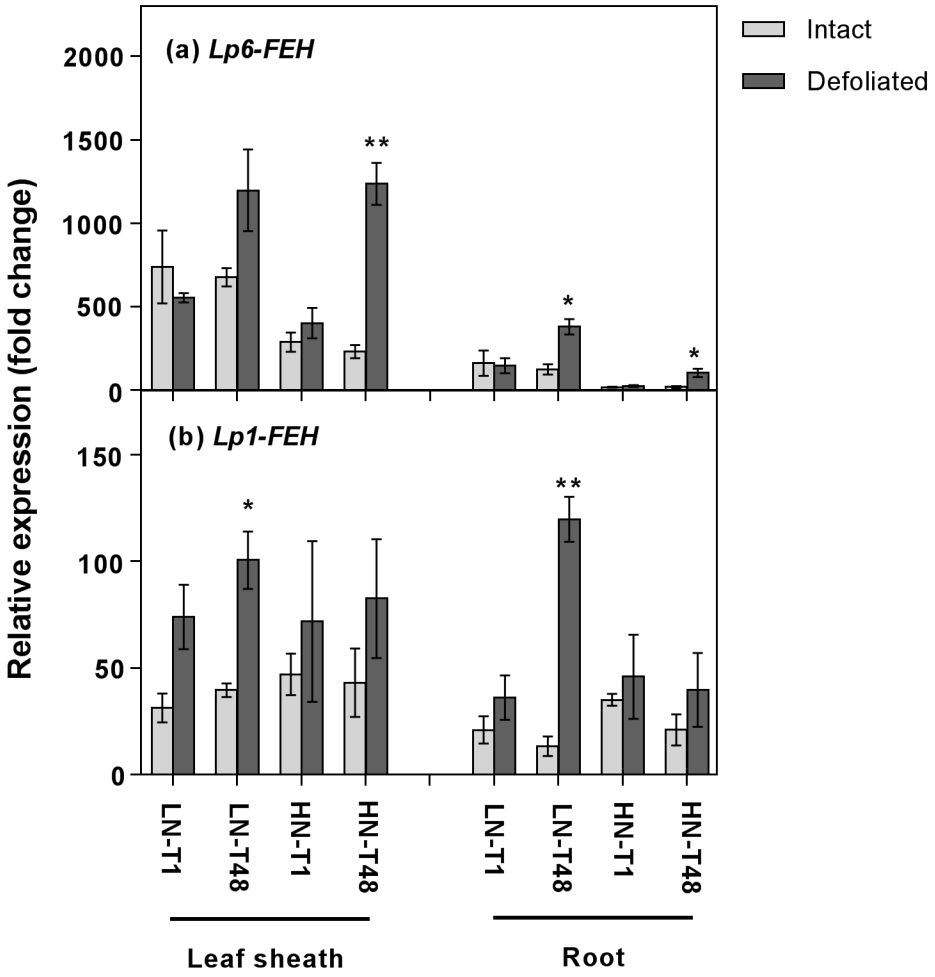

Fig 2. 6 Expression of putative *Lp6-FEH* and *Lp1-FEH* in *L. perenne* plants grown under either 0.05 mM (LN) or 5 mM NO_3^- (HN) supply.

0.05 mM (LN) or 5 mM NO_3^- (HN) supply, 1 h and 48 h after defoliation. Each data point was normalised against reference genes *eEF-1α* and *GAPDH*. Values are means ±SEM (n=3 pools of five plants each). *denotes significantly different means between intact plants (grey bars) and defoliated plants (black bars) (* $P<0.05$, ** $P<0.01$).

2.3.3. Nitrate uptake rate and N allocation

To better understand changes in NO_3^- uptake in response to defoliation, plants were exposed to 0.05 mM and 5 mM NO_3^- to stimulate either the nitrate high-affinity uptake system (HATS) or the low-affinity uptake system (LATS), respectively. The concentrations chosen were well below or above the point at which HATS or LATS would be saturated (Siddiqi *et al.* 1990; Garnett *et al.* 2013). The NO_3^- HATS and LATS responses in both HN and LN plants were measured using ^{15}N isotopically labelled NO_3^-. During the first 1 h after defoliation, no difference in NO_3^- uptake rate via HATS or LATS was observed in LN plants compared to intact plants, whereas NO_3^- uptake via both HATS and LATS in defoliated HN plants was significantly greater relative to intact plants (Fig. 2.7a). In intact plants, HATS uptake in LN plants was greater than that in HN plants, while a much greater LATS uptake was induced in HN plants (Fig. 2.7a). 48 h after defoliation, both HATS and LATS uptake rate in HN plants dropped by 93% and 79%, respectively, relative to intact plants, reaching a final value of 0.12 µmol g^{-1} DW h^{-1} and 1.7 µmol g^{-1} DW h^{-1}, respectively (Fig. 2.7b). Likewise, the HATS and LATS uptake measured in LN plants 48 h after defoliation were 27% and 31% lower than those measured in intact plants grown under LN condition, respectively (Fig. 2.7b). The reduction in both HATS and LATS uptake in HN plants was markedly greater than that of LN plants 48 h after defoliation.

To investigate the impact of defoliation on N distribution, ^{15}N allocation to leaf sheaths following the incubations in ^{15}N-labelled NO_3^- was measured at 1 h and 48 h after defoliation. Relative allocation was determined as the proportion of labelled ^{15}N in leaf sheaths to that in the total plant (roots and leaf sheaths). During the first hour after defoliation, with exception of LN plants incubated in 5 mM ^{15}N-labelled NO_3^- and HN plants incubated in 0.05 mM ^{15}N-labelled NO_3^- , relative less ^{15}N was allocated to leaf sheaths in defoliated LN and HN plants than in the controls (Fig. 2.7c). By contrast, despite the decline in NO_3^- uptake rate 48 h after defoliation (Fig. 2.7b), the ^{15}N allocation to leaf sheaths was relatively greater in both HN and LN defoliated plants than in intact plants (Fig. 2.7d).

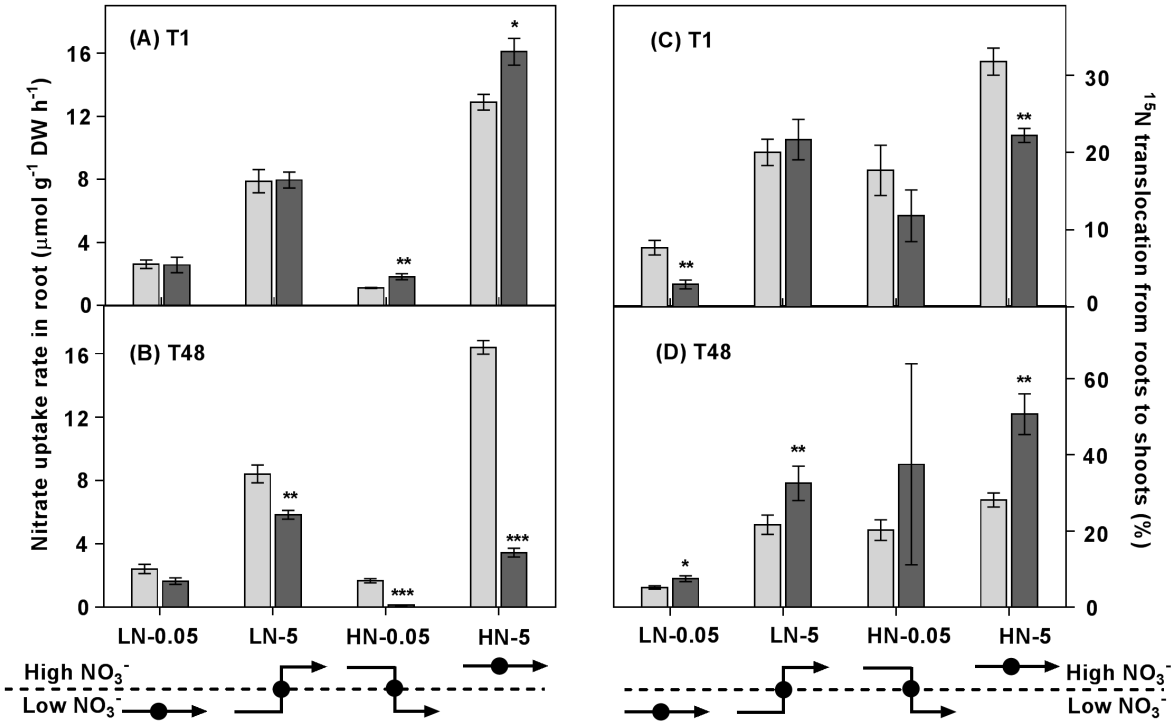

Fig 2. 7 The impact of defoliation on NO_3^- uptake and translocation in *L.perenne*.

In order to investigate HATS and LATS uptake capacity, plants were grown under low NO_3^- (LN: 0.05 mM) or high NO_3^- (HN: 5 mM), and then defoliated (or left intact). Plants were then exposed for 1 h to either 0.05 mM or 5 mM ^{15}N-labelled NO_3^- either immediately after defoliation or 48 h after defoliation. During the period of ^{15}N-labelling, NO_3^- uptake rate (a) and translocation rate from roots to leaf sheaths (b) were measured. ^{15}N allocation to leaf sheaths was determined as the proportion of ^{15}N-labelled NO_3^- in leaf sheath to that in the total plant (roots and leaf sheaths). Values are means ±SEM (n=5, pools of five plants each). *denotes significantly different means between intact plants (grey bars) and defoliated plants (black bars) (* $P<0.05$, ** $P<0.01$, *** $P<0.001$).

2.3.4. *NRT*, *NR* and *NiR* transcript levels

At the whole-root level, *NRT2* and *NAR* transcript levels in LN roots were generally greater than those in HN roots (Fig. 2.8a-e). This was particularly evident for the putative HAT candidate genes *LpNRT2.1a* and *LpNRT2.1b*, where transcript expression in roots of LN plants were 20-50 fold greater relative to HN plants (Fig. 2.8b). In addition, 48 h after defoliation, an increasing trend in transcript abundance of *LpNRT2.1b* was observed in LN roots, relative to intact plants, whereas no significant difference was observed between defoliated and intact LN plants during the first hour after defoliation. Although transcript levels were relatively low in HN roots following the 1 h incubation in 0.05 mM or 5 mM ^{15}N-labelled NO_3^-, a reduction in *LpNRT2.1b* transcript abundance was apparent 48 h after defoliation. Notably, within 1 h of defoliation, *LpNRT2.1b* expression was induced in HN roots incubated with 5 mM ^{15}N-labelled NO_3^- (P=0.06, Fig. 2.8b). *LpNRT2.5* and *LpNRT2.7* showed similar patterns of response, but with approximately 100-fold less transcript abundance relative to *LpNRT2.1a* and *LpNRT2.1b* (Fig. 2.8a-d). Similarly, *LpNAR* displayed a similar pattern to *LpNRT2.1a* and *LpNRT2.1b*, suggesting an important role in the function of NRT2.1 in NO_3^- uptake (Fig. 2.8e).

With regard to *NRT1,* another set of NRT gene family members involved in nitrate uptake, the transcript levels of *LpNRT1.1*, *LpNRT1.2*, *LpNRT1.3*, *LpNRT1.4* and *LpNRT1.5* were about 1000-fold less than those of *LpNRT2.1a* and *LpNRT2.1b* (Fig. 2.8). Generally, apart from *LpNRT1.1*, *NRT1* members did not show clear differences between low N and high N treatments (Fig. 2.8f-j).

In order to determine whether N assimilation is tightly coordinated, the influence of C/N balance on the expression of nitrate reductase (*NR*) and nitrite reductase (*NiR*) genes was assessed. Similar to nitrate transporter gene expression, transcript levels of genes involved in nitrate assimilation (*LpNR1*, *LpNRb* and *LpNiR*) were more abundant in plants grown under LN conditions relative to those under HN conditions (Fig. 2.9). With exposure to HN conditions, expression of *LpNR1* and *LpNRb* in sheaths was significantly induced 48-h after defoliation, whereas *LpNR* expression in roots showed a trend of reduction 48 h after defoliation (Fig. 2.9a-d). Notably, in HN roots, *LpNR1* and *LpNRb* expression was induced during the first hour after defoliation (Fig. 2.9b,d). The transcripts of *LpNiR* showed a similar pattern to that of *LpNR1* and *LpNRb*. In LN conditions, *LpNR1*, *LpNRb* and *LpNiR* expression was induced in roots 48 h after defoliation, whereas there was no change in leaf sheaths (Fig. 2.9b,d,f).

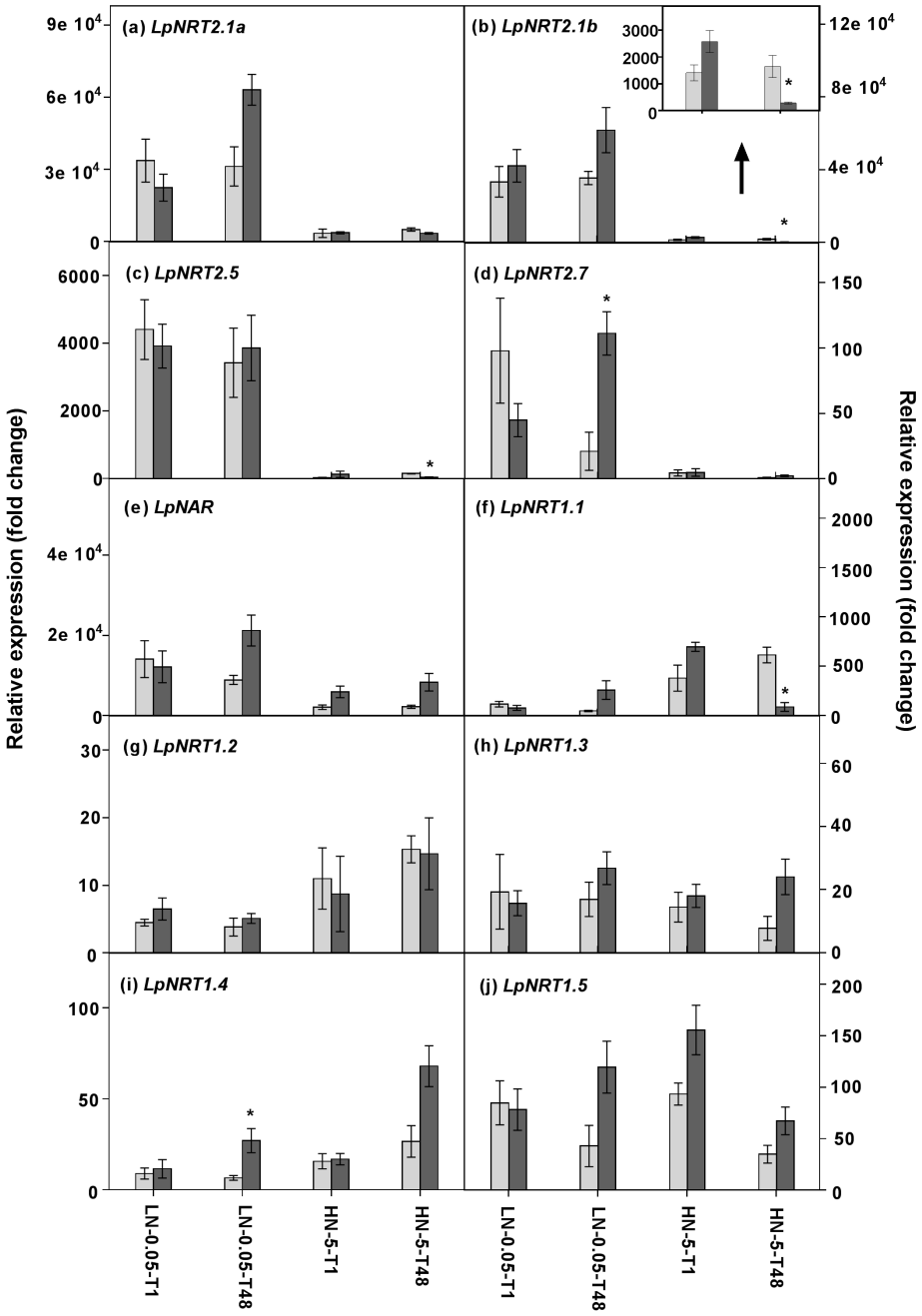

Fig 2. 8 Expression of putative high-and low-affinity (*NRT1*, *NRT2* and *NAR*) NO_3^- transporters in roots of *L.perenne*.

Plants were grown at either 0.05 mM (LN) or 5 mM (HN) NO_3^- , and then defoliated (or left intact). The expression level of *LpNRT2.1b* in HN roots is shown in the inserted bar graph in (b). Each data point is normalized against reference genes *eEF-1α* and *GAPDH*. Values are means ± SEM (n=3 pools of five plants each). *denotes significantly different means between intact plants (grey bars) and defoliated plants (black bars) at $P<0.05$.

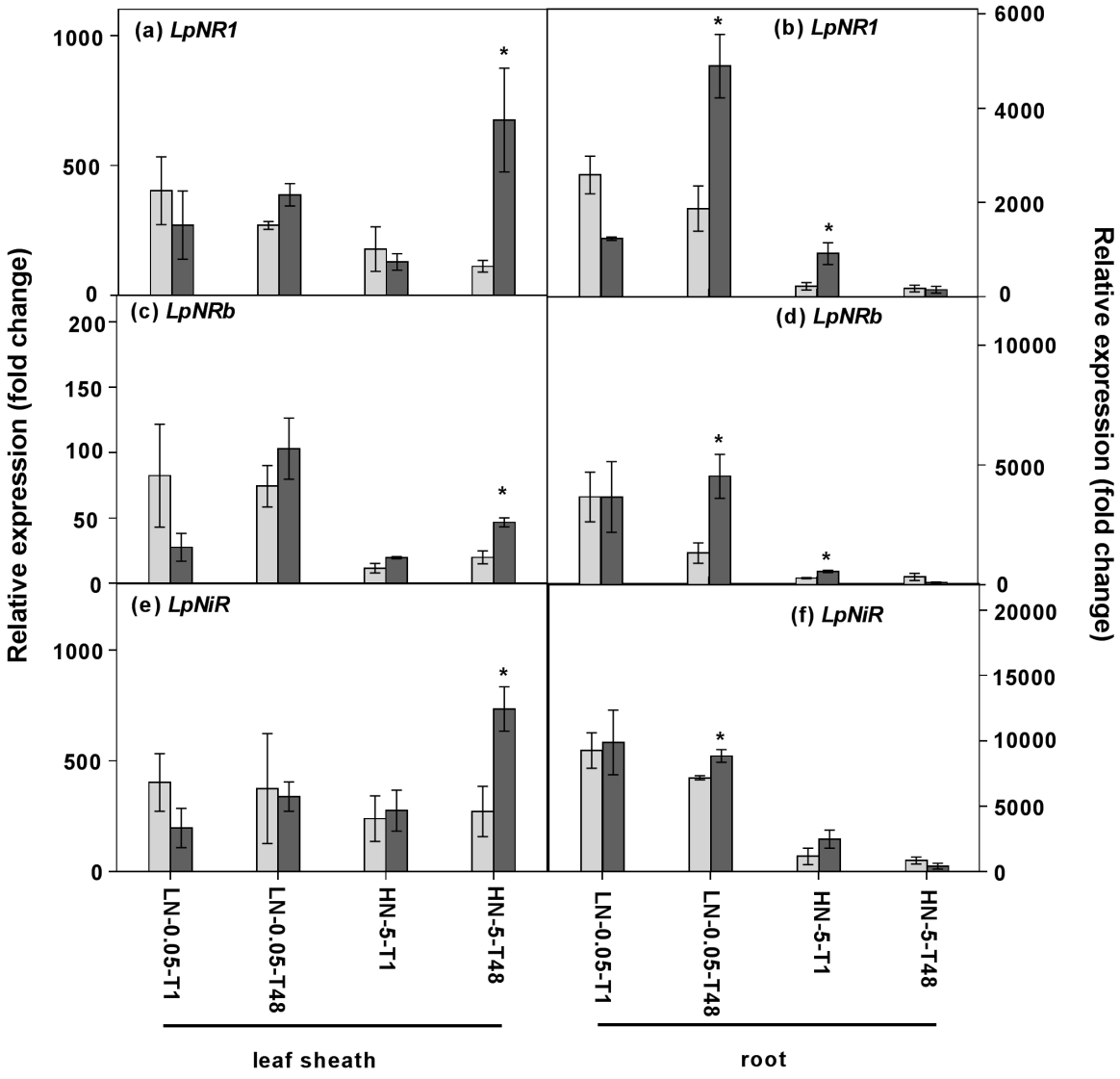

Fig 2. 9 Expression of putative NO_3^- reductase (*NR*) and nitrite reductase (*NiR*) genes in *L. perenne*.

Plants were grown at either 0.05 mM (LN) or 5 mM (HN) NO_3^- , and then defoliated (or left intact). Each data point is normalized against reference genes *eEF-1α* and *GAPDH*. Values are means ± SEM (n=3, pools of five plants each). *denotes significantly different means between intact plants (grey bars) and defoliated plants (black bars) at $P<0.05$.

2.3.5. Glucose supplement

To further distinguish the relationship between carbon change dynamics following defoliation and N uptake responses, a subset of the HN plants were subjected to exogenous glucose treatment 42 h after defoliation. After 6 h of treatment with 0.1%-glucose, fructan abundance in roots increased compared with the mannitol control and this increase was more pronounced when the glucose concentration was increased to 1% (Fig. 2.10b). With 0.1% glucose treatment, LMW WSCs increased 5-fold while HMW WSC levels did not change. When glucose concentration increased to 1%, LMW WSCs in roots were increased by 10-fold compared to those in control plants, and HMW WSCs also increased significantly (bar graph inserts in Fig. 2.10b). However, there was no significant difference as a result of the 6 h glucose supplement on fructan abundance in leaf sheaths (Fig. 2.10a).

After 6 h of glucose treatment, a subset of HN plants was moved to 5 mM ^{15}N isotopically labelled NO_3^- for LATS measurement. With 0.1% glucose treatment, LATS uptake was increased slightly compared to that in the mannitol treatment (Fig. 2.10c). When the concentration of glucose was increased to 1%, this difference was significantly increased, with LATS uptake over 2-fold greater than in the control (Fig. 2.10c). The 1% glucose supplement induced a significant decline in the percentage of NO_3^- translocated from roots to leaf sheaths (Fig. 2.10d).

The transcript profiles of *LpNRT2.1a* and *LpNRT2.1b* were also investigated following the glucose treatments. At the concentration of 0.1% glucose, the transcript level of *LpNRT2.1b* was significantly enhanced (Fig. 2.10f). Increasing glucose concentration to 1% resulted in a 400-fold increase in the transcript level of *LpNRT2.1b* relative to the mannitol control (Fig. 2.10f). There was no significant change in the transcript abundance of *LpNRT2.1a* following glucose treatment (Fig. 2.10e).

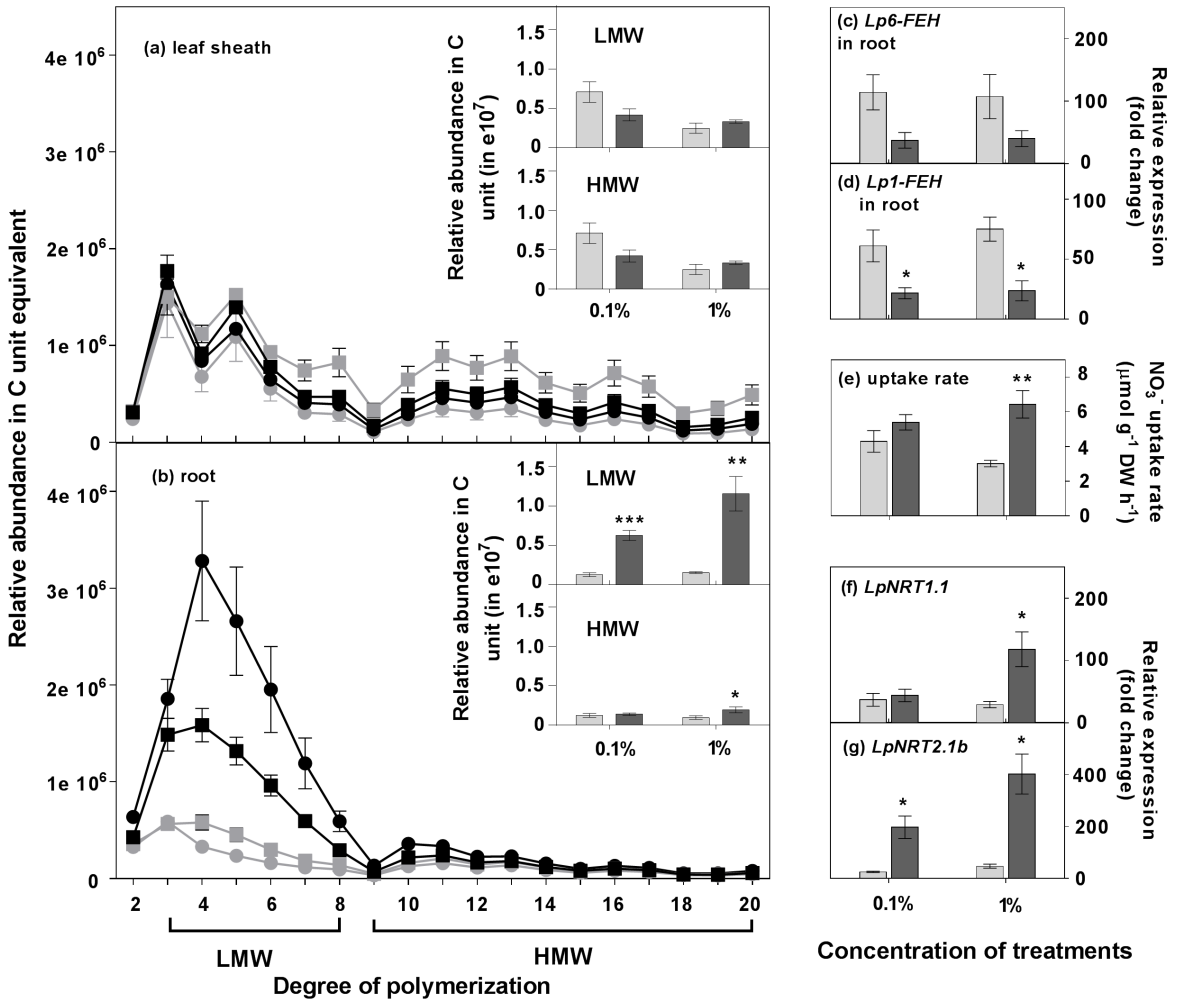

Fig 2. 10 WSC contents, NO_3^- uptake and *Lp6*-FEH, Lp1-*FEH*, *LpNRT1.1*, *LpNRT2.1a* expression in *L. perenne* roots with 6 h of supplemental glucose.

Plants were grown in HN conditions and supplied with 0.1% or 1% glucose 42 h after defoliation. After 6 h, the impact of supplemental 0.1% (squares) or 1% (circles) glucose treatment on: (a, b) the relative abundance (in carbon units) of water-soluble carbohydrate (WSC); (c) and (d) Lp6-FEH and Lp1-FEH expression; (e) NO_3^- uptake rate; (e) and (f) nitrate transporter gene expression were investigated. Values are means ±SEM (n=5, pools of five plants each).*denotes significantly different means between mannitol (grey) and glucose (black) treatment (* $P<0.05$, ** $P<0.01$, ***$P<0.001$).

2.3.6. Changes in endogenous cytokinin content following defoliation

To better understand the role of cytokinin in communicating the root-shoot C/N balance at the whole-plant level, cytokinins and their conjugates were quantified in *L. perenne* plants. Overall, the total cytokinin complement was greater in the leaf sheaths and roots of HN plants compared with LN plants, irrespective of defoliation. Under HN, both *t*Z and *t*Z riboside (*t*ZR) had decreased in the leaf sheaths 48 h after defoliation, whereas both iP and iP riboside (iPR) decreased in the roots 48 h after defoliation, relative to intact controls (Fig. 2.11). In the LN plants, with the exception of an accumulation of iPR in leaf sheaths 48 h after defoliation, there was little change in other cytokinins. In addition, iP and iPR in leaf sheaths was greater in HN defoliated plants following the 6-h 1% glucose treatment relative to HN defoliated plants without glucose treatment. Although there were no significant changes in iPR contents between glucose and mannitol treatment, iPR contents were greater in roots with 1% glucose treatment relative to HN defoliated roots without glucose or mannitol addition (Fig. 2.11). Substantial amounts of *cis* Z-type CKs were found in *L. perenne*. Among them, *cis*-zeatin (*c*Z) accumulated in leaf sheaths in the 48 h following defoliation of HN plants, compared with the leaf sheaths of control plants (Fig. 2.11). Further, cZ contents decreased in leaf sheaths and roots of plants treated with glucose relative to HN defoliated plants without glucose or mannitol treatment. This decrease was also observed in the 1% mannitol treatment (Fig. 2.11).

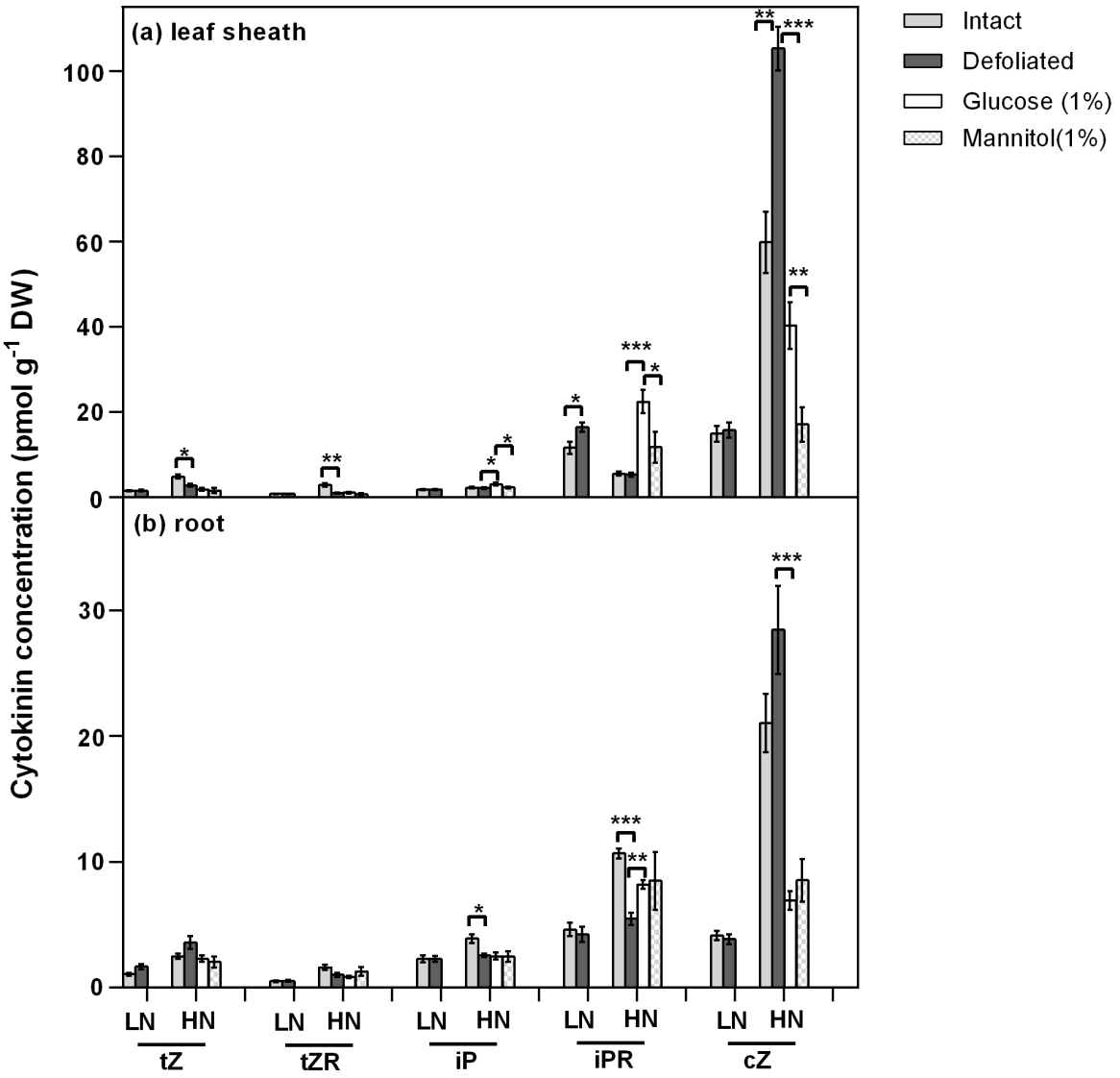

Fig 2. 11 Cytokinin concentrations in low (LN) and high (HN) *L. perenne* roots and leaf sheaths 48 h after defoliation.

Values are means ±SEM (n=5, pools of five plants each).*denotes significantly different means between intact plants (grey bars) and defoliated plants (black bars), or between defoliated plants (black bars) and defoliated plants supplemented with 1% glucose (white bars) or 1% mannitol (hatched bars) (* $P<0.05$, ** $P<0.01$, ***$P<0.001$).

2.3.7. Expression of cytokinin response regulator and cytokinin oxidase/dehydrogenase gene family members.

Based on the RNA-Seq transcriptome database of perennial ryegrass cv. Nui, most of the putative *LpCKX* and *LpRR* orthologous sequences in *L. perenne* were identified. Here, the transcript levels of *LpCKX4*, *LpCKX6* and those of the *RR* genes, *LpRR2*, *LpRR3*, *LpRR6, LpRR10*, *LpRR12a* and *LpRR12b* were profiled. Generally, strong differences were observed in transcript levels of *LpCKX* and *LpRR* family members under HN (Fig. 2.12). *LpCKX4* and *LpCKX6* showed the same expression patterns in leaf sheaths: relatively greater expression in LN plants and, relative to intact plants, greater expression was induced 48 h after defoliation in HN plants (Fig. 2.12a,b). The transcript level of *LpCKX4* was significantly greater in HN leaf sheaths relative to intact plants 48 h after defoliation (Fig. 2.12a). In roots, significant *LpCKX4* induction was observed in LN and HN plants 48 h after defoliation (Fig. 2.12a).

All of the six *LpRR* family members showed similar expression patterns in leaf sheaths. In comparison with intact plants, increases in *RR* transcript abundances were displayed in leaf sheaths of HN plants 48 h after defoliation, whereas no significant differences were displayed in leaf sheaths of LN plants (Fig. 2.12c-h). In roots, transcript levels of *LpRR* were greater in both LN and HN conditions 48 h after defoliation (Fig. 2.12c-h). A decrease in *LpCKX* and *LpRR* expression was displayed in both leaf sheaths and roots of plants following the 6 h glucose treatment (Fig. 2.13). Expression of *LpCKX4*, *LpCKX6*, *LpRR2*, *LpRR6*, *LpRR10*, *LpRR12a* and *LpRR12b* were strongly reduced in roots by 1% glucose (Fig. 2.13 a,b,c,d,e,f,h).

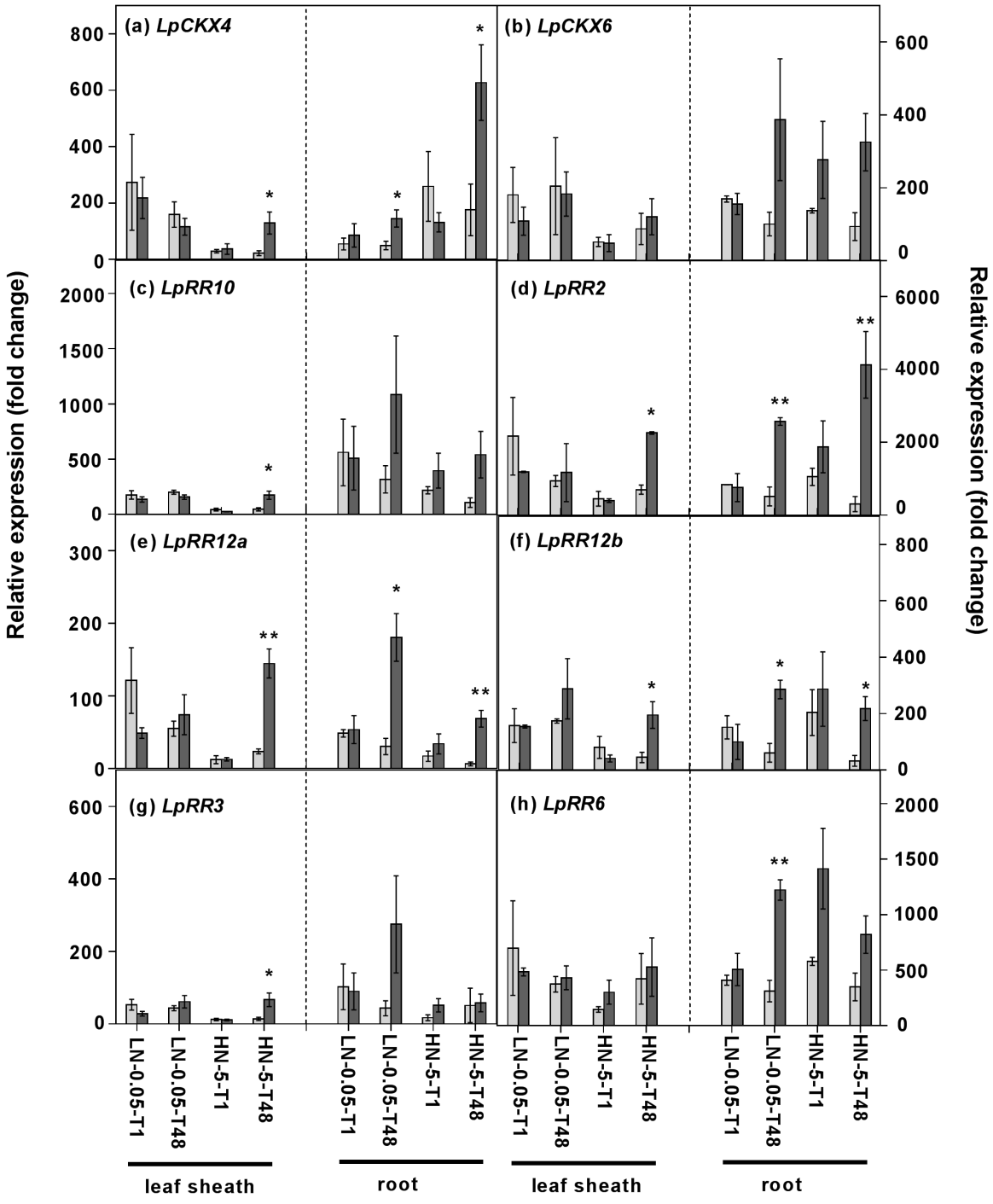

Fig 2. 2 Expression of putative *LpCKX* and *LpRR* in *L. perenne.* Plants were grown at either 0.05 mM (LN) or 5 mM (HN) NO_3^-, and then defoliated (or left intact).

Each data point is normalized against reference genes *eEF-1α* and *GAPDH*. Values are means ±SEM (n=3, pools of five plants each). *denotes significantly different means between intact plants (grey bars) and defoliated plants (black bars) (* $P<0.05$, ** $P<0.01$).

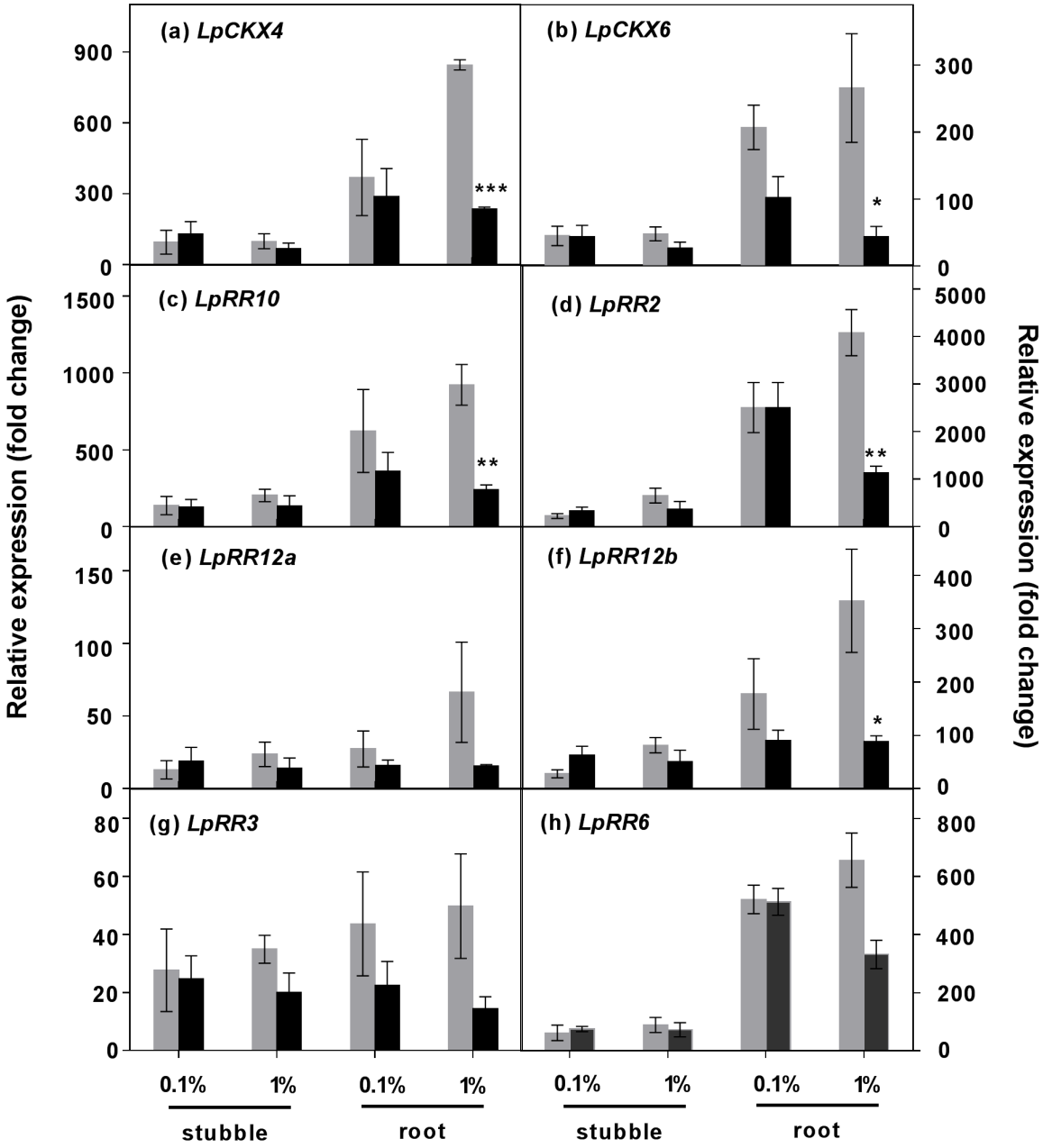

Fig 2. 3 Effects of glucose addition on putative *CKX* and *RR* gene expression in *L. perenne* grown in 5 mM NO_3^-, 48 h after defoliation.

Each data point is normalized against reference genes *eEF-1α* and *GAPDH*. Values are means ±SEM (n=3, pools of five plants each). *denotes significantly different means between mannitol (grey bars) and glucose (black bars) treatment (* $P<0.05$, ** $P<0.01$, *** $P<0.001$).

2.4 DISCUSSION

An understanding of the mechanisms linking C/N balance to N uptake and assimilation is vital for optimizing plant growth in the real-world scenario of defoliation by grazing followed by N-fertilizer addition. As shown in several studies, the fructan pool in elongating leaf bases and sheaths may be severely depleted to sustain regrowth following the removal of photosynthetically active tissues in grasses such as *L. perenne* (Morvan-Bertrand *et al.* 1999; Morvan-Bertrand *et al.* 2001). Here, by experimentally defoliating plants to interfere with C/N balance and by 'repairing' this with exogenous glucose supplementation, the dynamic relationships between the carbohydrate status of the plant and the nitrate-responsive uptake system, transporter gene expression and assimilation were uncovered. These results confirm and extend previous studies (Louahlia *et al.* 1999) by showing that NO_3^- HATS and LATS uptake changes in response to the rapid and large shift in carbon status induced by defoliation. The role of cytokinins in the regulation of changing C/N balance in response to defoliation was explored at the whole plant level. The results are discussed in relation to internal C/N balance under defoliation

2.4.1. Nitrate uptake and assimilation rely on labile carbohydrate availability

As expected, during the first 48 h of regrowth following defoliation, significant differences in both regrowth rate and regrowth biomass were observed when plants were grown under low nitrate (LN) or high nitrate (HN) supply, showing that N availability has effects on regrowth during the very early stages following defoliation (Fig. 2.4a,b). Consistent with previous studies (Louahlia *et al.* 2008; Roche et al. 2016), long term N-limitation led to a significant accumulation of fructans in both roots and shoots relative to N-sufficient plants, which is important in the context of this study (Fig. 2.5). Two days after defoliation, severe fructan depletion occurred in both roots and leaf sheaths of HN plants. However, in LN plants this depletion was only significant in roots, and was incomplete. Efficient regrowth following defoliation, therefore, requires balanced pools of stored C for energy, cell biosynthesis and C skeletons for nitrate reduction together with stored N. In contrast, sufficient N in HN plants stimulates remobilization of the available fructan pool in leaf sheaths, providing the required energy and C skeletons for regrowth. These observations imply carbohydrate remobilization to support regrowth occurs in an N-dependant manner.

The regulation of root nitrate uptake by C metabolites from photosynthesis has previously been demonstrated by diurnal stimulation of NO_3^- uptake. It has been established that sugars transported from shoots to roots play an important role in this diurnal stimulatory effect

(Rideout and Raper Jr 1994; Delhon *et al.* 1996; Lejay *et al.* 1999). Using defoliation as a treatment in the present study allowed us to reveal the response of root NO_3^- uptake to changes in endogenous C. During the first hour following defoliation, the immediate depletion of the fructan pool was observed in roots of HN plants, with 58% reduction in LMW WSC and 63% reduction in HMW WSC relative to intact plants (Fig. 2.5b). This immediate remobilization of the fructan pool in HN roots was associated with a rapid and significant stimulation of root NO_3^- uptake rate (Figs 2.5b & 2.7a). Given that there is a substantial amount of sucrose in phloem immediately after defoliation (Morvan-Bertrand *et al.* 2001), this stimulation of root NO_3^- uptake is mostly likely attributed to the initial increase in sucrose followed by fructan remobilization in roots, suggesting an instantaneous response of root NO_3^- uptake to C availability. By contrast, 48 h after defoliation, NO_3^- low- and high-affinity uptake decreased following a severe depletion of the fructan pool, irrespective of N status in plants (Figs 2.5 & 2.7). Interestingly, a relatively greater fructan remobilization in HN leaf sheaths than in LN leaf sheaths led to a much stronger repression of nitrate uptake rate in HN plants than in LN plants, implying that NO_3^- uptake is a carbon-dependent process. These observations strongly suggest a rapid regulation of root NO_3^- uptake by C metabolites at the whole plant level, which is consistent with the idea that photosynthate supply is closely balanced with mineral uptake and assimilation (Lejay *et al.* 1999; Coruzzi and Zhou 2001; Nunes-Nesi *et al.* 2010).

2.4.2. NO_3^- assimilation is regulated by the C-N balance.

According to Scheurwater *et al* (2002), the intact shoot of the eight grasses they tested is the predominant site for nitrate reduction. This can be explained by that when leaves in fully saturating light, nitrate assimilation in roots is inefficient because sugar (e.g. sucrose) has to be synthesised, transported to roots and respired in order to generate ATP and NAD(P)H for N assimilation (Nunes-Nesi *et al*., 2010). The results also support this tissue specific N assimilation regulated by local C availability. With relative high C availability in HN roots 1 h after defoliation, NO_3^- uptake was induced instantaneously compared to intact plants (Fig. 2.7a). This induction of nitrate uptake in HN roots was concomitant with stimulation of *LpNR1* and *LpNRb* transcript in HN roots (Fig. 2.9b, d). Given that light was non-saturating for young expanding leaf tissue in immediately defoliated plants because they were shaded by the sheath, it was suggested that relative greater proportion of NO_3^- was assimilated locally in HN roots during the first hour after defoliation. In the days (48 h) after defoliation, however, when root carbon was reduced in HN plants and the young leaves were emerged

relatively more N was allocated to shoots compared with intact plants, thereby stimulating shoot growth (Fig. 2.5d & 2.7d). This was concomitant with changes in the transcript levels of nitrate reductase genes. In HN plants, the transcript of *LpNR* and *LpNiR* in leaf sheaths was induced following the strong carbon remobilization in roots, whereas *LpNR* and *LpNiR* expression showed a repression in roots. These results suggested a shift in nitrate assimilation from roots to shoots when root carbon availability was reduced, implying the regulation of tissue-specific N assimilation by local C availability (Fig. 2.5c, d & 2.9).

With low N status associated with high C/N, the transcripts of *LpNR* and *LpNiR* genes were more abundant in roots compared with leaf sheaths (Fig. 2.5c, d & 2.9). It is suspected that in low NO_3^- condition, roots with high C/N had sufficient carbohydrate to assimilate most of the acquired NO_3^- into amino acids locally, and thus little N was allocated to shoots in LN plants, thereby potentiating root growth and foraging. Interestingly, 48 h after defoliation, the significant C remobilization in LN roots was accompanied by a strong induction of *LpNR* and *LpNiR* expression in roots, whereas there was no change in the fructan pool and the expression of *LpNR* and *LpNiR* in leaf sheaths (Fig. 2.5c, d & 2.9). These observations imply a mechanism that signals the availability of C metabolites for NO_3^- uptake and assimilation at the whole plant level. Within tissues, where stored C is available, it is apparent that NO_3^- is assimilated locally.

Given that the WSC content per mg DW was similar in leaf sheaths and roots (Fig. 2.5), and root fractions were much greater than shoot in LN plants, this study confirms that when leaf N is deficient more C is exported to roots whereas less C is delivered to roots when high leaf N promotes shoot growth (Bloom *et al.* 1993). The perturbation of C/N balance by defoliation was likely a stimulus for root growth in LN plants, but for shoot growth in HN plants. This conclusion is consistent with the report by Morvan-Bertrand *et al*. (2001) that leaf elongation rate in defoliated *L. perenne* plants grown in non-limiting N level was significantly greater than that of intact (non-defoliated) plants during the early regrowth stage.

2.4.3. HATS and LATS regulation at the transcriptional level in response to changing C/N ratio

Four *NRT* families have been characterized to be involved in nitrate uptake in *Arabidopsis* (Tsay *et al.* 2007). Among them, *NRT1* and *NRT2* are regarded as the main components controlling the high-affinity (HATS) and low-affinity (LATS) transport systems that function at low (<250 μM) or high (>1 mM) nitrate levels, respectively (Siddiqi *et al.* 1990; Tsay *et al.*

1993; Huang *et al.* 1999a; Wang *et al.* 2012b). In this study, as expected, the expression of *LpNRT2.1b* was significantly repressed in HN plants 48 h after defoliation, coinciding with reduced NO_3^- uptake activity (Fig. 2.7b & 2.8b). Interestingly, within 1 h of defoliation, the increased expression of *LpNRT2.1b* in HN roots (P=0.06) also coincided with the instantaneous induction of NO_3^- uptake activity (Figs 2.7a & 2.8b). This is consistent with observations that regulation of root NO_3^- uptake is correlated with changes in transcript levels of *NRT2.1* in response to N and C treatment (Zhuo *et al.* 1999; Lejay *et al.* 2003). Conversely, but as expected, this was not the case in LN status plants which showed lower reductions in NO_3^- uptake rate following defoliation relative to HN plants, with only small increases in *LpNRT2.1b* expression (Figs 2.7b & 2.8b). This discrepancy between nitrate uptake and transporter expression was apparent in LN 48-h defoliated plants following 1-h incubation in 5 mM NO_3^-. Indeed, the regulation of high-affinity nitrate uptake is complicated in low nitrate conditions. This result is consistent with previous studies showing that large and rapid increases in HATS uptake in low NO_3^- conditions are not accompanied by increased *AtNRT2.1* expression (De Jong *et al.* 2014). One possible interpretation for the discrepancy between *NRT2.1* transcript and nitrate uptake involves the potential for post-transcriptional regulation of existing transporter levels and activity, for example by phosphorylation (Laugier *et al.* 2012; Wang *et al.* 2012a).

In the hydroponic system, it was expected that HATS and LATS transcript levels would be dominant in LN and HN plants, respectively. Indeed, as expected, the baseline transcript abundance of *LpNRT2.1a* and *LpNRT2.1b* were generally much greater than other transporters in LN plants, while the transcript levels of *LpNRT2.1a* and *LpNRT2.1b* were extremely low in HN plants with 1-h incubation in either 0.05 mM or 5 mM NO_3^-, relative to those under LN conditions (Figs 2.8a,b). This confirms previous evidence in other plant species that *NRT2.1* is generally down-regulated when N levels are high (Vidmar *et al.* 2000; Okamoto *et al.* 2003; Santi *et al.* 2003). Despite their very low presence, *LpNRT2.5* and *LpNRT2.7* displayed a similar expression pattern to *LpNRT2.1a*/*LpNRT2.1b*, suggesting these two putative transporters may play a role in the HATS (Fig. 2.8c,d).

LpNAR2.1 and *LpNRT2.1a*/*2.1b* showed a similar transcript profile, with expression being much higher in LN plants than that in HN plants (Fig. 2.8e). These observations are consistent with the proposal that *AtNAR2.1* is essential to the function of *AtNRT2.1* in HATS (Okamoto *et al.* 2006; Orsel *et al.* 2006).

Although the transcript levels of *LpNRT1.1* were relatively quite low, the observation that transcript abundance contrasts with those of the two putative HATS (*LpNRT2.1a* and *LpNRT2.1b*), with each being generally higher in HN conditions than that in LN conditions, suggests that the putative *NRT1.1* may play an important role in the LATS (Fig. 2.8f). Unlike *LpNRT1.1*, other *LpNRT1* genes, *LpNRT1.2*, *1.3*, *1.4* and *1.5*, showed extremely low, but constitutive expression patterns in treatments, suggesting these putative *NRT1* genes might be less sensitive to changing N conditions.

2.4.4. Exogenous glucose rescues the reduced nitrate uptake rate in defoliated plants at the physiological and molecular level

Exogenous glucose supply for 6 h to HN plants largely restored LMW WSC levels in roots, which appears to have relieved the C-limitation on NO_3^- uptake and assimilation (Fig. 2.10a). The NO_3^- uptake rate in defoliated plants supplemented with glucose returned to a level considerably greater than that in plants maintained in 5 mM but without glucose supply. In contrast, application of 1% mannitol had no impact on LATS uptake compared to plants kept in 5 mM NO_3^-, confirming the carbohydrate-dependence of nitrate uptake as described above (Figs 2.7b & 2.10c). Interestingly, increasing C availability in roots was correlated with a decline in NO_3^- transportation to leaf sheaths, which supports my observations of C and N interactions in nitrate uptake and metabolism (Fig. 2.10b,d).

Following 1% glucose application, the NO_3^- uptake rescue was closely correlated with the transcript level for *LpNRT2.1b*, which is assumed to be the major player in nitrate high-affinity transport (Fig. 2.10c,f). This suggests strongly that there is regulation operating at the transcriptional level. In plants, glucose and sucrose have been found to regulate the expression of genes involved in metabolism and nutrient uptake (Li *et al.* 2006b; Lejay *et al.* 2008). Up-regulation of *AtNRT2.1* by sugars is not attributed to well-established specific sucrose or glucose sensing, although it relies on hexokinase [HXK]-mediated down stream of C metabolism in glycolysis (Sheen *et al.* 1999; Lejay *et al.* 2003; Rolland *et al.* 2006). As shown by De Jong *et al*. (2014), a glucose-regulated expression of *AtNRT2.1,* independent of nitrate-mediated mechanisms, can operate through HEXOKINASE1-mediated oxidative pentose phosphate pathway (OPPP) metabolism.

2.4.5. Cytokinin is involved in the regulation of N acquisition and assimilation in response to changes in C/N

N availability in soil and N demand in plants is communicated between the root and shoot to optimize plant growth and development (Forde 2002b; Ruffel *et al.* 2014). Cytokinins have been proposed as candidate signalling molecules relaying N status between the root and shoot (Kudo *et al.* 2010; Ruffel *et al.* 2011). It was shown here that the cytokinin content of HN-status plants is greater than that in plants of LN status. In contrast, but functionally relevant, the expression of *CKX* was generally lower in HN plants (Figs 2.11 & 2.12). This is consistent with the observations that N supply leads to cytokinin accumulation in roots, xylem sap and shoots in maize (Takei *et al.* 2001b), suggesting that cytokinin serves to signal N availability from the root to shoot (Sakakibara *et al.* 2006). After defoliation under HN, a decrease was observed in the *t*Z-type cytokinin in the leaf sheaths and the iP-type cytokinin in the roots which was associated with increased *CKX* expression (Figs 2.11 & 2.12a,b). Interestingly, 1% glucose addition in defoliated HN plants induced iP and iPR accumulation in leaf sheaths and roots which was associated with a significant decline in expression of *LpCKX4* and *LpCKX6* in roots, implying that iP-type cytokinin might signal the availability of C and N metabolites in plants (Figs 2.11 & 2.12a,b).

By contrast, cZ-type cytokinins increased in the HN leaf sheaths, as did expression of the *LpRRs* 48 h after defoliation (Figs 2.11 & 2.13). Considerable amounts of *c*Z-type cytokinins have been found previously in, for example, rice (Izumi *et al.* 1988), maize (Veach *et al.* 2003) and ryegrass (Izumi *et al.* 1988; Veach *et al.* 2003; Roche et al. 2016). Several studies have demonstrated that *c*Z-type cytokinins can bind to cytokinin receptor kinases (CHKs), and activate the signalling cascade in plants (Yonekura-Sakakibara *et al.* 2004; Romanov *et al.* 2006; Lomin *et al.* 2011). The maize receptor *ZmHK1* and rice receptors, *OsHK3* and *OsHK4*, showed a similar binding affinity for *c*Z compared to tZ- and iP-type cytokinins (Yonekura-Sakakibara *et al.* 2004; Lomin *et al.* 2011; Choi *et al.* 2012). Additionally, *c*Z up-regulated the expression of a subset of rice response regulator family members (Kudo *et al.* 2012), and a maize response regulator (Yonekura-Sakakibara *et al.* 2004) with comparable activity to *t*Z. In this context, it is possible that the *LpRRs* could be responding to the *cis*-cytokinins with the downstream activation of N assimilation in the leaf sheaths. Consistently, while *c*Z-type cytokinins content declined, *LpRR* expression was reduced in roots following 6 h of 1% glucose addition (Figs 2.11 & 2.13). However, this decline of *c*Z also occurred in plants with 1% mannitol treatment (Fig. 2.11). The decreased *c*Z content under 1% mannitol

treatment was not consistent with salt or osmotic stress which is suggested to induce *c*Z (HavlovA *et al.* 2008; Vyroubalová *et al.* 2009; Macková *et al.* 2013). As the *LpRR* expression decreased under glucose treatment but not under mannitol treatment, a cytokinin response to mannitol is not supported. Taken together with the increased NO_3^- uptake rate, fructan levels and *RR* gene profiles under glucose treatment, the glucose supplement does indeed appear to cause a cytokinin response via its impact on carbon.

2.5. SUMMARY

In conclusion, the results of these experiments provide clear evidence that the rapid and large shifts in carbon storage triggered by defoliation had significant impact on nitrate uptake in an N-status dependent manner. Further, the evidence is provided that cytokinins are implicated as a possible coordinator of C and N metabolism and acquisition at the whole plant level. In addition to carbon, root development is another important factor that determines N uptake efficiency. In the following two chapters, how root system architecture responds to different N sources is investigated and the functional significance of root traits in N uptake is assessed.

Chapter 3-A comprehensive analysis of root morphological changes in *Brassica napus* in response to different nitrogen forms

3.1. INTRODUCTION

Root system architecture (RSA) is the three-dimensional arrangement of the root system, comprising aspects of root topology, morphology and distribution. This is shaped by the intrinsic genetic background in the plant species and environmental cues under field conditions (Lynch 1995; Malamy 2005). Root systems display a considerable degree of plasticity during plant development and growth in terms of elongation, branching and spacing to cope with fluctuating environments. In other words, plant root plasticity is a consequence of plant perception and integration of environmental messages into root development (Novoplansky 2002; Magyar *et al.* 2007). The overall RSA is modulated by not only local nutrient availability that elicits local signalling, but also the internal nutrient status of the plant that elicits systemic signalling (Giehl *et al.* 2014). To date, it has been established that N availability in the soil could elicit extremely sophisticated and complex responses in the root system (Krouk *et al.* 2011). Apart from their direct nutritional effect, some nutrient molecules can also function as signals which control plant development, for example nitrate, glutamate and phosphate (Martín *et al.* 2000; Sakakibara *et al.* 2006; Forde and Walch-Liu 2009; Ho *et al.* 2009a; Krouk *et al.* 2010).

Nitrate (NO_3^-) is a major nitrogen form used in agricultural systems. It has been shown to have a significant impact on RSA. By using a split root system in *Arabidopsis*, it has been established that localized NO_3^- supply stimulates lateral root (LR) growth rate but not lateral root initiation (Zhang and Forde 1998). LR elongation in a localized nitrate-enriched zone may be stimulated by the nitrate ion itself rather than assimilated products of nitrate, suggesting that a nitrate sensing pathway regulating root response is independent of its nutritional effects (Zhang *et al.* 1999). However, another study in *Arabidopsis* showed that localized nitrate supply induces LR initiation and elongation (Linkohr *et al.* 2002). These discrepancies could be explained by the differences in plant genotypes and experimental conditions. The stimulating effect on LR branching by localized nitrate is regulated by the *ANR1* gene, a member of the MADS-box family of transcription factors in plants. *NRT1.1*, a dual nitrate transporter, has also been identified to trigger preferential lateral root growth in response to localized nitrate supply (Remans *et al.* 2006). Apart from the LR response to external nitrate, LR branching is feedback-regulated by intrinsic N status of the plant. Several studies have suggested that LR development is suppressed by nitrate accumulation in shoots that then triggers a systemic signalling response (Scheible *et al.* 1997; Zhang *et al.* 1999). Although the mechanism for long distance signalling remains unknown, several studies have

proposed that plant hormones may be recruited for long distance signalling from the shoot to modulate LR outgrowth in response to external nitrate supply, such as cytokinins, auxin and abscisic acid (ABA) (Signora *et al.* 2001; Forde 2002a; Walch-Liu *et al.* 2006a; Kiba *et al.* 2011). While local NO_3^- supply stimulates LR elongation, another important N source, ammonium (NH_4^+), can induce LRs initiation and higher-order LR branching, suggesting distinct RSA responses to different nutrients (Lima *et al.* 2010).

In addition to inorganic N resources, organic N, including protein and amino acids, may provide N for plant growth. A high-affinity transporter, LYSINE HISTIDINE TRANSPORTER (LHT) has been identified in *Arabidopsis* (Hirner *et al.* 2006; Xu *et al.* 2012). Among the amino acids, L-glutamate is noteworthy due to its specific modulation of root growth and branching. It was found that root development specifically responded to the presence of external L-glutamate, implying a specific sensory mechanism for L-glutamate in plants (Sivaguru *et al.* 2003; Walch-Liu *et al.* 2006b). Although a family of Glu receptor-like genes (*GLR*) has been proposed as potential candidates for a Glu sensor in *Arabidopsis*, the underlying mechanism is still unknown (Walch-Liu and Forde 2007).

Improving N utilization efficiency is a priority to maintaining food production while alleviating the deleterious environmental effects of N. In this context, a comprehensive investigation of how root system architecture responds to variation of nitrogen supply is essential for further improving NUE. In this study, using a plate-culture system, the comprehensive morphological changes in root system architecture in response to different N sources and a wide range of N concentrations was investigated in *Brassica napus*. In parallel, the impact of N sources on RSA was also investigated in *Lolium perenne* using a germination paper culture system. Unfortunately, the paper system was not able to be successfully adopted in the time available due to technical difficulties (see Appendix 2), and so a decision was made to focus this analysis on *B. napus*.

3.2. PLANT MATERIAL AND METHODS

3.2.1. *B. napus* growth and treatments

Forage brassica*, B. napus* cv. Greenland, seeds were sterilized with 70% (v/v) ethanol for 5 min, then with 0.5% SDS for 15 min, and then rinsed five times in sterile water. Surface sterilized *B. napus* seeds were germinated in petri dishes (120 × 120 mm) containing N-free ½ x MS medium (Caisson Laboratories, USA) for 24 h in the dark at 22 °C, and then

transferred to light for 24 h. The nutrient composition of ½ x MS medium is available at the online website of Caisson Laboratories, USA. The pH of treatment solutions was maintained at 6.0. Two days after germination, uniform seedlings were selected and transferred to a transparent plate with a hole on the top on solid MS medium containing different nitrogen sources (KNO_3, $(NH_4)_2SO_4$ and glutamate) or without nitrogen as control. The seedlings were treated with NO_3^- (0.5, 5 and 10 mM), NH_4^+ (0.5, 5 and 10 mM) and glutamate (0.01, 0.05 and 0.1 mM). To achieve the desired N concentrations, KNO_3 (0.5, 5 and 10 mM), and $(NH_4)_2SO_4$ (0.25, 2.5 and 5 mM) were applied to the medium, respectively. In order to avoid disruption from light, the traditional phytogel plate-culture system was improved by making a hole on one side of each plate and covering the whole surface of the plate with aluminium foil, so that the emerging shoots were not in direct contact with the medium and the roots were shielded from the light (Fig. 1a, b). The plates were placed vertically in a growth chamber at 22 °C under a 16/8 h photoperiod.

3.2.2. Morphometric analyses of exploratory root system

At Day 8 after transfer to ½ x MS medium with different N sources (10 dpg), root length, lateral number, lateral root density, root angle and root exploration area were analysed using RootNav (Pound et al. 2013). Shoot and root dry weights were subsequently measured. The lateral root density (LRD) is defined as the number of emerged LRs per unit length within the root branching zone (the zone that extends from the shoot base to the youngest emerged LR (Dubrovsky and Forde 2012)). The convex hull area [i.e. the area that encompasses all root material belonging to a given plant as defined by Pound et al. (2013)] was measured using RootNav, and is referred to as the root exploration area. The root growth angle is defined as the angle of emergence of the first LR, calculated relative to the primary root to which it is attached (Pound et al. 2013).

3.2.3. Statistical analysis

For morphometric analysis of roots grown in different N treatments, 20 independent seedlings per treatment were tested and the values presented are the mean ± SE. Statistical analyses were performed on GraphPad Prism statistical software version 7.00. Differences between means were tested for significance using ANOVA. Tukey's multiple comparisons test was used in the analysis.

3.3. RESULTS

3.3.1. High-throughput 2-D root system architecture phenotyping platform

RSA is a complex developmental trait involving many signals. In order to avoid the light-induced morphological and physiological response affecting the whole plant growth, an existing solid agar vertical-plate system were modified to allow roots to be shielded from light without sucrose addition and the emerging shoot to be grown without direct contact with medium, thereby mimicking more closely the environmental conditions in nature (Fig.3.1A, B). For root phenotyping, a 2D vertical plate system coupled with the recently developed package RootNav was used in this study (Pound *et al.* 2013). A flatbed scanner was used to non-destructively acquire images of seedling roots grown on an agar surface (Fig. 3.1C). Once captured, the images were analysed efficiently by RootNav (Fig. 3.1D). To evaluate this root software, the result obtained 20 manually measured architectures by RootNav and Image J was compared. The comparison demonstrated that RootNav is an efficient, user-friendly and accurate tool for high-throughput RSA phenotyping analysis (Fig. 3.2).

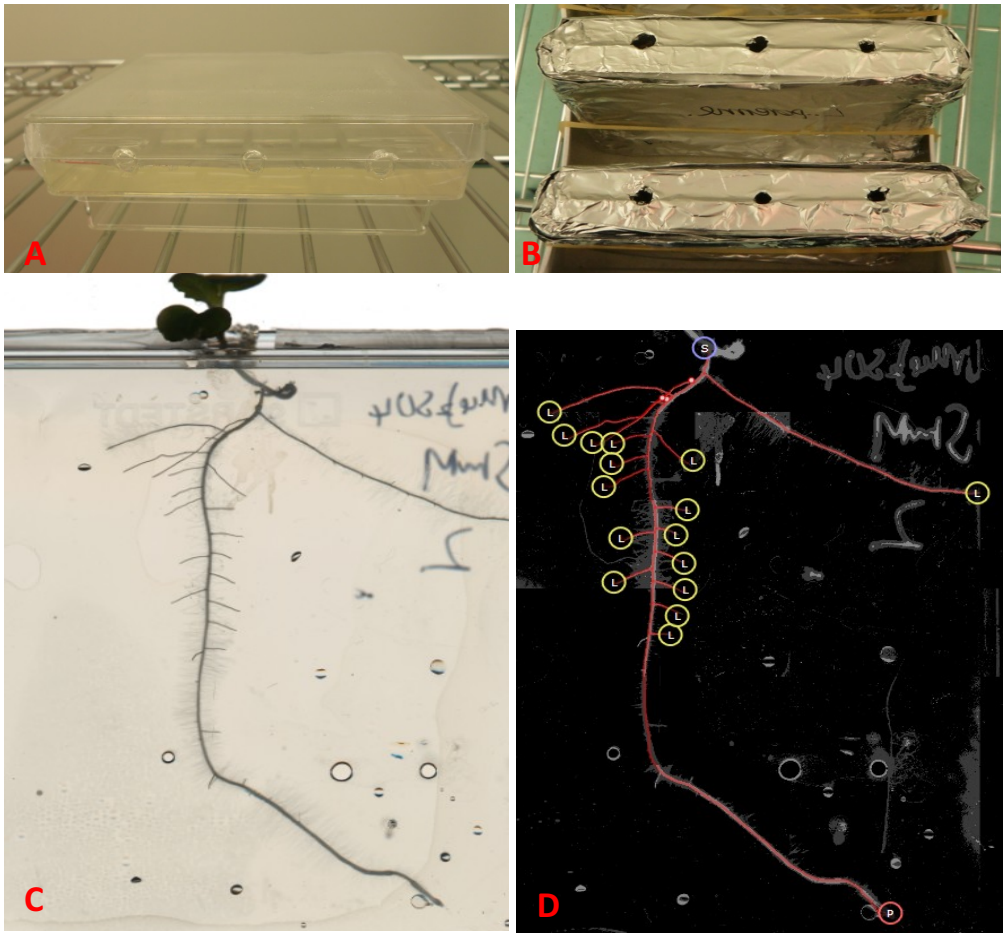

Fig 3. 1 High-throughput 2-D root system architecture phenotyping platform.

(A) and (B): The phytogel-plate culture system for studying root growth of *B. napus*. (A) Side view of the plate. (B) Vertical plates with the whole surface covered with aluminium foil. (C) and (D): An image of a *B. napus* root growing on phytogel captured by flatbed scanner (C) and analysed by RootNav (D).

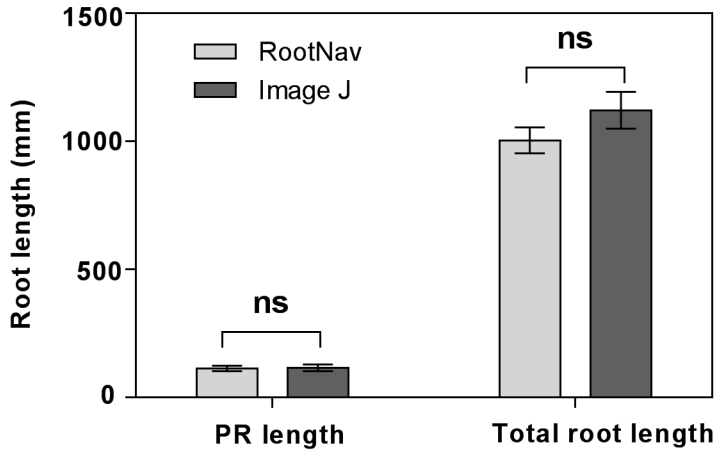

Fig 3. 2 The comparison of primary root length and total root length in *B. napus* measured by RootNav and Image J, respectively.

To assess the accuracy of RootNav, 10-days-old B. napus seedlings grown in N-free medium were analysed using RootNav and Image J, respectively. Values are mean ± SE of 20 plates with one seedling per plate.

3.3.2. Morphological responses of *B. napus* root system architecture to NO_3^-

In the growth conditions, visible LR development started at Day 2 after transfer (4 dpg). At Day 8 after transfer (10 dpg), the primary root (PR) length, lateral root (LR) density (number of emerged LR mm^{-1} primary root), LR branching zone (the zone that extends from the shoot base to the youngest emerged LR), root growth angle, root exploration area (the physical square of root occupied in the plates) and root/shoot dry biomass were analysed. Distinct differences were observed in the RSA of seedlings treated with different nitrate concentrations. Representative examples are shown in Fig. 3.3. Broadly, the seedlings supplied with 0.5 mM nitrate appeared to have a wider and more branched root system, while the root system of seedlings with 10 mM nitrate exhibited a relatively narrow and less branched root system (Fig. 3.3). Quantitatively, total root length, LR density and root exploration area decreased with increasing external NO_3^- concentrations from 0.5 mM to 10 mM, confirming the inhibitory effect of high NO_3^- concentration (>5 mM) on LR growth (Fig. 3.4). Interestingly, LR density and total root length were greater in 0.5 mM KNO_3 treatments than in the 0 mM KNO_3 treatments (as controls). In addition, the lateral root branching zone was shorter at high NO_3^- concentration (10 mM) relative to the other NO_3^-treatments. In contrast, the root and shoot biomass was much greater in the high NO_3^- (5 mM and 10 mM) treatments relative to 0.5 and 0 mM NO_3^- treatments, while root weight percentage was reduced with increasing concentration of NO_3^- (Fig. 3.4). However, within these various NO_3^- treatments, the primary root length and root angle did not change significantly (Fig. 3.4).

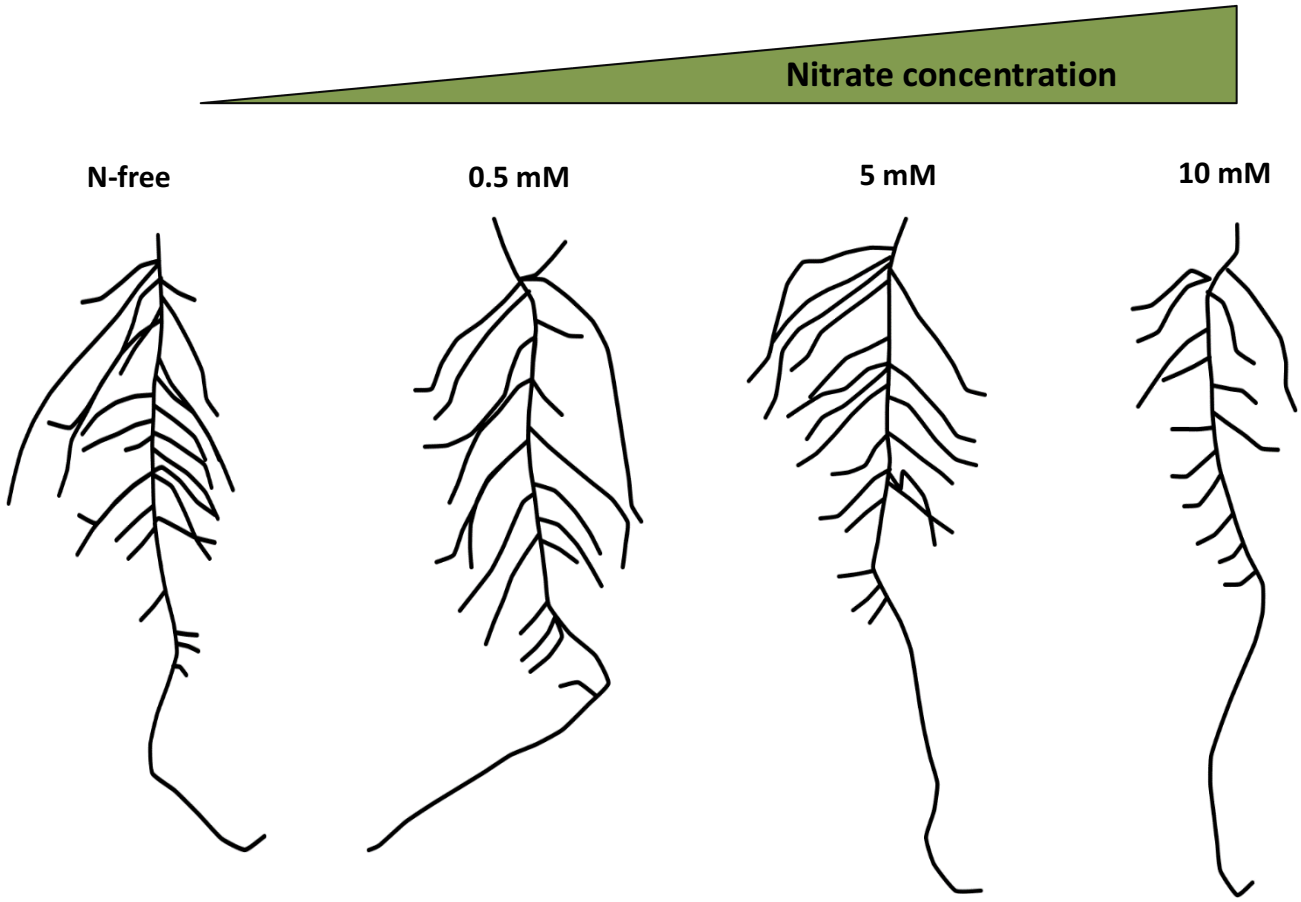

Fig 3. 3 RSA of representative 10-day-old *B. napus* seedlings in response to nitrate availability.

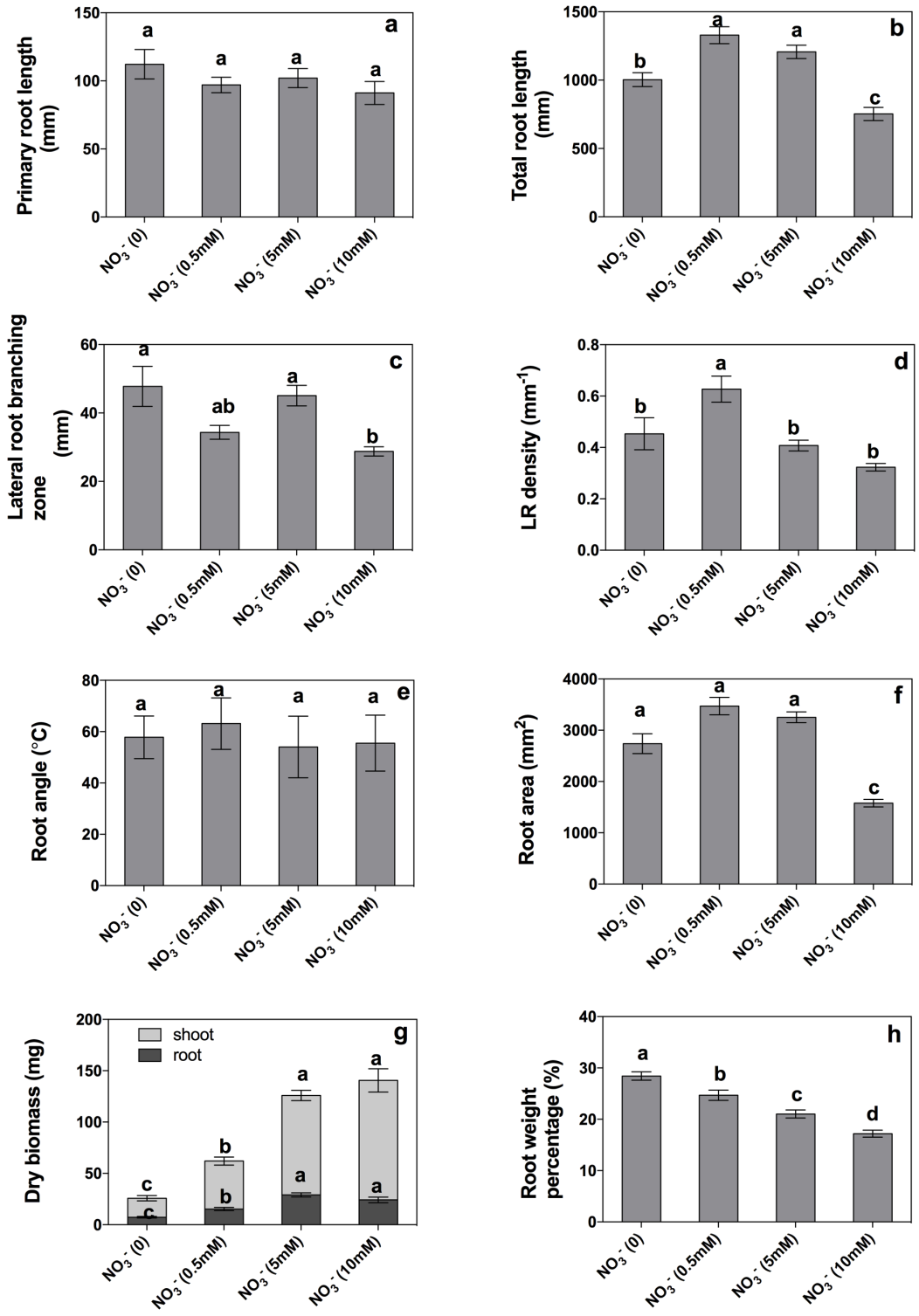

Fig 3.4 The effect of different NO_3^- concentrations on *B. napus* roots

The effect of different NO_3^- concentrations on *B. napus* primary root length, total root length, lateral root branching zone (the zone that extends from the shoot base to the youngest emerged LR), lateral root density (number of emerged LR mm^{-1} primary root), root angle, root exploration area (the physical square of root occupied in the plates), shoot and root dry

biomass, and root weight percentage (the percentage of root dry weight to total plant dry weight), respectively. Values are mean ± SE of 20 plates with one seedling per plate.

3.3.3. Morphological response of *B. napus* root system architecture to NH_4^+ supply

Changes in root traits of *B. napus* seedlings treated with different NH_4^+ concentrations were observed during an 8 d treatment. Representative examples are shown in Fig. 3.5. Quantitatively, with increasing NH_4^+ concentration from 0.25 mM to 5 mM, primary root length, total root length, LR branching zone, LR density and root exploration area were reduced (Fig. 3.6). The root angle did not change significantly in different NH_4^+ concentrations. In addition, the dry biomass of roots was greater in 0.25 mM NH_4^+ treatments while the dry biomass of shoots was greater in 2.5 mM NH_4^+ treatments. However, the root weight percentage was much less in the 2.5 and 5 mM NH_4^+ treatments than in the 0.25 mM NH_4^+ treatment (Fig. 3.6).

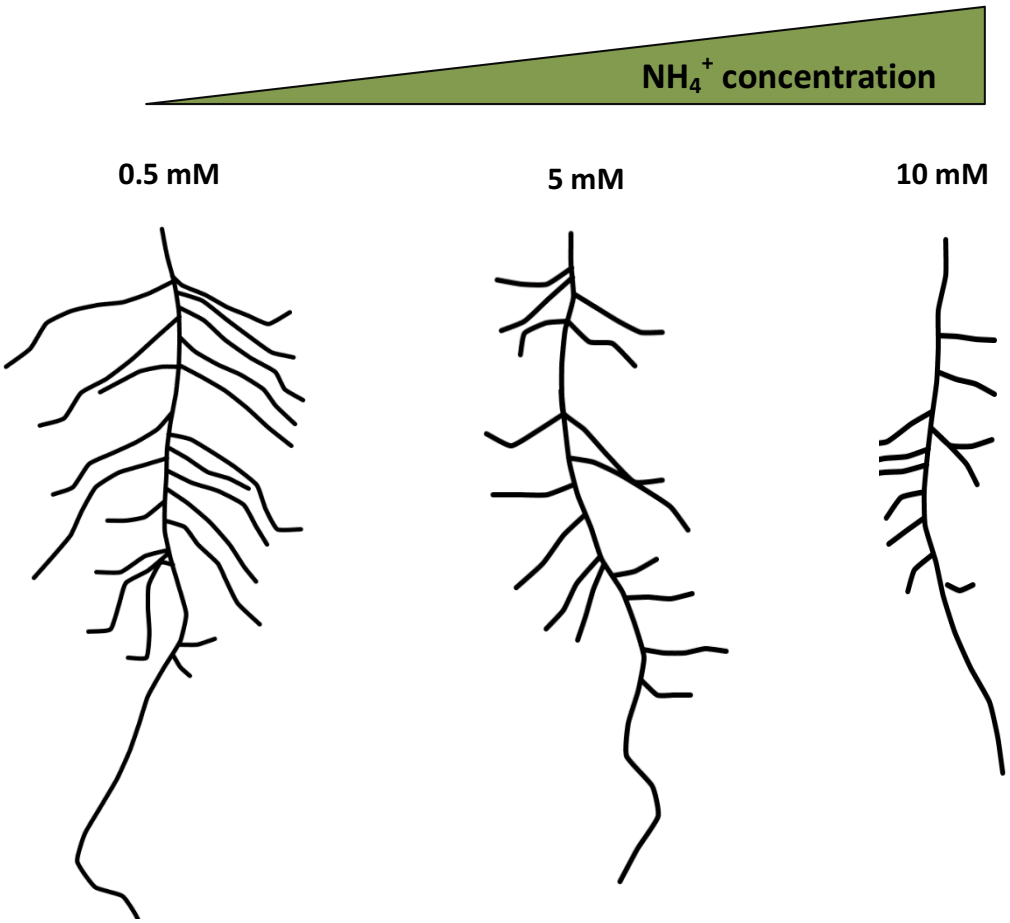

Fig 3. 5 RSA of representative 10-day-old *B. napus* seedlings in response to NH_4^+

.

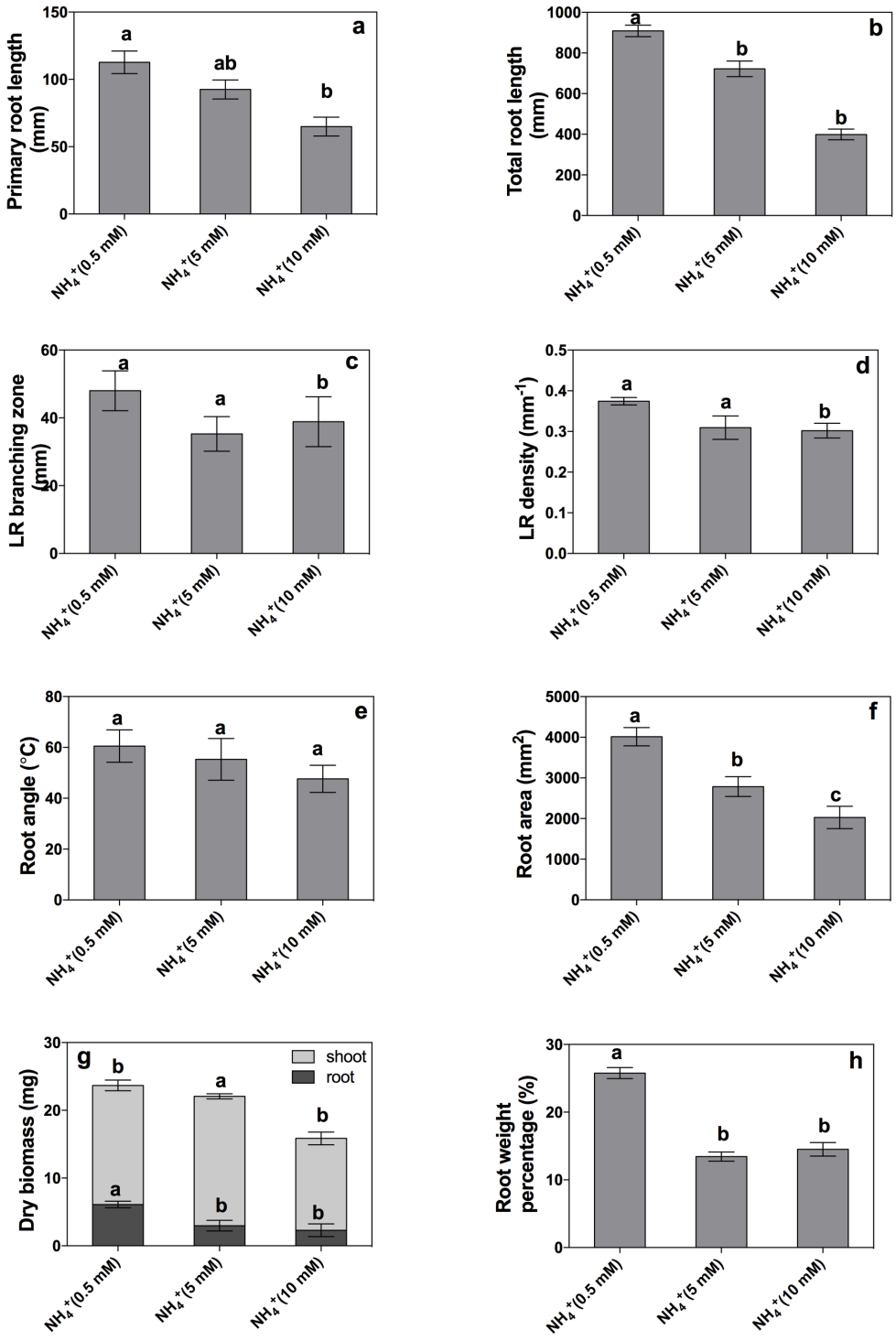

Fig 3. 6 The effect of different NH_4^+ concentrations on 10-day-old *B.napus*

The effect of different NH_4^+ concentrations on 10-days *B.napus* primary root length, total root length, lateral root branching zone, lateral root density, root angle, root exploration area, shoot and root dry biomass, and root weight percentage, respectively. Values are mean ± SE of 15 plates with one seedlings per plate.

3.3.4. The morphological responses of *B. napus* root system architecture to L-glutamate

After eight days growth, *B. napus* plants displayed significant differences in root traits between treatments with various concentrations of L-glutamate from 0.01 mM to 0.1 mM as representative examples show in Fig.3. 7. With an increasing concentration of L-glutamate, primary root length, total root length and root exploration area were reduced relative to control treatments (0 mM L-glutamate) (Fig. 3.8). LR branching zone was slightly reduced in 0.05 and 0.1 mM L-glutamate treatments compared to the control, whereas LR density did not changed significantly relative to the control, with exception of the 0.05 mM treatment (Fig. 3.8). Despite a slight increase in dry biomass of both root and shoot in the highest L-glutamate concentration (0.1 mM), there was no change observed in root weight percentage between these L-glutamate treatments. Similarly, no significant difference in root angle was shown across treatments (Fig. 3.8).

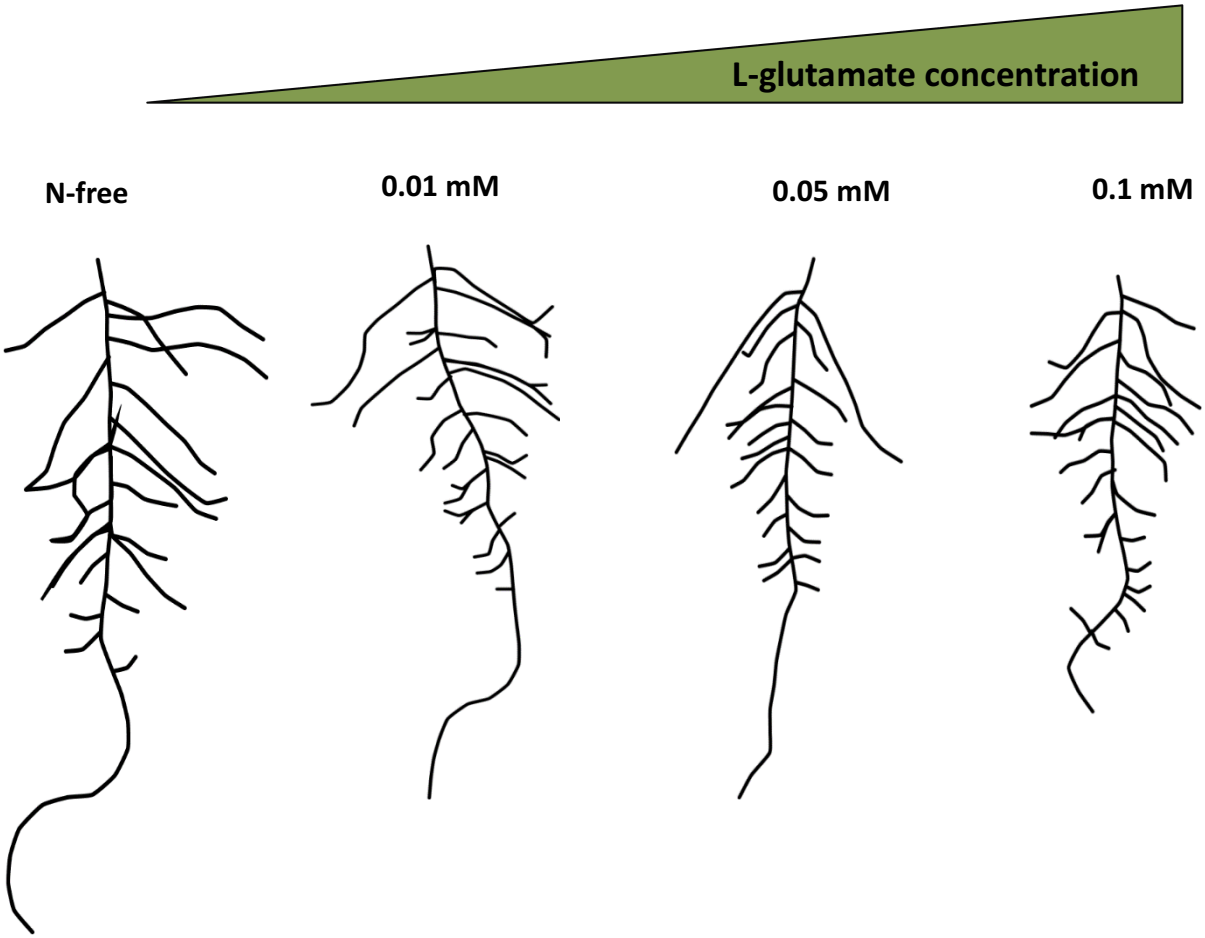

Fig 3. 7 RSA of representative 10-day-old *B. napus* seedlings in response to L-glutamate supply

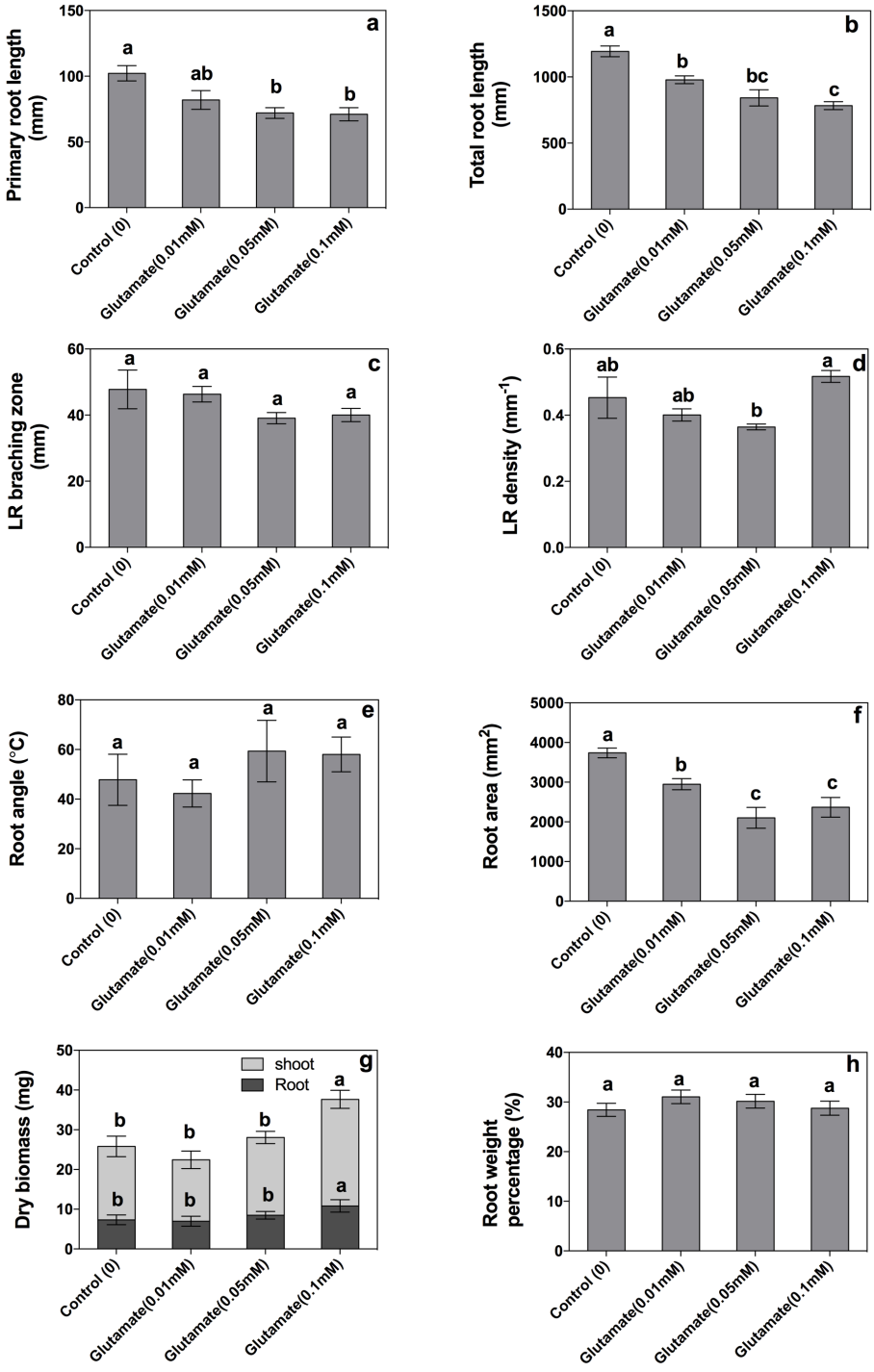

Fig 3.8 The effect of different L-glutamate concentrations on 10-day-old *B. napus*

The effect of different L-glutamate concentrations on 10-day-old *B. napus* primary root length, total root length, lateral root branching zone, lateral root density, root angle, root exploration area, shoot and root dry biomass, and root weight percentage, respectively. Values are mean ± SE of 15 plates with one seedlings per plate.

3.4. DISCUSSION

To conveniently explore physiological and molecular mechanisms in roots in response to environmental signals, cultivation of seedlings in transparent petri dishes with agar has been used in numerous previous laboratory experiments. However, as several photoreceptors have been shown to express and be active in roots, it is not surprising that exposure of plant roots to light induces morphological and physiological response affecting the whole seedling (Yokawa *et al.* 2011; Burbach *et al.* 2012). Light can stimulate root elongation in *Arabidopsis* roots via root-localized photoreceptors and this induced root elongation may be a root response to a light signal (Costigan *et al.* 2011; Wan *et al.* 2012). In addition to illumination, exposure of plant roots to the sucrose typically used in culture systems also affects root growth and response (Lei *et al.* 2011). Recent studies have confirmed that such cultivation systems lead to artificial perturbations in terms of root growth and response to environmental signals (Xu *et al.* 2013; Yokawa *et al.* 2013; Novák *et al.* 2015). Novák *et al.* (2015) reported that cultivation in transparent vertical-plates may interfere with nutrient sensing and uptake in *Arabidopsis*. This showed that shading roots by covering petri dishes with a layer of aluminium foil reduced the root to hypocotyl ratio and induced root hair elongation relative to illuminating roots in transparent petri dishes. The cytokinin receptor AHK3 was reported as the major mediator of root to hypocotyl signalling in response to root illumination (Novák *et al.* 2015). In this context, solid media vertical-plate culture system was modified to allow roots to be shielded from lights without sucrose addition and the emerging shoot to be grown without direct contact with medium, thereby mimicking more closely to the environmental conditions in nature. Coupling with the RootNav package, this improved the plate-culture system and allowed to investigate RSA plasticity in response to N availability.

Although similar studies have been reported in model species, such as *Arabidopsis*, comprehensive investigation of modifications of root system architecture in *B. napus* responding to N availability have not yet been presented in detail. N deficiency was shown to induce the growth of a more exploratory root system with greater lateral root length in *B. napus*, which is in agreement with the previous findings for *Arabidopsis* (López-Bucio *et al.* 2003). The reason for this effect in the present study was that low nitrate induced greater total root length and lateral root density (Fig. 3.4). The application of 0.5 mM NO_3^- induced more branching in the root system relative to the treatments with higher N concentrations (5 mM and 10 mM). This observation is consistent with the findings that addition of 0.55 mM N to N-deficient *Arabidopsis* seedlings resulted in greater total root length and average LR length

compared to the addition of higher N concentration (11.4 mM) (Gruber *et al.* 2013). Gruber et al (2013) also reported that primary root length decreased with the increasing the N concentration from 0.55 mM to 11.4 mM, but this was not observed in the present study (Fig. 3.4). Hormones are proposed to be involved in the regulatory mechanisms involved in the responses to changing N availability. Under mild N deficiency, the accumulation of auxin in non-emerged LR primordia leads to LR growth in *Arabidopsis* (Krouk *et al.* 2010). The accumulation is associated with up-regulation of the expression of the auxin biosynthesis gene *TRYPTOPHAN AMINOTRANSFERASE RELATED 2* (*TAR2*) in the root pericycle cells (Ma *et al.* 2014). In maize, it has been reported that the inhibition of lateral root elongation and initiation by high nitrate concentration was associated with decreased IAA levels in roots (Tian *et al.* 2008). From the available transcriptome data for *Arabidopsis*, it is clear that several root development related genes may be induced by N limitation. Both the shootward auxin transporter MULTIDRUG RESISTANCE 4/P-GLYCOPROTEIN 4 (MDR4/PGP4) and the WALL ASSOCIATED KINASE 4 (WAK4) induce PR and LR growth, and are responsive to mild N limitation (Lally *et al.* 2001; Terasaka *et al.* 2005). Members of the *CLAVATA3/ESR-RELATED* (*CLE*) gene family are also involved in the regulation of the LR system in response to N deficiency in *Arabidopsis*. N deficiency stimulated the expression of *CLE1*, *3*, *4* and *7* in the root pericycle cells, whereas the overexpression of these genes reduced LR growth (Araya *et al.* 2014).

Interestingly, total root length and LR density was increased in plants grown under low nitrate concentration (0.5 mM) relative to N-free medium, suggesting that plants are able to use different strategies in root modification in response to the amount of nitrate (Giehl and von Wirén 2014). Several studies reported that the expression of *AUXIN RESISTANT* (*AXR5*) and *ARABIDOPSIS CRINKLY 4* (*ACR4*), which are involved in LR formation, are down-regulated under severe N limitation, suggesting the reduction of LR formation under severe N deficiency (Yang *et al.* 2004; De Smet *et al.* 2008). These results indicated that LR production and development are behaviours which combine not only genetic variations but also environmental factors (Ruffel *et al.* 2011). The effective root exploration area decreased with the increasing NO_3^- concentration, which means N deficiency led to greater exploratory area by roots. These data are consistent with the greater total root length and LR density observed in low NO_3^- treatments.

As expected, sufficient N stimulated shoot growth, with dry biomass being considerably greater in 5 mM and 10 mM NO_3^- treatment than in 0 and 0.5 mM NO_3 treatments (Fig. 3.4).

Although N deficiency elicited a root system that proliferated more and had longer lateral roots that could explore more unavailable nutrient resource, the dry biomass of roots was much less than in the N sufficient treatments. It is clear that low N stimulates thinner and longer LRs to account for the economic trade-off between nutrient acquisition and utilization. This is consistent with observations in maize that low nitrogen stress decreased the size of cortex and stele, resulting in much thinner crown roots (Gao *et al.* 2015). The proportion of biomass allocation occupied by roots, however, was greater in low NO_3^- treatment relative to high NO_3^- treatments (Fig. 3.4), reflecting the fact that plants invested more resources in their roots when nutrient uptake from the environment was limited (Paul and Driscoll 1997; Scheible *et al.* 1997; Martin *et al.* 2002). These observations suggest that plants are able to cope with N shortage by modifying the allocation of resource to root and root system architecture to efficiently explore the limited nutrients in the soil. The molecular mechanisms by which plants respond to N limitation by biomass allocation have previously been investigated. Analysis of *Arabidopsis* microarray data showed that N limitation induced transcriptional changes in genes that are involved in the accumulation of sugars and starch (including starch metabolism, glycolysis and disaccharide metabolism) in shoots and the increased translocation of sucrose to the root. (Scheible *et al.* 1997; Scheible *et al.* 2004). Sugars mat be involved in the regulatory mechanism influencing carbohydrate partitioning between source and sink tissues in response to N deficiency (Fischer *et al.* 1998).

Root elongation was suppressed with increasing concentration of $(NH_4)_2SO_4$. The primary root length was greater in low $(NH_4)_2SO_4$ supply (0.25 mM) relative to high $(NH_4)_2SO_4$ supply (2.5 mM and 5 mM), a finding which is in agreement with previous observations that high ammonium concentration may arrest primary root development (Li *et al.* 2010b; Liu *et al.* 2013). The total root length and lateral root density were also largely reduced in 5 mM $(NH_4)_2SO_4$, suggesting that LR elongation and branching were inhibited by high NH_4^+ concentration. Unlike the effect of NO_3^- on biomass allocation, the dry biomass of roots in low NH_4^+ was much greater than in high NH_4^+, while shoot biomass was much less in high NH_4^+ condition relative to low NH_4^+, demonstrating the toxic effect of high NH_4^+ on plant metabolism and flow-on effects on plant growth (Givan 1979; Britto and Kronzucker 2002; Krupa 2003). Taken together, these results indicated that NH_4^+ toxicity usually leads to a stunted root system in most plants, whereas a low concentration of NH_4^+ is an optimal nitrogen resource for plant growth (Kronzucker *et al.* 2000; Kronzucker *et al.* 2001; Balkos *et al.* 2010).

Glutamate plays a critical role in amino acid metabolism in plants. The regulation of root growth and development by glutamate is independent of its nutritional role (Walch-Liu and Forde 2008; Forde and Walch-Liu 2009). Previous studies have reported that only micromolar amounts of exogenous L-glutamate can inhibit primary root growth in *Arabidopsis* (Walch-Liu *et al.* 2006a). Similarly, in *B. napus*, increasing the concentration of L-glutamate from 0.01 mM to 0.1 mM suppressed primary root length, whilst the LR branching zone did not change in the different L-glutamate treatments (Fig. 3.8), possibly explaining why the LR density was slightly increased in the high L-glutamate treatment (0.1 mM). Total root length and root exploration area, however, was reduced in the relatively high L-glutamate conditions. These results suggested that L-glutamate even at micromolar level could arrest primary root growth and LR branching in plants. Several studies suggested that the effect of L-glutamate on root development is highly specific. No similar effects were observed with the structurally related amino acids aspartate, ɤ-aminobutyric acid (GABA) and D-glutamate (Walch-Liu *et al*. 2006). This effect on PR growth was occurred only when the root tip directly contacted with L-glutamate (Walch-Liu *et al*. 2006). These evidences suggest that L-glutamate could serve as an external signal to regulate root development and growth. Although the mechanism underpinning L-glutamate signalling is still unknown, it has been proposed that the mGluR family is prabobly involved in sensing glutamate in plants (Forde and Lea 2007).

3.5 SUMMARY

Using RootNav to capture information on RSA from *B. napus* displayed the convenience and effectiveness of the tool. The PR length and total root length results were consistent with the manual measures using Image J. Root analysis using RootNav was found to be much easier and faster than manual methods that produced similar results, demonstrating that RootNav is applicable, accurate and user-friendly in high-throughput RSA phenotyping analysis. Coupling with the RootNav package, the improved plate-culture system allowed an investigation of RSA plasticity in response to N availability. This high-throughput 2-D RSA phenotyping platform provided a chance to investigate the functional significant of root system architecture in *B.napus*. By using the improved plate culture system and RootNav tool, this study provided a systematic comparison of root system plasticity in response to different N forms and concentrations. This should provide basic understanding which is necessary for improving nitrogen use efficiency in forage brassica breeding.

In conclusion, external N availability induced changes in the overall root morphology, with root elongation decreasing under an extremely N impoverished environment, but increasing under relatively mild N deficiency (for both NO_3^- and NH_4^+). This implies that plant roots can finely employ different strategies to cope with N availability. The results in this chapter confirm that plants alter root system architecture in response to N availability. In the following chapter, I extend this analysis by assessing the functional significance of differences in RSA in terms of their impact on N uptake.

Chapter 4- Insights into the functional relationship between cytokinin-induced root system phenotypes and nitrate uptake in *Brassica napus*

4.1. INTRODUCTION

In the agricultural system, nitrate (NO_3^-) is the major form of applied nitrogen (Miller and Cramer 2005). As plants acquire NO_3^- though roots from the soil, root system architecture and uptake capacity are the main determinants of N acquisition efficiency (Kiba and Krapp 2016). Root system architecture (RSA) is described by the rate of growth, angle within the soil and type and placement of individual roots contributing to the root system. In broad terms, the root system can be divided into the exploratory root system, comprising primary roots (PRs), and the exploitative root system, comprising lateral roots (LRs) and root hairs. Lateral roots are fully post-embryonic events co-ordinated by intrinsic genetic background and environmental cues, reflecting a plastic plant adaptation to environmental variation (Péret *et al.* 2009; Giehl *et al.* 2014). Overall root morphology is affected by both exogenous nutrient availability and the internal nutrient status of the plant (Giehl and von Wirén 2014). Taking nitrogen as an example, low N availability may induce a greater exploratory root system with longer PR and LRs in order to increase root foraging for nutrients (Linkohr *et al.* 2002; López-Bucio *et al.* 2003; Gruber *et al.* 2013). In contrast, with a heterogeneous NO_3^- supply, LR elongation may be induced by local NO_3^- availability within a NO_3^--containing patch, whereas the growth of lateral roots in N limited patches may be repressed by systemic signals reporting the N status within the plant (Zhang and Forde 1998; Remans *et al.* 2006; Ruffel *et al.* 2011). The modification of RSA, controlled by co-ordinating local nitrate signals and systemic signals, enables plants to forage for sparingly available resources with more efficiency (Zhang *et al.* 1999; Forde 2002a). In terms of root function, fine roots (crucial for the acquisition of soil resources in perennial plants) can be divided into two classes: absorptive fine-roots and transport fine-roots (McCormack *et al.* 2015). Absorptive fine-roots are the distal roots which function in water and nutrient acquisition and uptake, whilst transport fine roots represent the higher-order branching roots that are involved in anchoring the plant to the soil and which also fulfil transport functions (McCormack *et al.* 2015). In this context, a comprehensive understanding of root morphology and functionality is needed to achieve the greatest impact on improving NUE.

Cytokinins negatively regulate PR elongation and LR formation (Medford *et al.* 1989; Hewelt *et al.* 1994; Li *et al.* 2006a). Cytokinins can exert a significant impact on RSA by antagonising auxin in the root meristem during early embryogenesis (Del Bianco *et al.* 2013). Application of exogenous cytokinins or overexpression of the bacterial gene ATP/ADP isopentenyltransferases (*IPT*) in *Arabidopsis*, which controls the rate-limiting step of

cytokinin biosynthesis, can lead to inhibited root growth and reduced root meristem activity (Ioio *et al.* 2007; Kuderová *et al.* 2008). In contrast, cytokinin deficiency, achieved by overexpression of cytokinin oxidase/dehydrogenase (*CKX*), may induce greater root meristem activity (Werner *et al.* 2003; Ioio *et al.* 2007). In addition, higher order *ipt* mutants and higher order signalling *ahk* mutants have been shown to induce root growth and branching (Higuchi *et al.* 2004; Miyawaki *et al.* 2006). However, it has been established that cytokinins mediate the rate of meristematic cell differentiation at the transition zone (TZ) to determine root meristem size via the cytokinin two-component signalling pathway (Ioio *et al.* 2007). Furthermore, plants may recruit hormone signals regulating RSA in response to environmental cues, including NO_3^-. Using a split-root experimental framework, a NO_3^--cytokinin relay has been proposed to mediate a shoot-root systemic N signal controlling LR growth (Ruffel *et al.* 2011). This indicates that a cytokinin modulation of lateral root organogenesis, together with a cytokinin-nitrate feedback loop, attenuates nitrate uptake in response to N satiety (Ruffel *et al.* 2011; Marhavý *et al.* 2014).

In addition to RSA, NO_3^- uptake ability is also a major determinant of plant nitrate acquisition. NO_3^- levels in the soil can fluctuate by more than four orders of magnitude (Crawford and Glass 1998). Consequently, plants have evolved two types of membrane transport systems to cope with fluctuations in soil nitrate, one involving high-affinity transporters (HATS), and the other involving low-affinity (LATS) transporters. The HATS operate at low external nitrate levels (<250 μM), whereas LATS operate at high external nitrate concentrations (>1 mM) (Siddiqi *et al.* 1990;Tsay *et al.* 1993; Huang *et al.* 1999a). Nitrate uptake kinetics determine the rate of NO_3^- absorption by a localized root segment. In maize, nitrate uptake kinetics depends on root class (seminal, lateral, crown, or brace), plant age and nitrate deprivation time (York *et al.* 2016).

Michaelis-Menten kinetics are generally used to define root nutrient uptake capacity. The Michaelis-Menten kinetic parameters, V_{max} and K_m, describe the relationship between uptake rate and external NO_3^- concentration. This mathematical expression is based on the assumption that transporters (enzymes) are actively involved in the NO_3^- uptake process. Genes that encode nitrate transporters have been identified and constitute two families: *NRT1* and *NRT2*. Among them, *NRT1.1*/*CHL1* and *NRT1.2*, and three *NRT2* transporters, *NRT2.1*, *NRT2.2* and *NRT2.4*, have been identified as molecular components of nitrate uptake in roots (Tsay *et al.* 1993; Huang *et al.* 1999a; Kiba *et al.* 2012; Wang *et al.* 2012b). In addition, several *NRT* transporters are involved in the regulation of long-distance NO_3^- transport

between roots and shoots (Wang and Tsay 2011b; Han *et al.* 2016). It has been confirmed that *NRT1.5* is responsible for nitrate loading into the xylem while *NRT1.8* is responsible for NO_3^- removal from the xylem sap (Lin *et al.* 2008a; Li *et al.* 2010a).

This study investigated functional aspects of RSA with respect to N acquisition and internal resource investment in *Brassica napus*. Forage brassica cultivars are grown in a wide range of environments as a supplement for grazing animals when ryegrass growth is limited during early summer to late winter due to drought and low temperature (de Ruiter *et al.* 2009; Hampton *et al.* 2012). *Brassica napus* provides the main supply of nutrients in winter for grazing cows and sheep in New Zealand agriculture (Hampton *et al*. 2012). I first characterized morphological and molecular phenotypes induced by exogenous cytokinin and antagonist treatments. The compound PI-55 [6-(2-hydroxy-3-methylbenzylamino) purine] is structurally close to 6-benzylaminopurine (BA), and can competitively inhibit the binding activity of natural *trans*-zeatin to the *Arabidopsis* cytokinin receptors CRE1/AHK4 through substitutions at specific positions within the aromatic side chain of BA (Spíchal *et al.* 2009). This mechanism allows us to pharmacologically generate morphological and molecular phenotypes of functional interest.

Using the improved culture system and the high-throughput 2-D RSA phenotyping platform, I assessed the relationship between RSA (composed of primary roots and lateral roots) and N uptake, by determining the nitrate uptake rate, N translocation from root to shoot, C allocation and the expression of nitrate transporter genes. The hypothesis is that the phenotypes with contrasting root traits in the pharmacological treatments would lead to functional differences in relation to N acquisition.

4.2. MATERIAL AND METHODS

4.2.1. Plant materials

Forage brassica*, Brassica napus* cv. Greenland, seeds were sterilized with 70% ethanol for 5 min, then with 0.5% SDS for 15 min, followed by five rinses in sterile water. Surface sterilized *B. napus* seeds were germinated in Petri dishes (120 × 120 mm) containing normal ½ MS (Caisson Laboratories, USA) for 24 h in the dark at 22 °C, and then transferred to a growth chamber under 16/8 h photoperiod for 24 h. The germinated seedlings were selected and transferred into plates containing phytogel-solidified ½ MS containing either PI -55 (0.05,

1 or 10 µM), BA (0.005, 0.1 or 1 µM), or a combination of both. A phytogel-plate culture system for studying root growth and response of *Brassica napus* was developed by making two holes on one side of each plate and covering the whole surface of the plates with aluminium foil, so that the emerging shoots were not in direct contact with the medium and the roots were shielded from the light. All the treatments were supplied with KNO_3 (1 mM) as sole N source. The plates were placed vertically in a growth chamber at 22 °C under 16/8 h photoperiod.

4.2.2. Morphometric analyses of exploratory root system

A 2D vertical plate system coupled with the recently developed package RootNav was used to analysis root phenotypes (Pound *et al.* 2013). A flatbed scanner was used to non-destructively acquire images of seedling roots grown on the phytogel surface. Once captured, the images were analysed by RootNav

4.2.3. Net $K^{15}NO_3$ uptake and isotope analysis and carbon content measurement

B. napus seedlings were grown in plates containing phytogel-solidified 1/2 x MS containing either 10 uM PI -55, 1 uM BA, or a combination of both. The plant growth medium was supplemented with KNO_3 (^{15}N atom %: 0.8%) for measurement of net uptake of nitrate. Plant samples were harvested at 24, 48, 72 and 96 h after treatment, respectively. At sampling time, seedlings were rinsed with 0.1 mM $CaSO_4$ for 1 min. Shoots and roots were separated, and freeze dried for 3 d. Total N and ^{15}N in the samples harvested at each time point (24, 48, 72 and 96 h) were determined with an isotope ratio mass spectrometer (Waikato University, New Zealand). The calculation was used as described by Hayes (2004). The cumulative ^{15}N uptake was calculated as ^{15}N content obtained by roots over 96 h of treatments. The ^{15}N uptake rate after 96 h was averaged rate over the entire 96 h and calculated as nmol h^{-1}. root cm^{-1}.

The total C content in both roots and shoots of the samples harvested at 96 h after treatments was measured by Waikato University, New Zealand. The percentage of C distribution in roots was determined as the proportion of C content in roots to that in the total plants (roots and shoots).

4.2.4. Michaelis-Menten kinetics experiment

B. napus seedlings were grown in plates containing phytogel-solidified ½ MS containing either 10 uM PI -55, 1 uM BA, or a combination of both. All treatments were supplied with 0.01, 0.05, 0.1, 1 or 5 mM KNO_3 (^{15}N atom %: 0.8%) as sole nitrogen source. The experiment was repeated three times independently. Each experiment included 10 plates per treatment, and each replicated plate included two seedlings. All the plates were placed vertically in a growth chamber at 22 °C under 16/8 h photoperiod. After 96 h, seedlings were rinsed with 0.1 mM $CaSO_4$ for 1 min. Shoots and roots were separated, and freeze dried for 3 d. Total N and ^{15}N in the samples were determined with an isotope ratio mass spectrometer (Waikato University, New Zealand). The Michaelis-Menten parameters were obtained by GraphPad Prism statistical software version 7.00.

4.2.5. RNA isolation and cDNA synthesis

For gene expression analysis, total RNA was extracted from up to 100 mg of frozen samples using RNase Plant Mini Kit (Qiagen, Germany), following the manufacturer's protocols. Then total RNA was incubated in DNase I Set (Qiagen) before integrity and quality checking by running on a 1% (w/v) agarose gel. The concentration and purity of the total RNA was determined using a Nanodrop™ spectrophotometer. Up to 1 µg of isolated total RNA , 100 pmol random primers, 50 pmol oligo (dT) primers and 50 U Expand Reverse Transcriptase (Roche, Germany) were used in 20 µl reactions for cDNA synthesis. The final 20 µl reaction mix was incubated at 25°C for 10 min, then 42°C for 1 h, and then at 70°C for 15 min to inactivate the reaction. The cDNA was diluted 10-fold with nanopure water and stored at -20°C.

4.2.6. Gene isolation and sequence analysis

Sequences of candidate target gene family members in *B. napus* were determined through BLAST searching the NCBI database and an RNA-seq transcriptome database using prfect BLAST 2.0 software (Song *et al.* 2015).

4.2.7. Quantitative RT-PCR

Specific PCR primers were designed for each family member of the target genes using Primer Premier 6.20. Whenever possible, primer pairs were designed to span at least one intron to avoid/detect genomic contamination. In most cases, four primer pair combinations were designed and the best one was chosen for gene expression analysis. Primer sequences for reference genes and target genes are shown in Table S7 in Supplementary data.

The relative expression levels of *NRT* gene family members were determined using RT-qPCR. A volume of 15 µl was used for all qPCR reactions containing 1 µl of 10-fold diluted cDNA, the relevant primers and home-made SYBR Green master mix, in a Rotor-Gene Q real-time PCR machine (Qiagen, Germany). PCR products were Sanger sequenced to confirm homology to genes which are already identified in NCBI gene databases. Three technical replicates for each of three biological replicates were carried out for each sample set. Relative expression (fold change) of each target gene was corrected using the geometric means of two housekeeping genes from *B. napus*, elongation factor (*eEF-1α*) and *GAPDH*, and calculated using the $2^{-\Delta\Delta Ct}$ method as described in previous studies (Schmittgen and Livak 2008; Song *et al.* 2015).

4.2.8. Statistical analysis

For morphometric analyses of RSA, values are the mean ± SE of 30 plates with two seedlings per plate. For N and ^{15}N content, and gene expression analysis, three biological replicates, each comprising a pool of 20 seedlings, were tested and values are the mean ± SE. For C content analysis, values are the mean ± SE of n=6 experiments, with each experiment including 4 plates with 2 seedlings per plate. Statistical analyses were performed on GraphPad Prism statistical software version 7.00. Differences between means were tested for significance using ANOVA. Tukey's multiple comparisons test was used in the analysis.

4.3. RESULTS

4.3.1. Effect of PI-55 and BA on the exploratory root system

Changes in root branching and elongation were examined for 2-day-old seedlings grown in phytogel-solid medium containing 1 mM KNO_3 with various BA or PI-55 concentrations (Fig. 4.1). The primary root length and total root length showed a declining trend relative to controls (1 mM KNO_3) with an increase in PI-55 concentration from 0.05 µM to 10 µM. BA treatments showed a similar pattern as the concentration of BA increased from 0.005 to 1 µM (Fig. 4.1A). The lateral root (LR) number decreased significantly in the 10 µM PI-55 treatment while the LR number decreased significantly in all the BA treatments relative to control (Fig. 4.1B). The lateral root branching density (LRD) in this study is defined as the number of emerged LRs per unit length within the root branching zone (the zone that extends

from the shoot base to the youngest emerged LR) (Dubrovsky and Forde 2012). LRD was greater in the 10 μM PI-55 treatment than the control, whereas increasing the BA concentration significantly reduced LRD (Fig. 4.1B). In order to obtain the most contrasting phenotypes in root length and LRD, 10 μM PI-55 and 1 μM BA were chosen as the optimal pharmacological concentrations for the N uptake study.

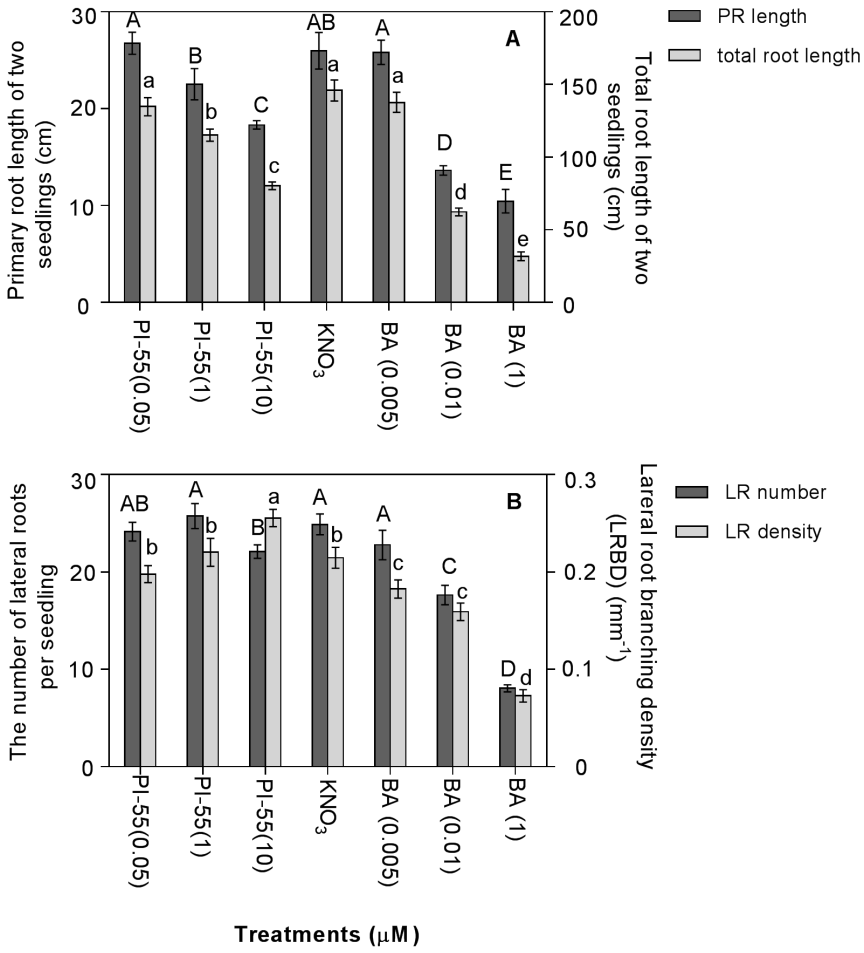

Fig 4. 1 Dose responses to PI-55 and BA treatments of *B. napus* roots

Dose responses to PI-55 and BA treatments of *B. napus* roots. After 96 h of the treatments, (a) primary and total root length, and (b) lateral root number and lateral root density (LBD) were measured in *B.napus* grown on phytogel plates with a homogeneous supply of 1 mM KNO_3. LR density is the number of emerged LRs per unit length within the root branching zone (the zone that extends from the shoot base to the youngest emerged LR). Values are mean ± SE of 30 plates with 2 seedlings per plate. Bars with different upper case letters denote means that are significantly different within the measurements of PR length and LR number, respectively (P<0.05). Bars with different lower case letters denote means that are significantly different within the measurements of total root length and LR density, respectively (P<0.05).

In the plants grown in the medium containing 1 mM ^{15}N-labelled KNO_3 with 10 μM PI-55, 1 μM BA or a combination of both, changes in the PR length, total root length and LRD were investigated after 24, 48, 72, 96 h of treatment (Fig. 4.2). During the first 24 h, the elongation of the primary root was significantly inhibited by PI-55, BA and the combination treatments compared to control (1 mM KNO_3^-) (Fig. 4.2A). Lateral roots appeared at 48 h. After 96 h, the inhibition of PR length and total root length by PI-55 and BA was pronounced (Fig. 4.2A and B). LR density was slightly increased by application of PI-55 relative to controls, whereas LR density was reduced in BA treatment after 96 h (Fig. 4.2C). In order to access the exploration efficiency of RSA, the convex hull of RSA was measured using RootNav and defined as root exploration area in this study. Consequently, the specific root exploration area (calculated as cm^2 per mg root dry weight) was reduced in both the PI-55 and BA treatments relative to control (Fig. 4.2C). This significant difference in the extent of the exploratory root system between control and treatments enabled an investigation of the functional relationship between root system architecture and nitrate uptake in *B. napus*.

To investigate the effect of the changes in root morphology on C allocation to the roots, the relationship between percentage C allocated to roots and total root length was analysed and this showed an exponential relationship (Fig. 4.2D). The percentage of total C allocated to roots and the shoot/root carbon ratio are shown in Supplementary Figures (Fig. S6). The dry weight of shoots and roots was reduced in the BA treatments relative to PI-55 and control

treatments (Fig. S7). The N content of the shoots in the PI-55, BA and the combination treatments was reduced relative to the control, whereas the N content in the BA- treated roots was only slightly decreased relative to those in PI-55 and control treatments (Fig. S7).

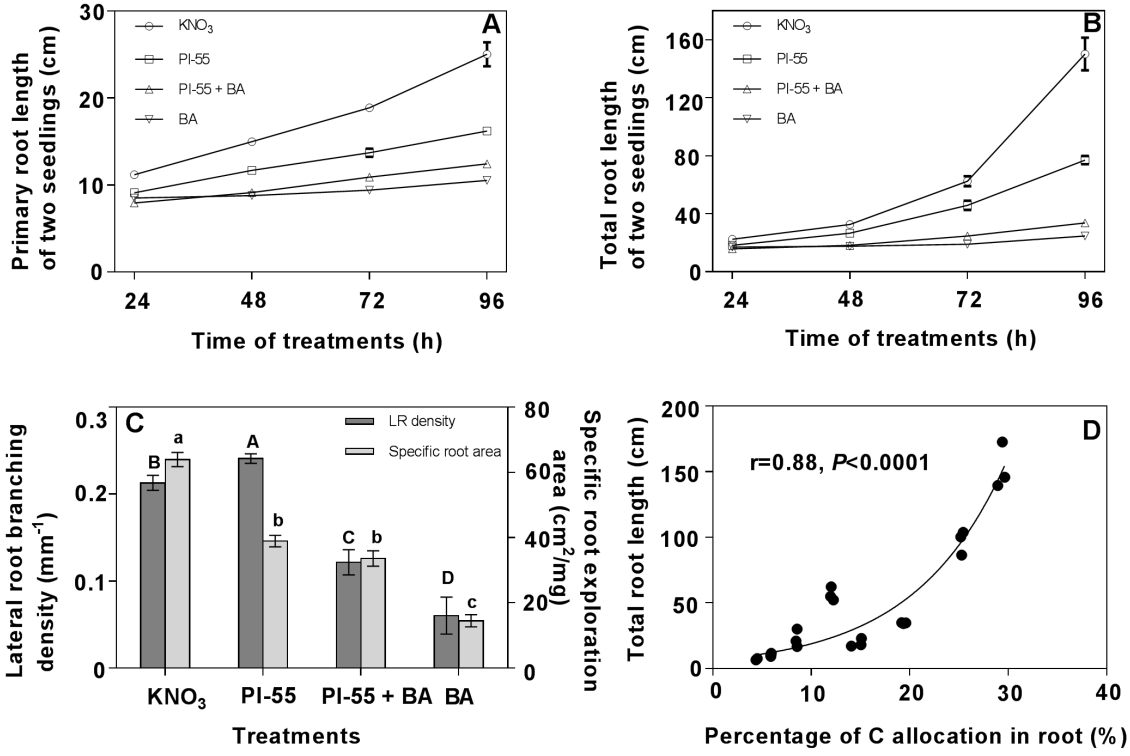

Fig 4. 2 Effects of PI-55 and BA on root growth and C allocation in *B.napus* during 96 h of growth with a homogeneous supply of 1 mM KNO_3.

(A), (B) Time-course of response of of primary root length and total root length. (C) Impact of PI-55 and BA on LR density and specific root exploration area after 96 h. (D) The

relationship between total root length and the percentage of whole plant C allocated to roots. LR density is the number of emerged LRs per unit length of the root branching zone (the zone that extends from the shoot base to the youngest emerged LR). Specific root exploration area is referred to as root exploration area (the convex hull obtained from RootNav) per unit dry weight, and calculated as cm^2 per mg root dry weight. Values are mean ± SE of 30 plates with two seedlings per plate. In panel (A), (B) and (C), values are mean ± SE of 30 plates with two seedlings per plate. In panel (D), the data points comprise the analysis in plants with the control and pharmacological treatments for 96 h, each treatment running 6 replicates and each replicate including 4 plates with 2 seedlings per plate. In panel (C), bars with different upper and lower case letters denote means that are significantly different within the measurements of LR density and specific root exploration area, respectively (P<0.05).

4.3.2. The relationship between root architecture and ^{15}N uptake in plants

In order to assess the relationship between RSA and N uptake, N uptake was measured using ^{15}N isotopically labelled NO_3^- during the 96 h of pharmacological treatments (Fig. 4.3). Based on the measurements of ^{15}N and root system components every 24 h, a logarithmic relationship was established between the ^{15}N content in plants and the total root length (Fig. 3A). It was shown that after 96 h, ^{15}N content was significantly reduced in the PI-55 treatment compared to control (1mM KNO_3), and this reduction in ^{15}N accumulation was pronounced in treatments with a combination of PI-55 and BA, and BA. To better understand the functional relationship between root structure and N uptake, ^{15}N uptake rate (determined as nmol h^{-1} cm^{-1} root length) was measured after 96 h. The results revealed that BA-treated seedlings, which had the the smallest root systems, had the highest ^{15}N specific uptake rate, whereas the control plants, which had largest root systems, had the lowest ^{15}N specific uptake rate (Fig. 4.3B). Consequently, the relationship between ^{15}N uptake rate and total root length was found to be negative (Fig. 4.3C). In addition, ^{15}N uptake rate per unit root length was negatively correlated with specific root area (Fig. 4.3D).

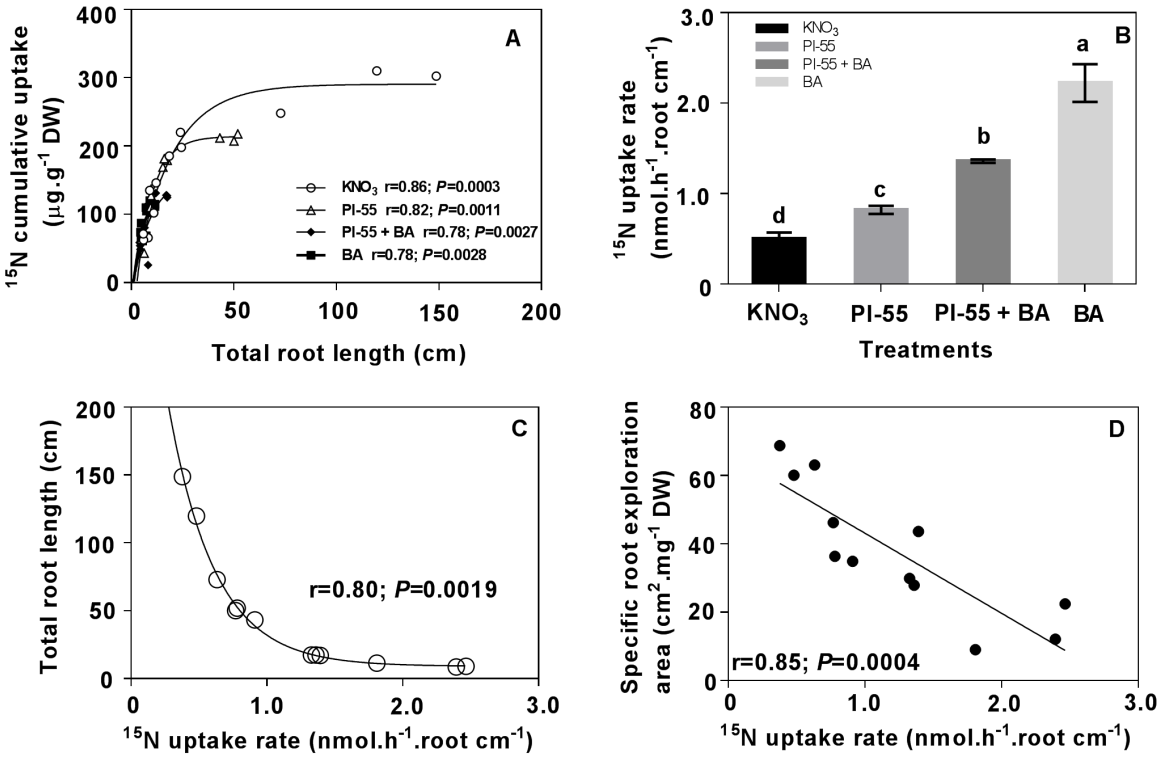

Fig 4. 3 ^{15}N uptake analysis in *B. napus* after 96 h of treatment.

(A) Relationship between ^{15}N cumulative uptake (at 24, 48, 72 and 96 h, respectively) and total root length (measured at 24, 48, 72 and 96 h, respectively). (B) Impact of PI-55 and BA on ^{15}N uptake rate per unit root length (The ^{15}N uptake rate was averaged rate over the entire 96 h and calculated as nmol h^{-1}. root cm^{-1}). (C) Relationship between total root length and ^{15}N uptake rate per unit root length. (D) Relationship between ^{15}N uptake rate and specific root exploration area. In panel (a), (c) and (d), each point represented a pool comprising 10 plates with two seedlings per plate. In panel (c) and (d), the data points comprise the analysis in plants with the control and pharmacological treatments for 96 h. In panel (B), vertical bars indicate mean ± SE of n=3 experiments, where each experiment included 10 plates with two seedlings per plate. Bars with different lower case letters denote means that are significantly different (P<0.05).

To investigate how effective cumulative N content or N metabolism was in terms of resource investment and distribution in roots proliferated, daily root elongation was examined over the time course. The daily root elongation of plants treated with BA was much less relative to PI-55 and control treatments over 96 h, consistent with the previous results for total root length (Fig. 4.4A and Fig. 4.2). There was an exponential relationship between daily root elongation and ^{15}N acquisition by plants during the previous 24-h period (Fig. 4.4B). This positive correlation suggests that root proliferation is associated with the N status of the plant.

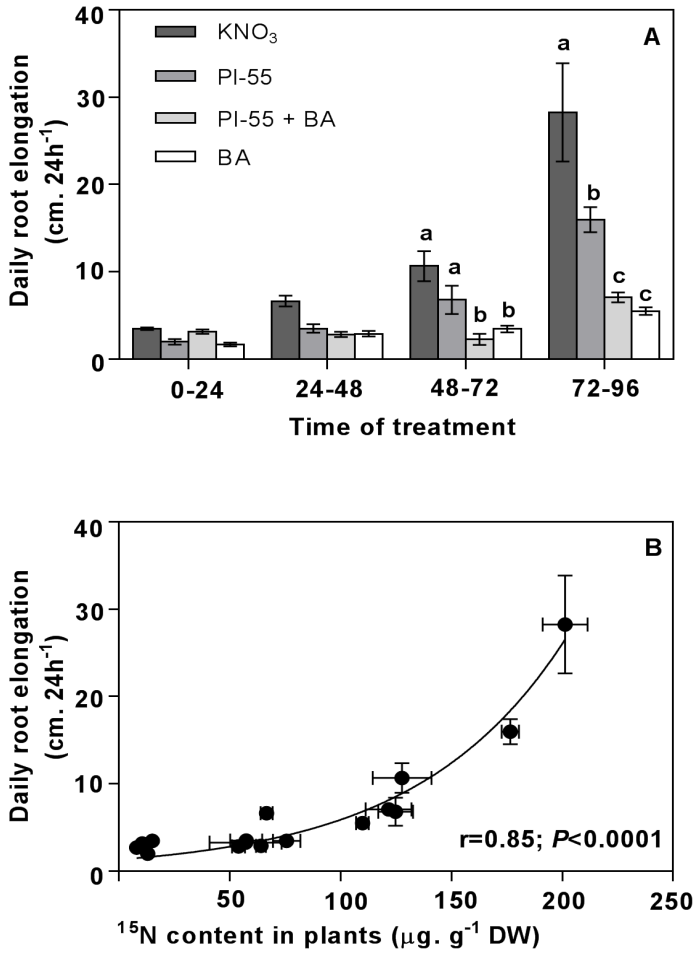

Fig 4. 4 Response of daily root elongation and ^{15}N accumulation in PI-55 and BAP treated *B. napus* seedlings.

(A) Daily root elongation over 96 h. (B) Relationship between daily root elongation and ^{15}N content in the whole plant (measured during the 24-h period before root elongation was determined). Vertical bars indicate mean ± SE of n=3 experiments, with each experiment including 10 plates with 2 seedlings per plate. Values are mean ± SE of 30 plates with two seedlings per plate. In panel (A), bars with different lower case letters denote means that are significantly different (P<0.05). In panel (B), the data points comprise the analysis in plants with the control and pharmacological treatments.

4.3.3. Correlation between root to shoot ratio and ^{15}N uptake

In order to investigate the value of root investment in terms of N uptake, the root and shoot biomass were estimated, and the correlation between root/shoot ratio and ^{15}N cumulative uptake. Under treatments with the same amount of nitrate (1 mM), root/shoot biomass ratio was greater in PI-55 and control treatments compared with BA treatment and the combination of PI-55 and BA treatments (Fig. 4.5A). The ^{15}N cumulative uptake was positively correlated with root/shoot biomass ratio ($r=0.92$, $P<0.0001$), suggesting a strong positive correlation between root investment and function in terms of N uptake (Fig. 4.5B).

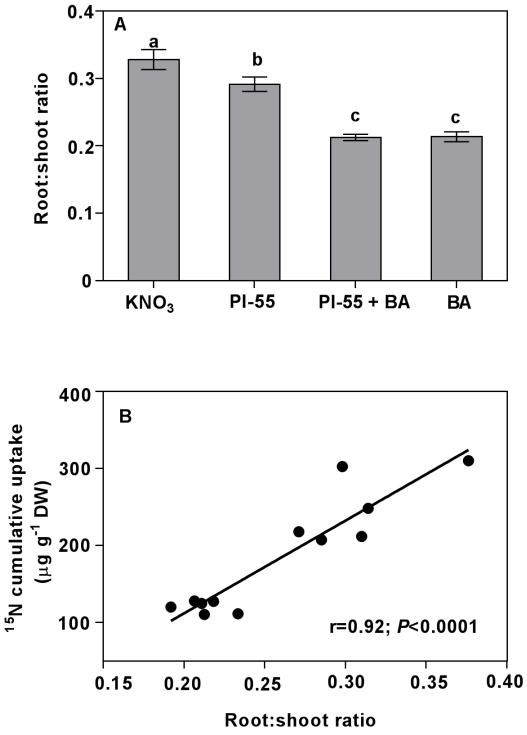

Fig 4. 5 The effects of PI-55 and BA on root/shoot ratio and the relationship between R:S ratio and ^{15}N uptake in *B. napus*.

The effects of PI-55 and BAP on root/shoot biomass ratio (A) and the relationship between root/shoot ratio and ^{15}N uptake of roots (B) in plants grown for 96 h. In panel (B), the data points comprise the analysis in plants with the control and pharmacological treatments for 96 h. Vertical bars indicate mean ± SE of n=3 experiments, with each experiment including 10 plates with 2 seedlings per plate.

4.3.4. Expression of nitrate transporter genes (*BnNRT*) and *BnPHO1* genes

I investigated whether the changes in ^{15}N uptake induced by PI-55 and BA were associated with transcriptional regulation of nitrate transporters. Consistent with the changes in N uptake, PI-55 treated plants, with reduced cumulative N uptake, showed less expression of *BnNRT2.1* relative to control plants after 96 h (Fig. 4.6A). The greatest reduction in *BnNRT2.1* was observed in the BA treatment where less cumulative N was measured relative to control plants. The expression of another important transporter gene in nitrate uptake, *BnNRT1.1*, displayed a different pattern to *BnNRT2.1*, with greater expression of *BnNRT1.1* in PI-55 than in the control. However, the expression of *BnNRT1.1* was inhibited by BA and the combination of PI-55 and BA treatments (Fig. 4.6B).

The expression of nitrate transporters involved in NO_3^- translocation from root to shoot was also examined. *BnNRT1.5*, responsible for loading NO_3^- into xylem, showed a similar expression pattern to *BnNRT1.1*, with greater expression in response to PI-55 treatment and reduced expression in response to BA and the combination of treatments in comparison to the control (Fig. 4.6C). In contrast, the expression of *BnNRT1.8*, a nitrate transporter responsible for unloading NO_3^- from the xylem, was up-regulated by BA treatment and slightly repressed by PI-55 relative to the control (Fig. 4.6D). *BnPHO1a* and *BnPHO1b* showed similar expression patterns to *BnNRT1.1*, being greater in both the PI-55 and control treatment relative to the BA treatment (Fig. 4.6E and F).

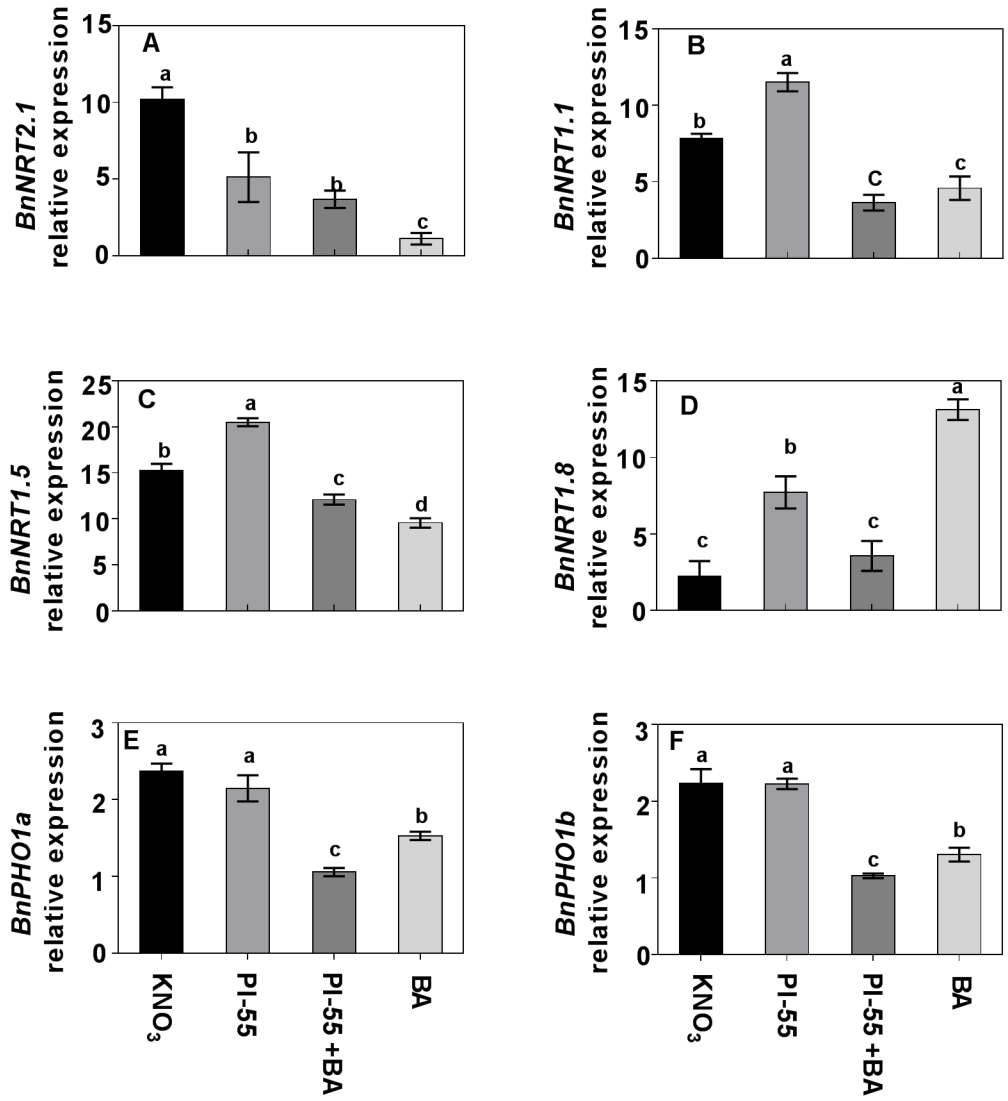

Fig 4. 6 Expression of *BnNRT2.1, BnNRT1.1, BnNRT1.5, BnNRT1.8*, *BnPHO1*a and *BnPHO1b* in *B. napus* roots after 96 h.

Vertical bars indicate mean ± SE of n=3 experiments, with each experiment including 10 plates with two seedlings per plate. Bars with different lower case letters denote means that are significantly different (P<0.05).

4.3.5. Nitrate uptake kinetics

In order to determine nitrate uptake kinetics among the different root architectures, *Brassica* seedlings from the various pharmacological treatments were supplied with ^{15}N isotopically labelled NO_3^- at concentrations ranging from 0.01-5 mM (Fig. 4.7). Cumulative ^{15}N content (calculated as µg g^{-1} DW) and ^{15}N uptake during 96 h of treatments (calculated as nmol h^{-1} cm^{-1} root length) increased with increases in external NO_3^- concentration according to Michaelis-Menten kinetics, indicating the capacity for nitrate uptake in roots saturated at high N. K_m and I_{max} values were calculated (Fig. 4.7A and B) and NO_3^- uptake kinetics varied among different RSAs induced by the pharmacological treatments. Maximum total N uptake per unit dry weight (I_{maxdw}) values of 325.8, 225.9, and 186.0 µg g^{-1} DW were determined in PI-55, the combination of PI-55 and BA, and BA treatments, respectively. Control plants without pharmacological treatment displayed a I_{maxdw} of 464.8 0 µg g^{-1} DW (Fig. 4.7A). Together with total root length, the maximum uptake rate per unit root length (I_{maxrl}) was estimated. I_{maxrl} varied among different RSAs induced by the pharmacological treatments, with the greatest I_{maxrl} being 312.7 nmol cm^{-1} root length observed in RSA induced by BA treatment and the slowest I_{maxrl} being 76.09 nmol cm^{-1} root length observed in control roots. Root systems induced by PI-55 and the combination of PI-55 and BA treatments exhibited values of 179.4 and 227.9 nmol h^{-1} cm^{-1} root length , respectively (Fig. 4.7B).

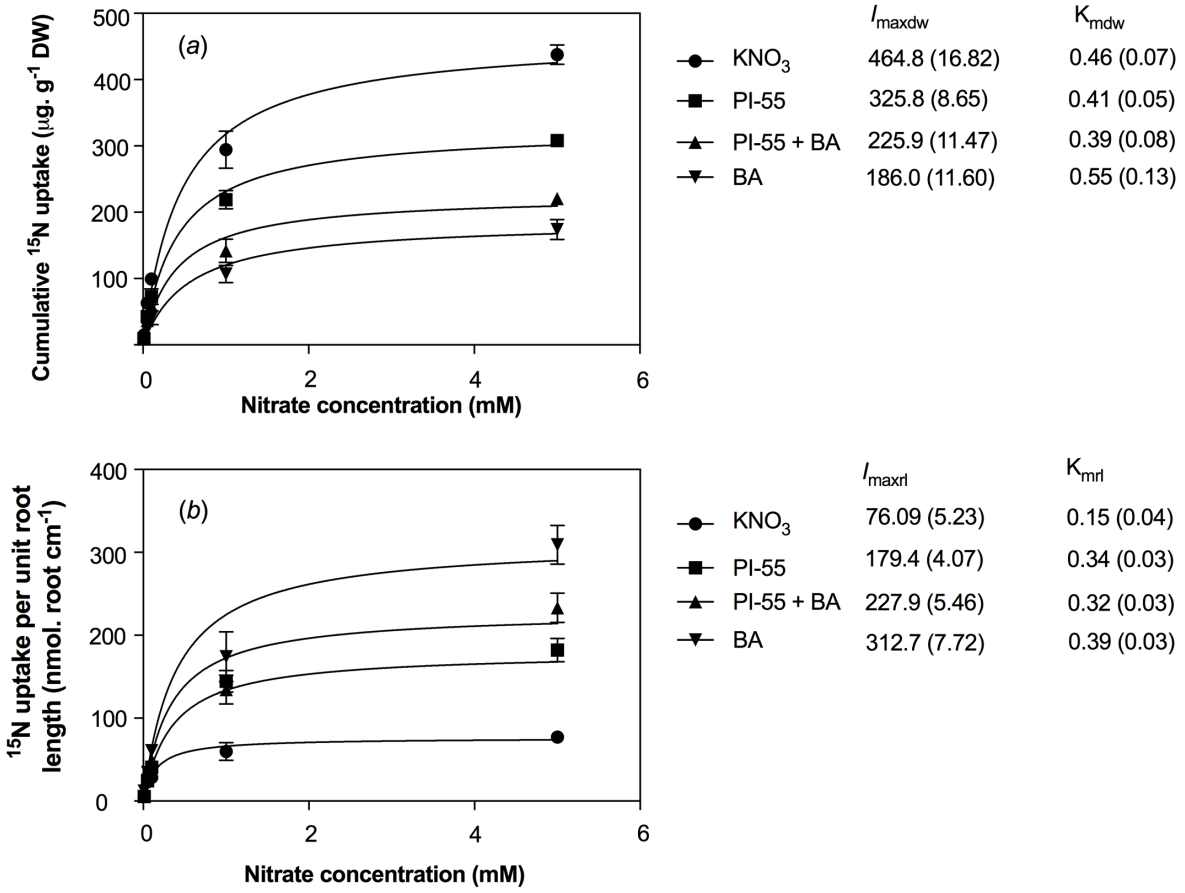

Fig 4. 7 Fitted Michaelis-Menten curves for ^{15}N uptake in *B. napus* roots in response to PI-55 and BAP treatment over 96 h.

Vertical bars indicate mean ± SE of n=3 experiments, where each experiment included 10 plates with two seedlings per plate. I_{maxdw} and I_{maxrl} represented I_{max} on a dry weight and root length basis, respectively. Estimated I_{maxdw}, I_{maxrl} and K_m values (± SE) for each curve are also shown.

4.3.6. Relationships between roots and ^{15}N uptake in a wide range of N concentrations.

In order to further dissect the relationships between structural and functional adjustments induced by pharmacological treatments, the quantity of ^{15}N translocated from roots to shoots was investigated systematically (Fig. 4.8B). The percentage of ^{15}N translocated from roots to shoots varied from 8.6% to 44.7% with changes in external nitrate concentration. A significant relationship was observed between cumulative ^{15}N uptake and translocation from roots to shoots. With increasing external NO_3^- concentration from 0.01 mM to 5 mM, the slopes of this positive relationship increased, being greatest in 5 mM NO_3^- and least in 0.01 mM NO_3^- (Fig. 4.8B). Cumulative ^{15}N uptake was correlated with specific root exploration area under various external nitrate concentrations (Fig. 4.8A). In addition, the transcripts levels of *BnNRT2.1* in the different phenotypes induced by the pharmacological treatments were strongly associated with the total root length (Fig. 4.8C).

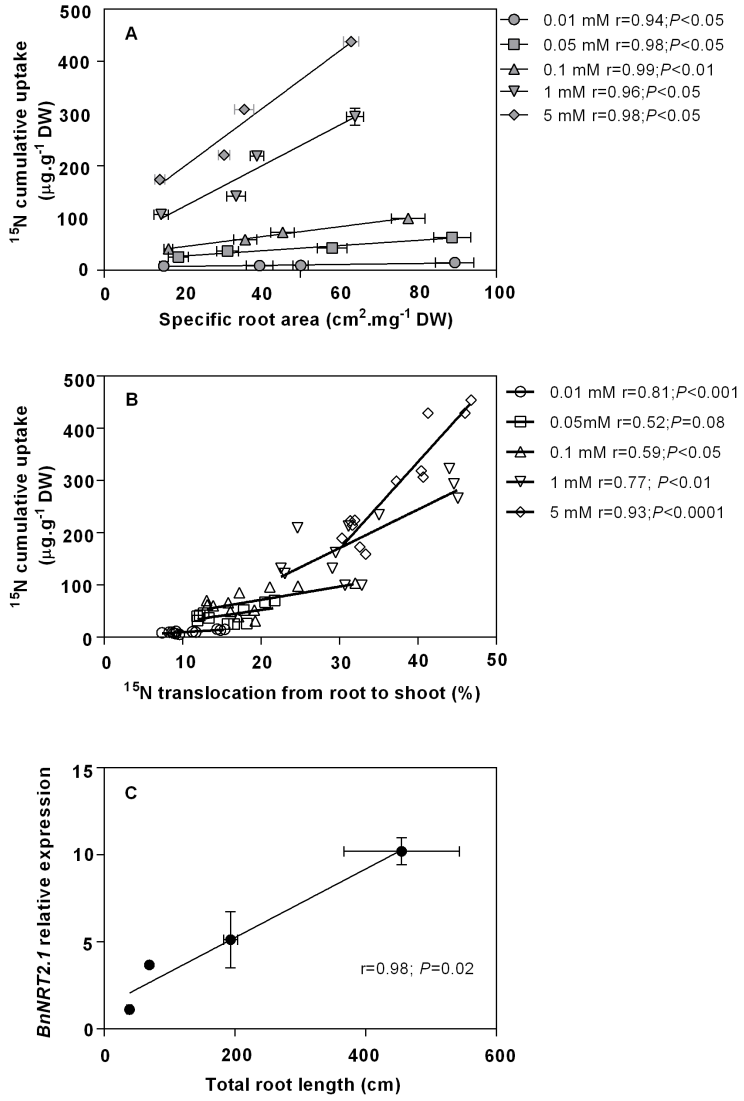

Fig 4. 8 Relationship between cumulative ^{15}N uptake and (A) specific root exploration area, and (B) ^{15}N translocation from root to shoot in *B. napus*

Relationship between cumulative ^{15}N uptake and (A) specific root exploration area, and (B) ^{15}N translocation from root to shoot, in PI-55 and BA-treated seedlings with differing external concentrations of NO_3^-. (C) Relationship between *BnNRT2.1* expression and total root length. Vertical bars indicate mean ± SE of n=3 experiments, where each experiment included 10 plates with two seedlings per plate (the error bars of the two lowest points in C are smaller than the symbols).

4.4. DISCUSSION

In this study, BA induced a RSA phenotype with shorter PR, reduced LR density and reduced total root length, indicating that the application of BA significantly inhibited LR formation and elongation (Fig. 4.2). These data are consistent with results showing that treatment with BA led to strong inhibition of root growth and LR formation in 10-day old *Arabidopsis* seedlings (Laplaze *et al.* 2007). The underlying mechanism could be that cytokinin disrupts an auxin gradient that is required for lateral root primordia formation, via perturbation of PIN-mediated polar auxin transport (Benková *et al.* 2003; Laplaze *et al.* 2007; Marhavý *et al.* 2014). In addition, exogenous application of the cytokinin receptor antagonist, PI-55, induced a root phenotype with increased LR density but reduced root elongation, supporting its function in supressing activity of endogenous cytokinin (Spíchal *et al.* 2009). This is in agreement with findings that treatment with 10 µM PI-55 may lead to increased LR primordia and emerged LRs in 7 and 12 day-old seedlings of pea (Long *et al.* 2012). However, as shown with my data, and also with in *Arabidopsis* (Spíchal *et al.* 2009), a combined treatment of 10 µM PI-55 and 1 µM BA was found to partially, but not completely, reverse the effect of exogenous application of BA on lateral root branching.

The significant changes in root branching in these phenotypes allowed this study to investigate the functional significance of RSA in terms of N uptake. Exogenous application of BA led to a reduction in biomass and carbon allocation to the roots (Fig. 4.2C, S6 and S7). As N concentration in the culture medium was the same in these treatments (1 mM KNO_3), it can be assumed that the changes in root architecture induced by PI-55 and BA were associated with perturbation of C allocation to roots. Interestingly, a significant correlation between root elongation and C allocation to roots was observed (Fig. 4.2D), confirming that root growth is largely dependent on C availability in the root. This is consistent with the observation that root elongation rate and branching is positively related with local sugar concentration (Freixes *et al.* 2002). Although cytokinins are proposed to be involved in affecting the allocation of C to the root, it may be possible that cytokinins impeded N metabolism and thereby impaired C allocation in root tissue. It was also found that cytokinin signalling is involved in C partitioning between root and shoot in response to perturbation in the C/N balance by defoliation in *Lolium perenne* (Chapter 2).

These results show clearly that in BA-treated seedlings, or seedlings treated with the combination of PI-55 and BA, the decrease in their LR formation and root growth is accompanied by a dramatic reduction in total ^{15}N uptake relative to PI-55 and control

seedlings. Despite the greater LR density in PI-55-treated seedlings, total ^{15}N uptake was less than in control seedlings, which possessed lower LR density and longer LR length, reflecting the important role that root elongation has in increasing the total absorbing surface for nutrient acquisition. In terms of functional differences in RSA, I observed an exponential relationship between total root length and cumulative N uptake, confirming a major contribution of LR outgrowth to the ability of a plant to explore and exploit resources in the soil. Interestingly, the root/shoot biomass ratio was positively correlated with cumulative N uptake under these treatments (Fig. 4.5), suggesting a functional utility of the investment into roots in term of nutrient uptake. This root investment for resource acquisition in the soil is affected by metabolic costs and benefits (Lynch 2013).

N uptake rate per unit of root length showed a contrasting trend to that of cumulative N uptake (Fig. 4.3B), with BA-treated seedlings having the smallest root system but the greatest N uptake rate per unit of root length, implying a compensatory mechanism in regulating root N uptake. This compensatory effect in root segments is suggested to be associated with nitrate transporter *NRT2.1* expression (Lemaire *et al.* 2013). In my study, however, the smaller root systems in the BA-treated plants had the lowest expression of *BnNRT2.1*, which is consistent with the conclusion that cytokinin down-regulates the expression of nitrate transporter *NRT2.1* genes (Brenner *et al.* 2005; Kiba *et al.* 2011). Moreover, PI-55 partially relieved the repression of *BnNRT2.1* expression by BA. Given that all plants received the same amount of N resource supplied during the experiment (1 mM KNO_3), another possible conclusion is that the decrease in the N uptake efficiency per unit root length in plants with greater root branching may result from an increase in competition among individual lateral roots in terms of nutrients and water acquisition. This would have the effect of reducing N uptake efficiency per unit root length. These results are consistent with previous findings from functional-structural plant model system simulations of maize root architecture development with various lateral root branching densities and contrasting root architectures (Postma *et al.* 2014; Dathe *et al.* 2016). These support a negative correlation between ^{15}N uptake efficiency and specific root exploration area (root exploration area per unit dry weight). Fig. 4.3D clearly shows a linear decline in ^{15}N uptake rate per unit root length with increasing root specific exploration area, demonstrating that there is strong competition among lateral roots of the same plant. The shift in the relative amount of ^{15}N uptake by each root fraction suggests a trade-off between N uptake efficiency and root growth, which is in accordance with earlier studies (Berntson 1994).

It was also found that the kinetics of NO_3^- uptake varied among the treatments, with I_{max} being greatest for root systems in the BA treatment (Fig. 4.7B). This response was consistent even under varying concentrations of external nitrate from 0.01 mM to 5 mM, demonstrating the functional importance of variation in root phenotypes to nitrate uptake kinetics. Several studies have investigated N uptake plasticity by measuring nitrate uptake rate of different grass species grown in uniform soil or in a heterogeneous nitrate patch (Van Vuuren *et al.* 1996; Fransen *et al.* 1999). However, these studies lack an assessment of the functional importance of nitrate uptake kinetics. York *et al.* (2016) reported that V_{max} has greater effect on plant growth than K_m, and increasing V_{max} of nitrate uptake in localized root segments is associated with largely induced shoot growth from functional-structural plant model system simulations of maize root architecture development (York *et al.* 2016). These demonstrate a potential for targeting the plasticity of nitrate uptake kinetics in crop breeding research. High V_{max} and low K_m has been proposed as an ideotype for nitrate acquisition from soil (Lynch 2013).

After 96 h of treatment, the expression of *BnNRT1.1* was greater under PI-55 treatment, while the expression of *BnNRT2.1* decreased (Fig. 4.6A and B). *NRT1.1* has been proposed to act as a NO_3^- sensor and to play an important role in NO_3^-signalling in developmental processes governing root growth (Zhang *et al.* 1999; Remans *et al.* 2006; Ho *et al.* 2009a). Plants recruit cytokinin for shoot-root communication of plant N status. Ruffel *et al.* (2011) have proposed that a NO_3^--CK relay enables plants to efficiently control root growth to regulate plant N economics (Ruffel *et al.* 2011). Taken together, the application of exogenous cytokinin and its antagonist in *B.napus* provides evidence supporting the notion that *NRT1.1* is implicated in mediating NO_3^--dependent cytokinin biosynthesis (Takei *et al.* 2004a; Kiba *et al.* 2011).

In *Arabidopsis*, *AtPHO1* has been identified by genome-wide association mapping to be associated with changes in allometry of lateral roots, and to mediate root development through interactions with nitrate and hormonal signalling (Rosas *et al.* 2013). Here, I found the expression of *BnPHO1a* and *BnPHO1b* was greater in PI-55 and control treatments which possessed greater root growth and root branching relative to BA-treated plants. This supports the role of *BnPHO1* in mediating lateral root plasticity, as reported by Rosas *et al.* (2013) in *Arabidopsis*. Given that *PHO1* is mainly localized to the root vascular tissues and primarily functions to export phosphate into the xylem vessels of roots (Hamburger *et al.* 2002), the

reduction in *BnPHO1* expression under BA treatment may be partly explained by a decrease in phosphate acquisition due to the feedback of low N availability in the plants.

4.5. SUMMARY

In conclusion, by using a pharmacological approach, evidence is provided that the modification of RSA through disruption of endogenous cytokinin signalling is correlated with N uptake, with greater root proliferation in PI-55 treated and control plants leading to greater cumulative N uptake. However, considering the overall C cost and resource investment, this increased root proliferation did not bring much benefit in terms of plant growth because of increasing competition between individual lateral roots which resulted in reduced N uptake efficiency per unit root length. This could partly explain why, in the long-term, fertilised and unfertilised plants in the field do not display differences in final root length and proliferation (Gabrielle *et al.* 1998). This investigation of varying root traits and their impact on N uptake has shown that root proliferation in response to external N is a behaviour which integrates local N availability and the systemic N status of the plant. This integration is, at least in part, regulated by cytokinin signalling.

Chapter 5 – Final discussion and future directions

5.1. THESIS OBJECTIVES AND KEY RESULTS

This thesis attempted to address three major questions. There are listed below along with a summary of key results:

1. In *L. perenne*, how does nitrate uptake respond to two independent but coinciding metabolic demands on carbon: defoliation and nitrate addition?

- Nitrate uptake relies on labile carbohydrate availability in plants
- Nitrate assimilation is regulated by the C/N status of the plant
- Nitrate transporters *LpNRT2.1* and *LpNRT1.1* are regulated at the transcriptional level in response to changing C/N status.
- Cytokinin is involved in the regulation of N acquisition and assimilation in response to changes in C/N balance.

2. In *B. napus*, how does root system architecture respond to different N forms and availability?

- Root traits displayed distinct morphological changes in response to different nitrogen sources.

3. What is the functional significance of root system architecture in terms of N uptake?

- Cytokinin and the cytokinin antagonist PI-55 can induce contrasting root phenotypes in *B. napus*
- ^{15}N uptake was strongly related to the contrasting root traits induced by cytokinin and PI-55. Large root proliferation led to greater ^{15}N cumulative uptake rather than greater ^{15}N uptake rate per unit root length.
- The functional relationship between RSA and ^{15}N uptake was associated with changes in C and N resource distribution between the shoot and root.

5.2 GENERAL DISCUSSION OF RESULTS

5.2.1 C/N control of N uptake and assimilation

Carbon metabolism provides energy and C skeletons for N assimilation and incorporation into essential molecules such as amino acids, proteins and nucleic acids. It is not surprising that N uptake is not only determined by external N availability and internal N status in plants, but also by the availability of C metabolites from photosynthesis (Delhon *et al.* 1996; Forde 2002a). To cope with a wide range of environmental factors, plants recruit a complex regulatory and signalling network, and undergo morphological and metabolic responses to maintain their C/N balance.

The regulation of root nitrate uptake by C metabolites from photosynthesis has previously been demonstrated by diurnal stimulation of NO_3^- uptake. It has been established that sugars transported from shoots to roots play an important role in this diurnal stimulatory effect (Rideout and Raper Jr 1994; Delhon *et al.* 1996; Lejay *et al.* 1999). In the forage grass, *L. perenne*, defoliation and subsequent regrowth both impact C partitioning, thereby creating a significant point of interaction with soil N availability. The dramatic shift in C/N metabolic partitioning resulting from defoliation and regrowth in *Lolium* has the potential to reveal insights into the integration of C/N assimilation in plants that are otherwise not possible to observe in dicotyledonous species. Thus, using defoliation as an experimental treatment, this project showed high- and low-affinity NO_3^- uptake were reduced within 48 h in an N-dependent manner in response to the rapid and large shift in carbohydrate remobilization triggered by defoliation (Fig. 5.1). This reduction in NO_3^- uptake was rescued by an exogenous 1% glucose supplement, confirming the carbohydrate-dependence of NO_3^- uptake. Furthermore, the transport of NO_3^- from root to shoot, and its subsequent assimilation, appears to be regulated by the C-N condition of the plant, implying a mechanism that signals the availability of C metabolites for NO_3^- uptake and assimilation at the whole-plant level.

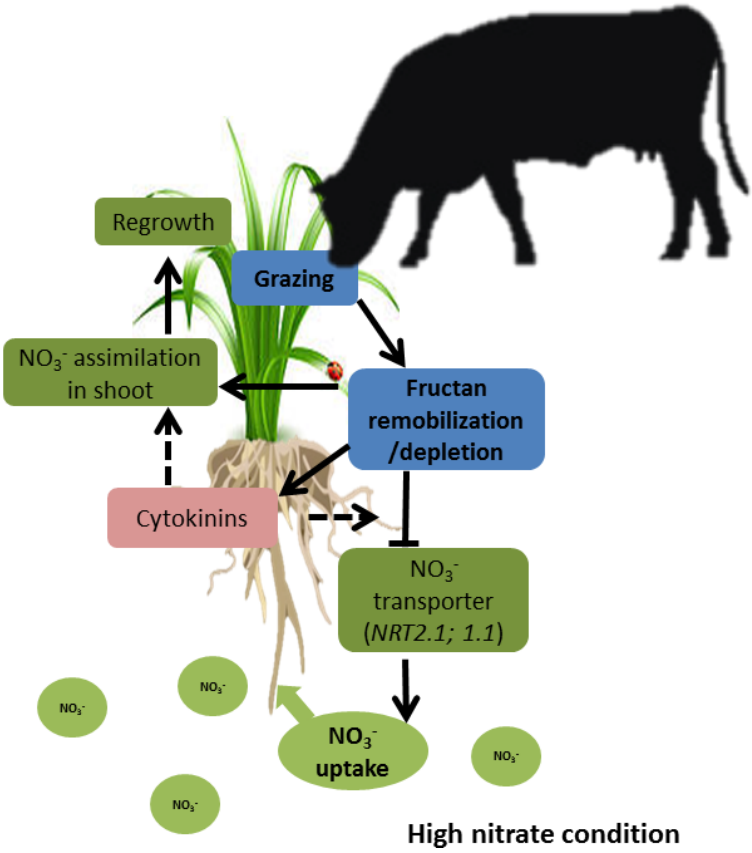

Fig 5. 1 A summary model depicting early responses to defoliation in *L. perenne*.

In *L. perenne* grown in high nitrate conditions, high- and low-affinity NO_3^- uptake is repressed in an N-dependent manner in response to a rapid and large shift in fructans triggered by defoliation. Nitrate assimilation in shoots is induced by fructan remobilisation to stimulate regrowth of shoot. Cytokinin plays a role in regulation of nitrate uptake and assimilatory genes in response to C availability.

At the molecular level, several genes that encode nitrate transporters in the roots have been found to be regulated by the products from photosynthesis in the shoots. Interestingly these genes are generally reported to be responsive to N. For instance, *NRT1.1*, *NRT2.1* and *NRT2.4* have been reported to be responsive to both carbon and nitrogen treatments (Lejay *et al.* 1999; Lejay *et al.* 2003; Kiba *et al.* 2012). In my study, nitrate transporter genes *LpNRT2.1* and *LpNRT1.1* were responsive to the perturbation of plant C/N balance (Fig. 5.1). These suggest the general existence of interactions between carbon and nitrogen signalling in plants. However, the molecular elements involved in the cross-talk between carbon and nitrogen signalling remain unclear. In *Arabidopsis*, TOR and SnRK1 kinases have been reported as central elements of signalling pathways involved in nutrient and carbon sensing (Robaglia *et al.* 2012; Dobrenel *et al.* 2013). However, no evidence supports these two kinases being involved in the regulation of root nitrate uptake by nitrogen and carbon. Up-regulation of *AtNRT2.1* by sugars is not attributed to well-established specific sucrose or glucose sensing, although glucose-regulated expression of *AtNRT2.1,* independent of nitrate-mediated mechanisms, can operate through HEXOKINASE1-mediated oxidative pentose phosphate pathway (OPPP) metabolism (Lejay *et al.* 2008; De Jong *et al.* 2014). Interestingly, changes in the expression of nitrate assimilatory genes in response to sucrose in the roots is also regulated by the signal coming from the OPPP pathway (Lejay *et al.* 2008; De Jong *et al.* 2014). However, the molecular components involved in this signalling pathway are still unknown. Thus, in the future, efforts to understand the signalling pathway linked to the OPPP are necessary to reveal how nitrogen and carbon signalling pathways are integrated to regulate nitrate uptake by the roots.

Recently however, findings demonstrating a direct regulatory function for the non-protein amino acid, gamma-aminobutyric acid (GABA) in ion flux, makes this a potential candidate for further investigations of plant C/N regulation in response to environmentally induced changes in C and N partitioning (Ramesh *et al.* 2015). In *Arabidopsis*, seed-targeted up-regulation of Glutamate-to-GABA decarboxylation has been shown to lead to significant changes in C/N balance and storage reserves, suggesting a role for a finely regulated GABA shunt in maintaining C/N equilibrium (Fait *et al.* 2011).

5.2.2 Cytokinin control of nitrogen uptake in response to C/N ratio

Despite several studies proposing possible mechanisms underlying C and N signalling in *Arabidopsis*, a definitive mechanistic understanding remains elusive. The results of the cytokinin metabolite profiling and *LpRR* expression (Chapter 2, Fig. 2.11) are consistent with cytokinins acting as a systemic N signal regulating N uptake and assimilation as suggested for *Arabidopsis* (Ruffel *et al*. 2011). By perturbing C assimilation and metabolism with a defoliation-regrowth treatment, it is proposed that cytokinin-mediated NO_3^- uptake and assimilation also acts to balance C and N resources at the whole plant level. A model is conceived whereby cytokinins serve as a signal to integrate C and N metabolism via tissue-specific function (Fig. 5.2). This involves (i) cytokinin-mediated reduction in NO_3^- uptake in roots and increase in NO_3^- assimilation in re-growing shoots under low C/high N status (low N demand); (ii) a shift in C allocation from shoots to roots which serves to stimulate NO_3^- assimilation in roots under high C/low N status (high N demand). Given that IAA biosynthesis is up-regulated by soluble sugars (LeClere *et al.* 2010; Lilley *et al.* 2012; Sairanen *et al.* 2012) and N deficiency tends to induce basipetal auxin transport in LR via AtNRT1.1 (Krouk *et al.* 2010), it is possible that auxin is also involved in the shoot-root bi-directional C-N signalling loop in relation to balancing C/N (Wang and Ruan 2016).

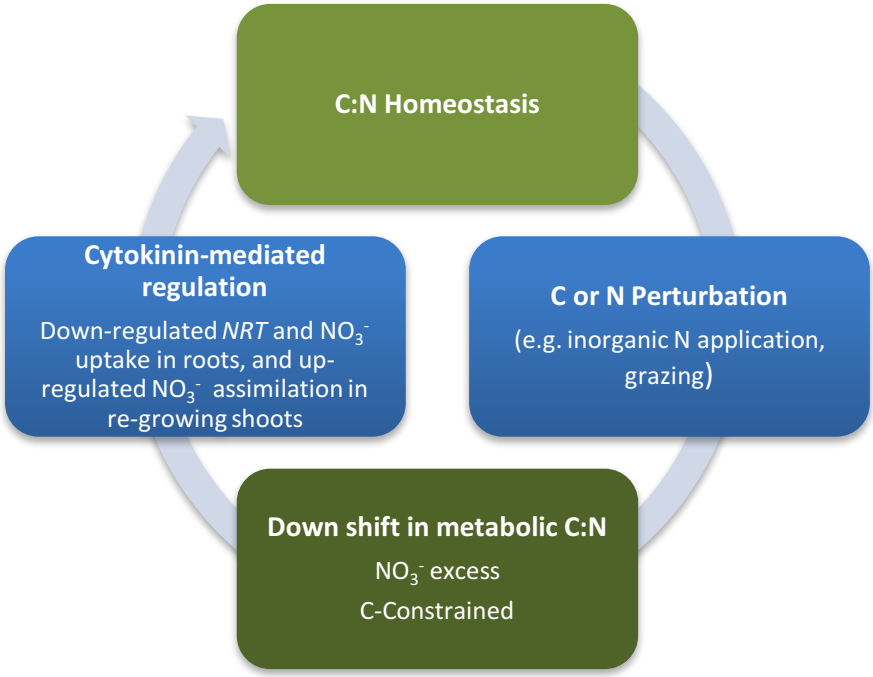

Fig 5. 2 A model depicting the role of cytokinin in C:N homeostasis

Cytokinin restores the C:N balance by down regulating NO_3^- uptake in a C-status dependent manner: when grazing or inorganic N application leads to a decrease in the C:N balance, cytokinin serves as a signal to mediate the down-regulation of NO_3^- uptake in roots and the up-regulation of NO_3^- assimilation in the re-growing shoots, thereby re-balancing the C and N resources at the whole plant level.

5.2.3 The importance of root foraging in nutrient uptake

Plant roots show a high degree of plasticity in response to N availability in the field. Following development of an improved plate culture system, root morphological changes in response to in a wide range of N sources and N conditions were investigated (Fig. 5.3). As summarized in Fig. 5.3, N deficiency induced the growth of more exploratory root system with greater lateral root length in *B. napus*, which is in agreement with previous findings in *Arabidopsis* (López-Bucio *et al.* 2003). However, the total root length and LR density was greater in plants grown in low nitrate condition relative to the N-free condition. These results indicate that plants are able to use different strategies to modify RSA in response to the amount of nitrate as also suggested by Giehl *et al.* (2014) and Giehl and von Wirén (2014).

In this study, the application of the cytokinin, 6-benzylaminopurine (BA) and the cytokinin antagonist, PI-55, induced contrasting phenotypes (Fig. 5.3). Based on these observations, the functional impact of RSA in relation to N uptake was investigated. *In situ* ^{15}N isotope labelling was used to investigate the spatiotemporal uptake of nitrate. This allowed an assessment of the relationship between root and N uptake. The contrasting root traits induced pharmacologically displayed differences in N uptake, with relatively high N cumulative uptake by more highly branching roots and low N cumulative uptake by the small, less branched root systems. However, it is worth noting that the N uptake rate per unit root length in the contrasting root systems showed the opposite trend. These data imply that plants are able to balance root foraging and N uptake rate. This investigation of varying root traits and its impact on N uptake has shown that root proliferation in response to external N is a behaviour which integrates local N availability and systemic N status in the plant. This integration is, at least in part, regulated by cytokinin signalling. Although it is difficult to interpret phenotypic root plasticity in a functional way, knowledge of functional differences between contrasting root traits in relation to nitrate capture should be helpful in guiding forage brassica breeding for high N acquisition.

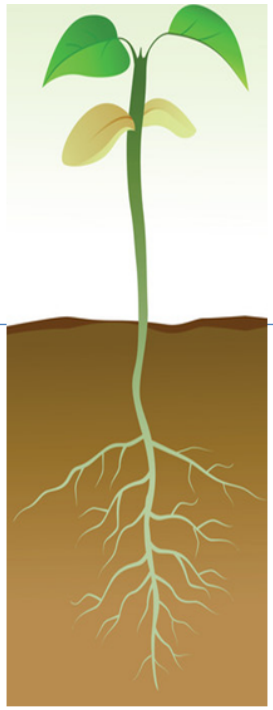

Mild low NO_3^-
1. Longer LRs
2. Greater LR density
3. Greater root exploration area
4. Greater root biomass ratio

High NO_3^-
1. Reduced LRs
2. Reduced LR density
3. Reduced root exploration area
4. Greater shoot and root biomass
5. Reduced root biomass ratio

PI-55 (cytokinin antagonist)-induced root phenotypes which possess
1. Reduced PR and LRs
2. Greater LR density
3. Reduced specific root exploration area

High NH_4^+
1. Reduced PR and LRs
2. Reduced LR density
3. Reduced root exploration area
4. Reduced shoot and root biomass

High glutamate
1. Reduced PR and LRs
2. Greater LR density
3. Reduced root exploration area
4. Induced shoot and root biomass

Fig 5. 3 Summary of morphological changes in *B. napus* roots in response to different N sources, cytokinin and the cytokinin antagonist PI-55.

5.3 CONCLUDING STATEMENT AND THOUGHTS FOR FUTURE WORK

In conclusion, using two major economic forage species in New Zealand agriculture system, *L. perenne* and *B. napus*, this project investigated three distinct but related components: 1) dynamic relationships between plant carbohydrate status and NO_3^--responsive uptake systems, transporter gene expression and N assimilation during early regrowth in *Lolium perenne*; 2) root morphological changes in response to a wide range of N availability; 3) the functional relationship between contrasting root systems induced pharmacologically, and N uptake. Each of these components contributes to our understanding of the mechanisms impacting on N uptake. Building on previous studies, the factors that impact on N uptake by the roots are summarized in Fig. 5.4. The results of Chapter 2 provide clear evidence that the rapid and large shifts in carbon storage triggered by defoliation have significant impact on nitrate uptake in an N-status dependent manner. Intact plants grown under high and low N conditions displayed distinct NO_3^- uptake rates (Chapter 2, Fig. 2.6), confirming that root NO_3^- uptake is regulated by both exogenous N availability and the internal N status of the plant. In addition, root system architecture that reflects a plastic plant adaptation to environmental variation is another important determinant of N uptake. The modification of RSA, controlled by co-ordinating local nitrate signalling and systemic signalling, enables plants to forage for sparingly available resources with greater efficiency (Chapter 4).

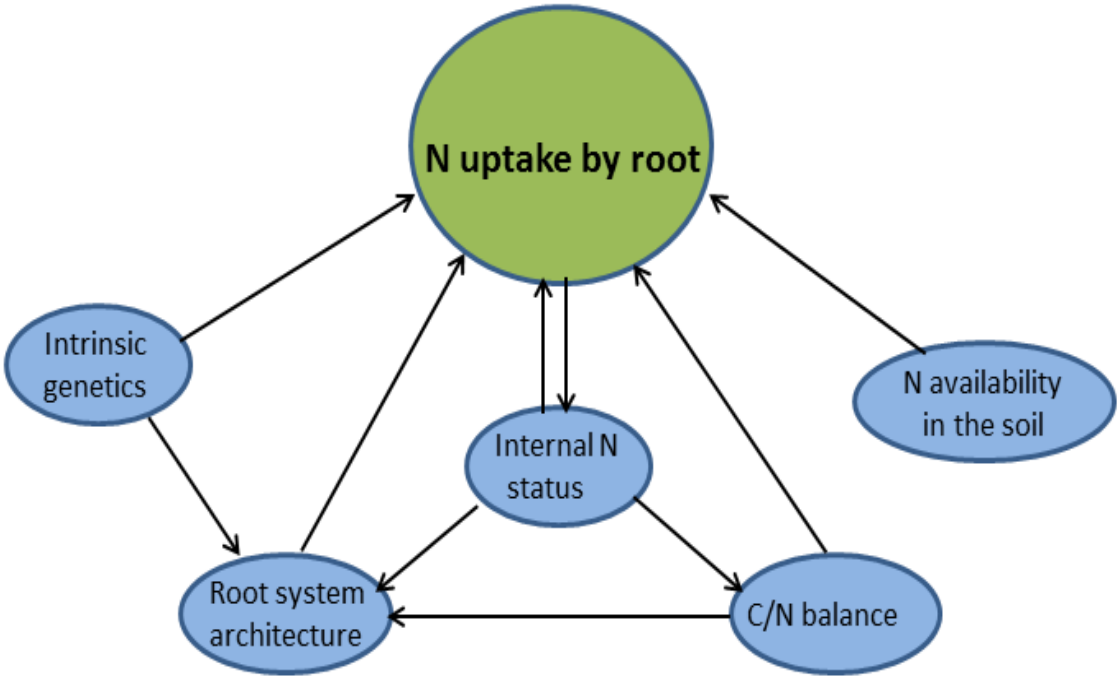

Fig 5. 4 Correlation network and regulatory components in N uptake by the roots

It is clear from this study, and others preceding it, that N uptake and assimilation are strongly linked to C metabolism. However, the signalling mechanisms underpinning the coordination between N and C metabolism are mostly unknown. By using high throughput sequencing, it may be possible for future studies to identify novel players correlated with changes in C and N status in plants experimentally manipulated to possess a wide range of C/N ratios. Root system architecture, as another important determinant of N uptake, was also investigated in this study. Modifications of RSA were correlated to N uptake in the plate-vertical culture system. This study helped assess the functional significance of root traits in N uptake. In future research, a wide range of architectural and anatomical root phenotypes should be used to investigate whether the variation of root traits is associated with N uptake under field conditions, and to what extent each root trait correlates to N uptake. Although not involved in this thesis, the impacts of plant roots and rhizosphere microbes on N uptake should be investigated. Understanding and manipulating interactions at the root /soil /microbe interface may be a productive tool, providing benefits for plant nutrient uptake under field conditions.

In order to increase yield, considerable amounts of N fertilisers are applied to crops each year. However, about 25-70% of applied N fertilisers in agricultural systems are leached and released to the environment, in the form of NO, N_2O and NH_3, with potentially severe negative environmental outcomes (Davidson *et al.* 2011; Sutton *et al.* 2011; De Vries *et al.* 2013; Qiao *et al.* 2015). Improving N utilization efficiency is a priority to maintain food production while alleviating the deleterious environmental effects of fertiliser N. The study of the impact of perturbing C/N on nitrate uptake (Chapter 2) threw light on how plants such as perennial grasses take up and use nitrogen during the gazing cycle. These findings will help further in efforts to improve nitrogen use efficiency. Advice to farmers would be to avoid addition of N fertiliser too soon after grazing, as this may result in relatively low N uptake due to the low carbon availability in recently defoliated plants. Appling N fertilizers at the right time could benefit the agricultural system by achieving greater production with lower inputs. However, the optimum timing for N fertilizer addition after grazing is yet to be established. A key point for the future work would be investigating the spatiotemporal changes in N uptake rate and carbohydrate remobilisation during several rotations of grazing to identify the optimal timing for N addition.

Literature Cited

Andrews, M (1986) The partitioning of nitrate assimilation between root and shoot of higher plants. *Plant, Cell & Environment* **9**, 511-519.

Antoniadi, I, Plačková, L, Simonovik, B, Doležal, K, Turnbull, C, Ljung, K, Novák, O (2015) Cell-type-specific cytokinin distribution within the *Arabidopsis* primary root apex. *The Plant Cell* **27**, 1955-1967.

Araya, T, Miyamoto, M, Wibowo, J, Suzuki, A, Kojima, S, Tsuchiya, YN, Sawa, S, Fukuda, H, Von Wirén, N, Takahashi, H (2014) CLE-CLAVATA1 peptide-receptor signaling module regulates the expansion of plant root systems in a nitrogen-dependent manner. *Proceedings of the National Academy of Sciences* **111**, 2029-2034.

Balkos, KD, Britto, DT, Kronzucker, HJ (2010) Optimization of ammonium acquisition and metabolism by potassium in rice (Oryza sativa L. cv. IR-72). *Plant, Cell & Environment* **33**, 23-34.

Bari, R, Pant, BD, Stitt, M, Scheible, W-R (2006) PHO2, microRNA399, and PHR1 define a phosphate-signaling pathway in plants. *Plant Physiology* **141**, 988-999.

Benková, E, Michniewicz, M, Sauer, M, Teichmann, T, Seifertová, D, Jürgens, G, Friml, J (2003) Local, efflux-dependent auxin gradients as a common module for plant organ formation. *Cell* **115**, 591-602.

Berntson, G (1994) Modelling root architecture: are there tradeoffs between efficiency and potential of resource acquisition? *New Phytologist* **127**, 483-493.

Bhalerao, RP, Eklöf, J, Ljung, K, Marchant, A, Bennett, M, Sandberg, G (2002) Shoot-derived auxin is essential for early lateral root emergence in *Arabidopsis* seedlings. *The Plant Journal* **29**, 325-332.

Bloom, A, Jackson, L, Smart, D (1993) Root growth as a function of ammonium and nitrate in the root zone. *Plant, Cell & Environment* **16**, 199-206.

Borch, K, Bouma, T, Lynch, J, Brown, K (1999) Ethylene: a regulator of root architectural responses to soil phosphorus availability. *Plant, Cell & Environment* **22**, 425-431.

Boucaud, J, Bigot, J (1989) Changes in the activities of nitrogen assimilation enzymes ofLolium perenne L. during regrowth after cutting. *Plant and Soil* **114**, 121-125.

Brenner, WG, Romanov, GA, Köllmer, I, Bürkle, L, Schmülling, T (2005) Immediate-early and delayed cytokinin response genes of *Arabidopsis thaliana* identified by genome-

wide expression profiling reveal novel cytokinin-sensitive processes and suggest cytokinin action through transcriptional cascades. *The Plant Journal* **44**, 314-333.

Britto, DT, Kronzucker, HJ (2002) NH_4^+ toxicity in higher plants: a critical review. *Journal of Plant Physiology* **159**, 567-584.

Burbach, C, Markus, K, Zhang, Y, Schlicht, M, Baluška, F (2012) Photophobic behavior of maize roots. *Plant Signaling & Behavior* **7**, 874-878.

Bussell, JD, Keech, O, Fenske, R, Smith, SM (2013) Requirement for the plastidial oxidative pentose phosphate pathway for nitrate assimilation in *Arabidopsis*. *The Plant Journal* **75**, 578-591.

Campbell, WH (1999) Nitrate reductase structure, function and regulation: bridging the gap between biochemistry and physiology. *Annual Review of Plant Biology* **50**, 277-303.

Canvin, D, Atkins, C (1974) Nitrate, nitrite and ammonia assimilation by leaves: effect of light, carbon dioxide and oxygen. *Planta* **116**, 207-224.

Cerezo, M, Tillard, P, Filleur, S, Muños, S, Daniel-Vedele, F, Gojon, A (2001) Major alterations of the regulation of root NO3− uptake are associated with the mutation of Nrt2. 1 and Nrt2. 2 genes in *Arabidopsis*. *Plant Physiology* **127**, 262-271.

Chalmers, J, Lidgett, A, Cummings, N, Cao, Y, Forster, J, Spangenberg, G (2005) Molecular genetics of fructan metabolism in perennial ryegrass. *Plant Biotechnology Journal* **3**, 459-474.

Chen, C-Z, Lv, X-F, Li, J-Y, Yi, H-Y, Gong, J-M (2012) *Arabidopsis* NRT1. 5 is another essential component in the regulation of nitrate reallocation and stress tolerance. *Plant Physiology* **159**, 1582-1590.

Chiu, CC, Lin, CS, Hsia, AP, Su, RC, Lin, HL, Tsay, YF (2004) Mutation of a nitrate transporter, AtNRT1 : 4, results in a reduced petiole nitrate content and altered leaf development. *Plant and Cell Physiology* **45**, 1139-1148.

Choi, J, Hwang, I (2007) Cytokinin: Perception, signal transduction, and role in plant growth and development. *Journal of Plant Biology* **50**, 98-108.

Choi, J, Lee, J, Kim, K, Cho, M, Ryu, H, An, G, Hwang, I (2012) Functional identification of OsHk6 as a homotypic cytokinin receptor in rice with preferential affinity for iP. *Plant and Cell Physiology* **53**, 1334-1343.

Clarkson, D, Deane-Drummond, CE (1983) 'Thermal adaptation of nitrate transport. In Nitrogen as an Ecological Factor. J.A. Lee, S. McNeill, and I.H. Rorison, eds (Oxford: Blackwell), pp. 211-224

Coruzzi, GM, Zhou, L (2001) Carbon and nitrogen sensing and signaling in plants: emerging 'matrix effects'. *Current Opinion in Plant Biology* **4**, 247-253.

Costigan, SE, Warnasooriya, SN, Humphries, BA, Montgomery, BL (2011) Root-localized phytochrome chromophore synthesis is required for photoregulation of root elongation and impacts root sensitivity to jasmonic acid in *Arabidopsis*. *Plant Physiology* **157**, 1138-1150.

Crawford, NM, Glass, AD (1998) Molecular and physiological aspects of nitrate uptake in plants. *Trends in Plant Science* **3**, 389-395.

Dathe, A, Postma, J, Postma-Blaauw, M, Lynch, J (2016) Impact of axial root growth angles on nitrogen acquisition in maize depends on environmental conditions. *Annals of Botany* **112**, 207-224.

Davidson, E, David, MB, Galloway, JN, Goodale, CL, Haeuber, R, Harrison, JA, Howarth, RW, Jaynes, DB, Lowrance, RR, Thomas, NB (2011) Excess nitrogen in the US environment: trends, risks, and solutions. *Issues in Ecology* **15**, 1092-8987.

Davies, PJ (1995) 'Plant hormones: physiology, biochemistry and molecular biology. DOI 10.1007/978-94-011-0473-9.

Dawar, K, Zaman, M, Rowarth, JS, Blennerhassett, J, Turnbull, MH (2010) The impact of urease inhibitor on the bioavailability of nitrogen in urea and in comparison with other nitrogen sources in ryegrass (*Lolium perenne* L.). *Crop and Pasture Science* **61**, 214-221.

De Jong, F, Thodey, K, Lejay, LV, Bevan, MW (2014) Glucose elevates NITRATE TRANSPORTER2. 1 protein levels and nitrate transport activity independently of its HEXOKINASE1-mediated stimulation of NITRATE TRANSPORTER2. 1 expression. *Plant Physiology* **164**, 308-320.

de Ruiter, J, Wilson, D, Maley, S, Fletcher, AL, Fraser, T, Scott, WR, Berryman, S, Dumbleton, A, Nichol, W (2009) Management practices for forage brassicas. *Christchurch: Forage Brassica Development Group*

De Smet, I, Vassileva, V, De Rybel, B, Levesque, MP, Grunewald, W, Van Damme, D, Van Noorden, G, Naudts, M, Van Isterdael, G, De Clercq, R (2008) Receptor-like kinase ACR4 restricts formative cell divisions in the *Arabidopsis* root. *Science* **322**, 594-597.

De Vries, W, Kros, J, Kroeze, C, Seitzinger, SP (2013) Assessing planetary and regional nitrogen boundaries related to food security and adverse environmental impacts. *Current Opinion in Environmental Sustainability* **5**, 392-402.

Deane-Drummond, CE, Clarkson, DT, Johnson, CB (1980) The effect of differential root and shoot temperature on the nitrate reductase activity, assayed in vivo and in vitro in roots of *Hordeum vulgare* (barley). *Planta* **148**, 455-461.

Del Bianco, M, Giustini, L, Sabatini, S (2013) Spatiotemporal changes in the role of cytokinin during root development. *New Phytologist* **199**, 324-338.

Delhon, P, Gojon, A, Tillard, P, Passama, L (1996) Diurnal regulation of NO_3^- uptake in soybean plants IV. Dependence on current photosynthesis and sugar availability to the roots. *Journal of Experimental Botany* **47**, 893-900.

Dobrenel, T, Marchive, C, Azzopardi, M, Clément, G, Moreau, M, Sormani, R, Robaglia, C, Meyer, C (2013) Sugar metabolism and the plant target of rapamycin kinase: a sweet operaTOR? *Frontiers in Plant Science* **4**, 93.

Dobrev, PI, Kamınek, M (2002) Fast and efficient separation of cytokinins from auxin and abscisic acid and their purification using mixed-mode solid-phase extraction. *Journal of Chromatography A* **950**, 21-29.

Dubrovsky, JG, Forde, BG (2012) Quantitative analysis of lateral root development: pitfalls and how to avoid them. *The Plant Cell* **24**, 4-14.

Fait, A, Nesi, AN, Angelovici, R, Lehmann, M, Pham, PA, Song, L, Haslam, RP, Napier, JA, Galili, G, Fernie, AR (2011) Targeted enhancement of glutamate-to-γ-aminobutyrate conversion in *Arabidopsis* seeds affects carbon-nitrogen balance and storage reserves in a development-dependent manner. *Plant Physiology* **157**, 1026-1042.

Fan, S-C, Lin, C-S, Hsu, P-K, Lin, S-H, Tsay, Y-F (2009) The *Arabidopsis* nitrate transporter NRT1.7, expressed in phloem, is responsible for source-to-sink remobilization of nitrate. *The Plant Cell Online* **21**, 2750-2761.

Filleur, S, Dorbe, M-F, Cerezo, M, Orsel, M, Granier, F, Gojon, A, Daniel-Vedele, F (2001) An *Arabidopsis* T-DNA mutant affected in *NRT2.1* genes is impaired in nitrate uptake. *FEBS letters* **489**, 220-224.

Fischer, E, Lohaus, G, Heineke, D, Heldt, H (1998) Magnesium deficiency results in accumulation of carbohydrates and amino acids in source and sink leaves of spinach. *Physiologia Plantarum* **102**, 16-20.

Fischer, R, Byerlee, D, Edmeades, GO (2009) Can technology deliver on the yield challenge to 2050. *Procedings of Expert Meeting on How to feed the World in 2050*, 24-26 June 2009. FAO, Rome.

Forde, BG (2002a) Local and long-range signaling pathways regulating plant responses to nitrate. *Annual Review of Plant Biology* **53**, 203-224.

Forde, BG (2002b) The role of long-distance signalling in plant responses to nitrate and other nutrients. *Journal of Experimental Botany* **53**, 39-43.

Forde, BG, Lea, PJ (2007) Glutamate in plants: metabolism, regulation, and signalling. *Journal of Experimental Botany* **58**, 2339-2358.

Forde, BG, Walch-Liu, P (2009) Nitrate and glutamate as environmental cues for behavioural responses in plant roots. *Plant, Cell & Environment* **32**, 682-693.

Fransen, B, Blijjenberg, J, de Kroon, H (1999) Root morphological and physiological plasticity of perennial grass species and the exploitation of spatial and temporal heterogeneous nutrient patches. *Plant and Soil* **211**, 179-189.

Freixes, S, Thibaud, MC, Tardieu, F, Muller, B (2002) Root elongation and branching is related to local hexose concentration in *Arabidopsis thaliana* seedlings. *Plant, Cell & Environment* **25**, 1357-1366.

Fukaki, H, Tasaka, M (2009) Hormone interactions during lateral root formation. *Plant Molecular Biology* **69**, 437-449.

Gabrielle, B, Justes, E, Denoroy, P (1998) 'Modelling of temperature and nitrogen effects on the rooting dynamics of winter oilseed rape, 16th International Society of Soil Science Congress.'

Gao, K, Chen, F, Yuan, L, Zhang, F, Mi, G (2015) A comprehensive analysis of root morphological changes and nitrogen allocation in maize in response to low nitrogen stress. *Plant, Cell & Environment* **38**, 740-750.

Garnett, T, Conn, V, Plett, D, Conn, S, Zanghellini, J, Mackenzie, N, Enju, A, Francis, K, Holtham, L, Roessner, U (2013) The response of the maize nitrate transport system to nitrogen demand and supply across the lifecycle. *New Phytologist* **198**, 82-94.

Giehl, RF, Gruber, BD, von Wirén, N (2014) It's time to make changes: modulation of root system architecture by nutrient signals. *Journal of Experimental Botany* **65**, 769-778.

Giehl, RF, Von Wirén, N (2014) Root nutrient foraging. *Plant Physiology* **166**, 509-517.

Gifford, ML, Dean, A, Gutierrez, RA, Coruzzi, GM, Birnbaum, KD (2008) Cell-specific nitrogen responses mediate developmental plasticity. *Proceedings of the National Academy of Sciences* **105**, 803-808.

Givan, CV (1979) Metabolic detoxification of ammonia in tissues of higher plants. *Phytochemistry* **18**, 375-382.

Good, AG, Shrawat, AK, Muench, DG (2004) Can less yield more? Is reducing nutrient input into the environment compatible with maintaining crop production? *Trends in Plant Science* **9**, 597-605.

Götz, K-P, Staroske, N, Radchuk, R, Emery, RN, Wutzke, K-D, Herzog, H, Weber, H (2007) Uptake and allocation of carbon and nitrogen in Vicia narbonensis plants with increased seed sink strength achieved by seed-specific expression of an amino acid permease. *Journal of Experimental Botany* **58**, 3183-3195.

Gruber, BD, Giehl, RF, Friedel, S, von Wirén, N (2013) Plasticity of the *Arabidopsis* root system under nutrient deficiencies. *Plant Physiology* **163**, 161-179.

Gutiérrez, RA, Lejay, LV, Dean, A, Chiaromonte, F, Shasha, DE, Coruzzi, GM (2007) Qualitative network models and genome-wide expression data define carbon/nitrogen-responsive molecular machines in Arabidopsis. *Genome Biology* **8**, R7.

Hamburger, D, Rezzonico, E, Petétot, JM-C, Somerville, C, Poirier, Y (2002) Identification and characterization of the Arabidopsis *PHO1* gene involved in phosphate loading to the xylem. *The Plant Cell* **14**, 889-902.

Hampton, J, Rolston, M, Pyke, N, Green, W (2012) Ensuring the long term viability of the New Zealand seed industry. *Agronomy New Zealand* **42**, 129-140.

Han, Y-L, Song, H-X, Liao, Q, Yu, Y, Jian, S-F, Lepo, JE, Liu, Q, Rong, X-M, Tian, C, Zeng, J (2016) Nitrogen use efficiency is mediated by vacuolar nitrate sequestration capacity in roots of *Brassica napus*. *Plant Physiology* pp. 01377.2015.

HavlovA, M, Dobrev, PI, Motyka, V, Štorchova, H, LIBUS, J, DobrA, J, Malbeck, J, GaudinovA, A, VankovA, R (2008) The role of cytokinins in responses to water deficit in tobacco plants over-expressing trans-zeatin O-glucosyltransferase gene under 35S or SAG12 promoters. *Plant, Cell & Environment* **31**, 341-353.

Hayes, JM (2004) An introduction to isotopic calculations. *Woods Hole Oceanographic Institution, Woods Hole, MA*. http://www. nosams.whoi.edu/research/staff_hayes.htm

He, C-J, Morgan, PW, Drew, MC (1992) Enhanced sensitivity to ethylene in nitrogen-or phosphate-starved roots of *Zea mays* L. during aerenchyma formation. *Plant Physiology* **98**, 137-142.

Hewelt, A, Prinsen, E, Schell, J, Onckelen, H, Schmülling, T (1994) Promoter tagging with a promoterless ipt gene leads to cytokinin-induced phenotypic variability in transgenic tobacco plants: implications of gene dosage effects. *The Plant Journal* **6**, 879-891.

Higuchi, M, Pischke, MS, Mähönen, AP, Miyawaki, K, Hashimoto, Y, Seki, M, Kobayashi, M, Shinozaki, K, Kato, T, Tabata, S (2004) In planta functions of the *Arabidopsis* cytokinin receptor family. *Proceedings of the National Academy of Sciences of the United States of America* **101**, 8821-8826.

Hirner, A, Ladwig, F, Stransky, H, Okumoto, S, Keinath, M, Harms, A, Frommer, WB, Koch, W (2006) *Arabidopsis* LHT1 is a high-affinity transporter for cellular amino acid uptake in both root epidermis and leaf mesophyll. *The Plant Cell* **18**, 1931-1946.

Hirose, N, Takei, K, Kuroha, T, Kamada-Nobusada, T, Hayashi, H, Sakakibara, H (2008) Regulation of cytokinin biosynthesis, compartmentalization and translocation. *Journal of Experimental Botany* **59**, 75-83.

Ho, C-H, Lin, S-H, Hu, H-C, Tsay, Y-F (2009a) CHL1 functions as a nitrate sensor in plants. *Cell* **138**, 1184-1194.

Ho, CH, Lin, SH, Hu, HC, Tsay, YF (2009b) CHL1 Functions as a Nitrate Sensor in Plants. *Cell* **138**, 1184-1194.

Huang, N-C, Liu, K-H, Lo, H-J, Tsay, Y-F (1999a) Cloning and functional characterization of an *Arabidopsis* nitrate transporter gene that encodes a constitutive component of low-affinity uptake. *The Plant Cell Online* **11**, 1381-1392.

Huang, NC, Liu, KH, Lo, HJ, Tsay, YF (1999b) Cloning and functional characterization of an *Arabidopsis* nitrate transporter gene that encodes a constitutive component of low-affinity uptake. *Plant Cell* **11**, 1381-1392.

Hwang, I, Sheen, J, Müller, B (2012) Cytokinin signaling networks. *Annual Review of Plant Biology* **63**, 353-380.

Hwang, S-J, Hamayun, M, Kim, H-Y, Na, C-I, Kim, K-U, Shin, D-H, Kim, S-Y, Lee, I-J (2007) Effect of nitrogen and silicon nutrition on bioactive gibberellin and growth of rice under field conditions. *J Crop Sci Biotech* **10**, 281-286.

Ioio, RD, Linhares, FS, Scacchi, E, Casamitjana-Martinez, E, Heidstra, R, Costantino, P, Sabatini, S (2007) Cytokinins determine *Arabidopsis* root-meristem size by controlling cell differentiation. *Current Biology* **17**, 678-682.

Izumi, K, Nakagawa, S, Kobayashi, M, Oshio, H, Sakurai, A, Takahashi, N (1988) Levels of IAA, cytokinins, ABA and ethylene in rice plants as affected by a gibberellin biosynthesis inhibitor, Uniconazole-P. *Plant and Cell Physiology* **29**, 97-104.

Jameson PE. 2017. Cytokinins. *Encyclopedia of Applied Plant Sciences* **1**, 391-402.

Jang, SW, Hamayun, M, Sohn, EY, Shin, DH, Kim, KU, Lee, BH, Lee, IJ (2008) Effect of elevated nitrogen levels on endogenous gibberellin and jasmonic acid contents of three rice (*Oryza sativa* L.) cultivars. *Journal of Plant Nutrition and Soil Science* **171**, 181-186.

Jiang, C, Gao, X, Liao, L, Harberd, NP, Fu, X (2007) Phosphate starvation root architecture and anthocyanin accumulation responses are modulated by the gibberellin-DELLA signaling pathway in *Arabidopsis*. *Plant Physiology* **145**, 1460-1470.

Jung, J-Y, Shin, R, Schachtman, DP (2009) Ethylene mediates response and tolerance to potassium deprivation in *Arabidopsis*. *The Plant Cell Online* **21**, 607-621.

Kakimoto, T (2001) Identification of plant cytokinin biosynthetic enzymes as dimethylallyl diphosphate: ATP/ADP isopentenyltransferases. *Plant and Cell Physiology* **42**, 677-685.

Khan, N, Mir, R, Khan, M, Javid, S (2002) Effects of gibberellic acid spray on nitrogen yield efficiency of mustard grown with different nitrogen levels. *Plant Growth Regulation* **38**, 243-247.

Kiba, T, Feria-Bourrellier, A-B, Lafouge, F, Lezhneva, L, Boutet-Mercey, S, Orsel, M, Bréhaut, V, Miller, A, Daniel-Vedele, F, Sakakibara, H (2012) The *Arabidopsis* nitrate transporter NRT2.4 plays a double role in roots and shoots of nitrogen-starved plants. *The Plant Cell Online* **24**, 245-258.

Kiba, T, Krapp, A (2016) Plant nitrogen acquisition under low availability: regulation of uptake and root architecture. *Plant and Cell Physiology* **4**, 707-714.

Kiba, T, Kudo, T, Kojima, M, Sakakibara, H (2011) Hormonal control of nitrogen acquisition: roles of auxin, abscisic acid, and cytokinin. *Journal of Experimental Botany* **62**, 1399-1409.

Kronzucker, H, Glass, A, Siddiqi, M, Kirk, G (2000) Comparative kinetic analysis of ammonium and nitrate acquisition by tropical lowland rice: implications for rice cultivation and yield potential. *New Phytologist* **145**, 471-476.

Kronzucker, HJ, Britto, DT, Davenport, RJ, Tester, M (2001) Ammonium toxicity and the real cost of transport. *Trends in Plant Science* **6**, 335-337.

Krouk, G, Lacombe, B, Bielach, A, Perrine-Walker, F, Malinska, K, Mounier, E, Hoyerova, K, Tillard, P, Leon, S, Ljung, K (2010) Nitrate-regulated auxin transport by NRT1.1 defines a mechanism for nutrient sensing in plants. *Developmental Cell* **18**, 927-937.

Krouk, G, Ruffel, S, Gutiérrez, RA, Gojon, A, Crawford, NM, Coruzzi, GM, Lacombe, B (2011) A framework integrating plant growth with hormones and nutrients. *Trends in Plant Science* **16**, 178-182.

Krupa, S (2003) Effects of atmospheric ammonia (NH_3) on terrestrial vegetation: a review. *Environmental Pollution* **124**, 179-221.

Kuderová, A, Urbánková, I, Válková, M, Malbeck, J, Brzobohatý, B, Némethová, D, Hejátko, J (2008) Effects of conditional IPT-dependent cytokinin overproduction on root architecture of *Arabidopsis* seedlings. *Plant and Cell Physiology* **49**, 570-582.

Kudo, T, Kiba, T, Sakakibara, H (2010) Metabolism and long-distance translocation of cytokinins. *Journal of Integrative Plant Biology* **52**, 53-60.

Kudo, T, Makita, N, Kojima, M, Tokunaga, H, Sakakibara, H (2012) Cytokinin activity of cis-zeatin and phenotypic alterations induced by overexpression of putative cis-zeatin-O-glucosyltransferase in rice. *Plant Physiology* **160**, 319-331.

Kushwah, S, Laxmi, A (2014) The interaction between glucose and cytokinin signal transduction pathway in *Arabidopsis thaliana. Plant, Cell & Environment* **37**, 235-253.

Lally, D, Ingmire, P, Tong, H-Y, He, Z-H (2001) Antisense expression of a cell wall–associated protein kinase, WAK4, inhibits cell elongation and alters morphology. *The Plant Cell* **13**, 1317-1332.

Lancien, M, Gadal, P, Hodges, M (2000) Enzyme redundancy and the importance of 2-oxoglutarate in higher plant ammonium assimilation. *Plant Physiology* **123**, 817-824.

Laplaze, L, Benkova, E, Casimiro, I, Maes, L, Vanneste, S, Swarup, R, Weijers, D, Calvo, V, Parizot, B, Herrera-Rodriguez, MB (2007) Cytokinins act directly on lateral root founder cells to inhibit root initiation. *The Plant Cell* **19**, 3889-3900.

Laugier, E, Bouguyon, E, Mauriès, A, Tillard, P, Gojon, A, Lejay, L (2012) Regulation of high-affinity nitrate uptake in roots of *Arabidopsis* depends predominantly on posttranscriptional control of the NRT2.1/NAR2.1 transport system. *Plant Physiology* **158**, 1067-1078.

Lea, P, Forde, B (1994) The use of mutants and transgenic plants to study amino acid metabolism. *Plant, Cell & Environment* **17**, 541-556.

Lea, P, Miflin, B (1974) Alternative route for nitrogen assimilation in higher plants. *Nature* **251**, 614-616.

Leakey, AD, Ainsworth, EA, Bernacchi, CJ, Rogers, A, Long, SP, Ort, DR (2009) Elevated CO2 effects on plant carbon, nitrogen, and water relations: six important lessons from FACE. *Journal of Experimental Botany* **60**, 2859-2876.

LeClere, S, Schmelz, EA, Chourey, PS (2010) Sugar levels regulate tryptophan-dependent auxin biosynthesis in developing maize kernels. *Plant Physiology* **153**, 306-318.

Lei, M, Liu, Y, Zhang, B, Zhao, Y, Wang, X, Zhou, Y, Raghothama, KG, Liu, D (2011) Genetic and genomic evidence that sucrose is a global regulator of plant responses to phosphate starvation in *Arabidopsis*. *Plant Physiology* **156**, 1116-1130.

Lejay, L, Gansel, X, Cerezo, M, Tillard, P, Müller, C, Krapp, A, von Wirén, N, Daniel-Vedele, F, Gojon, A (2003) Regulation of root ion transporters by photosynthesis: functional importance and relation with hexokinase. *The Plant Cell* **15**, 2218-2232.

Lejay, L, Tillard, P, Lepetit, M, Olive, FD, Filleur, S, Daniel-Vedele, F, Gojon, A (1999) Molecular and functional regulation of two NO_3^- uptake systems by N-and C-status of *Arabidopsis* plants. *The Plant Journal* **18**, 509-519.

Lejay, L, Wirth, J, Pervent, M, Cross, JM-F, Tillard, P, Gojon, A (2008) Oxidative pentose phosphate pathway-dependent sugar sensing as a mechanism for regulation of root ion transporters by photosynthesis. *Plant Physiology* **146**, 2036-2053.

Lemaire, L, Deleu, C, Le Deunff, E (2013) Modulation of ethylene biosynthesis by ACC and AIB reveals a structural and functional relationship between the $K^{15}NO_3$ uptake rate and root absorbing surfaces. *Journal of Experimental Botany* **64**, 2725-2737.

Lestienne, F, Thornton, B, Gastal, F (2006) Impact of defoliation intensity and frequency on N uptake and mobilization in *Lolium perenne*. *Journal of Experimental Botany* **57**, 997-1006.

Li, J-Y, Fu, Y-L, Pike, SM, Bao, J, Tian, W, Zhang, Y, Chen, C-Z, Zhang, Y, Li, H-M, Huang, J (2010a) The *Arabidopsis* nitrate transporter NRT1. 8 functions in nitrate removal from the xylem sap and mediates cadmium tolerance. *The Plant Cell* **22**, 1633-1646.

Li, Q, LI, BH, Kronzucker, HJ, SHI, WM (2010b) Root growth inhibition by NH4+ in *Arabidopsis* is mediated by the root tip and is linked to NH_4^+ efflux and GMPase activity. *Plant, Cell & Environment* **33**, 1529-1542.

Li, W, Wang, Y, Okamoto, M, Crawford, NM, Siddiqi, MY, Glass, AD (2007) Dissection of the AtNRT2. 1: AtNRT2. 2 inducible high-affinity nitrate transporter gene cluster. *Plant Physiology* **143**, 425-433.

Li, X, Mo, X, Shou, H, Wu, P (2006a) Cytokinin-mediated cell cycling arrest of pericycle founder cells in lateral root initiation of *Arabidopsis*. *Plant and Cell Physiology* **47**, 1112-1123.

Li, Y, Lee, KK, Walsh, S, Smith, C, Hadingham, S, Sorefan, K, Cawley, G, Bevan, MW (2006b) Establishing glucose-and ABA-regulated transcription networks in

Arabidopsis by microarray analysis and promoter classification using a Relevance Vector Machine. *Genome Research* **16**, 414-427.

Lilley, JLS, Gee, CW, Sairanen, I, Ljung, K, Nemhauser, JL (2012) An endogenous carbon-sensing pathway triggers increased auxin flux and hypocotyl elongation. *Plant Physiology* **160**, 2261-2270.

Lima, JE, Kojima, S, Takahashi, H, von Wirén, N (2010) Ammonium triggers lateral root branching in *Arabidopsis* in an AMMONIUM TRANSPORTER1; 3-dependent manner. *The Plant Cell* **22**, 3621-3633.

Lin, S-H, Kuo, H-F, Canivenc, G, Lin, C-S, Lepetit, M, Hsu, P-K, Tillard, P, Lin, H-L, Wang, Y-Y, Tsai, C-B (2008a) Mutation of the *Arabidopsis* NRT1. 5 nitrate transporter causes defective root-to-shoot nitrate transport. *The Plant Cell* **20**, 2514-2528.

Lin, S-H, Kuo, H-F, Canivenc, G, Lin, C-S, Lepetit, M, Hsu, P-K, Tillard, P, Lin, H-L, Wang, Y-Y, Tsai, C-B (2008b) Mutation of the Arabidopsis NRT1. 5 nitrate transporter causes defective root-to-shoot nitrate transport. *The Plant Cell Online* **20**, 2514-2528.

Linkohr, BI, Williamson, LC, Fitter, AH, Leyser, H (2002) Nitrate and phosphate availability and distribution have different effects on root system architecture of *Arabidopsis*. *The Plant Journal* **29**, 751-760.

Liu, K-H, Huang, C-Y, Tsay, Y-F (1999a) CHL1 is a dual-affinity nitrate transporter of *Arabidopsis* involved in multiple phases of nitrate uptake. *The Plant Cell Online* **11**, 865-874.

Liu, K-H, Huang, C-Y, Tsay, Y-F (1999b) CHL1 is a dual-affinity nitrate transporter of *Arabidopsis* involved in multiple phases of nitrate uptake. *The Plant Cell* **11**, 865-874.

Liu, K-H, Tsay, Y-F (2003) Switching between the two action modes of the dual-affinity nitrate transporter CHL1 by phosphorylation. *The EMBO Journal* **22**, 1005-1013.

Liu, Y, Lai, N, Gao, K, Chen, F, Yuan, L, Mi, G (2013) Ammonium inhibits primary root growth by reducing the length of meristem and elongation zone and decreasing elemental expansion rate in the root apex in *Arabidopsis thaliana*. *PLoS One* **8**, e61031.

Ljung, K, Hull, AK, Celenza, J, Yamada, M, Estelle, M, Normanly, J, Sandberg, G (2005) Sites and regulation of auxin biosynthesis in *Arabidopsis* roots. *The Plant Cell Online* **17**, 1090-1104.

Lomin, SN, Yonekura-Sakakibara, K, Romanov, GA, Sakakibara, H (2011) Ligand-binding properties and subcellular localization of maize cytokinin receptors. *Journal of Experimental Botany* **62**, 5149-5159.

Long, C, Held, M, Hayward, A, Nisler, J, Spíchal, L, Neil Emery, R, Moffatt, BA, Guinel, FC (2012) Seed development, seed germination and seedling growth in the R50 (sym16) pea mutant are not directly linked to altered cytokinin homeostasis. *Physiologia Plantarum* **145**, 341-359.

López-Bucio, J, Cruz-Ramírez, A, Herrera-Estrella, L (2003) The role of nutrient availability in regulating root architecture. *Current Opinion in Plant Biology* **6**, 280-287.

Lothier, J, Lasseur, B, Le Roy, K, Van Laere, A, Prud'homme, M-P, Barre, P, Van den Ende, W, Morvan-Bertrand, A (2007) Cloning, gene mapping, and functional analysis of a fructan 1-exohydrolase (1-FEH) from *Lolium perenne* implicated in fructan synthesis rather than in fructan mobilization. *Journal of Experimental Botany* **58**, 1969-1983.

Louahlia, S, Laine, P, MacDuff, J, Ourry, A, Humphreys, M, Boucaud, J (2008) Interactions between reserve mobilization and regulation of nitrate uptake during regrowth of *Lolium perenne* L.: putative roles of amino acids and carbohydrates. *Botany* **86**, 1101-1110.

Louahlia, S, Macduff, J, Ourry, A, Humphreys, M, Boucaud, J (1999) Nitrogen reserve status affects the dynamics of nitrogen remobilization and mineral nitrogen uptake during recovery of contrasting cultivars of *Lolium perenne* from defoliation. *New Phytologist* **142**, 451-462.

Lynch, J (1995) Root architecture and plant productivity. *Plant Physiology* **109**, 7-13.

Lynch, JP (2013) Steep, cheap and deep: an ideotype to optimize water and N acquisition by maize root systems. *Annals of Botany* **112**, 347-357.

Ma, Q, Tang, R-J, Zheng, X-J, Wang, S-M, Luan, S (2015) The calcium sensor CBL7 modulates plant responses to low nitrate in Arabidopsis. *Biochemical and Biophysical Research Communications* **468**, 59-65.

Ma, W, Li, J, Qu, B, He, X, Zhao, X, Li, B, Fu, X, Tong, Y (2014) Auxin biosynthetic gene TAR2 is involved in low nitrogen-mediated reprogramming of root architecture in *Arabidopsis*. *The Plant Journal* **78**, 70-79.

Macková, H, Hronková, M, Dobrá, J, Turečková, V, Novák, O, Lubovská, Z, Motyka, V, Haisel, D, Hájek, T, Prášil, IT (2013) Enhanced drought and heat stress tolerance of tobacco plants with ectopically enhanced cytokinin oxidase/dehydrogenase gene expression. *Journal of Experimental Botany* **131**, 247-257.

Magyar, G, Kun, Á, Oborny, B, Stuefer, JF (2007) Importance of plasticity and decision-making strategies for plant resource acquisition in spatio-temporally variable environments. *New Phytologist* **174**, 182-193.

Malamy, J (2005) Intrinsic and environmental response pathways that regulate root system architecture. *Plant, Cell & Environment* **28**, 67-77.

Marhavý, P, Duclercq, J, Weller, B, Feraru, E, Bielach, A, Offringa, R, Friml, J, Schwechheimer, C, Murphy, A, Benková, E (2014) Cytokinin controls polarity of PIN1-dependent auxin transport during lateral root organogenesis. *Current Biology* **24**, 1031-1037.

Martín, AC, Del Pozo, JC, Iglesias, J, Rubio, V, Solano, R, De La Peña, A, Leyva, A, Paz-Ares, J (2000) Influence of cytokinins on the expression of phosphate starvation responsive genes in *Arabidopsis*. *The Plant Journal* **24**, 559-567.

Martin, T, Oswald, O, Graham, IA (2002) *Arabidopsis* seedling growth, storage lipid mobilization, and photosynthetic gene expression are regulated by carbon: nitrogen availability. *Plant Physiology* **128**, 472-481.

Masclaux-Daubresse, C, Daniel-Vedele, F, Dechorgnat, J, Chardon, F, Gaufichon, L, Suzuki, A (2010) Nitrogen uptake, assimilation and remobilization in plants: challenges for sustainable and productive agriculture. *Annals of Botany* **105**, 1141-1157.

Matsumoto-Kitano, M, Kusumoto, T, Tarkowski, P, Kinoshita-Tsujimura, K, Václavíková, K, Miyawaki, K, Kakimoto, T (2008) Cytokinins are central regulators of cambial activity. *Proceedings of the National Academy of Sciences* **105**, 20027-20031.

Matt, P, Geiger, M, Walch-Liu, P, Engels, C, Krapp, A, Stitt, M (2001) The immediate cause of the diurnal changes of nitrogen metabolism in leaves of nitrate-replete tobacco: a major imbalance between the rate of nitrate reduction and the rates of nitrate uptake and ammonium metabolism during the first part of the light period. *Plant, Cell & Environment* **24**, 177-190.

McCormack, ML, Dickie, IA, Eissenstat, DM, Fahey, TJ, Fernandez, CW, Guo, D, Helmisaari, HS, Hobbie, EA, Iversen, CM, Jackson, RB (2015) Redefining fine roots improves understanding of below-ground contributions to terrestrial biosphere processes. *New Phytologist* **207**, 505-518.

Medford, JI, Horgan, R, El-Sawi, Z, Klee, HJ (1989) Alterations of endogenous cytokinins in transgenic plants using a chimeric isopentenyl transferase gene. *The Plant Cell* **1**, 403-413.

Miller, A, Cramer, M (2005) Root nitrogen acquisition and assimilation. In 'Root Physiology: from Gene to Function.'. 1-36.

Miyawaki, K, Matsumoto-Kitano, M, Kakimoto, T (2004) Expression of cytokinin biosynthetic isopentenyltransferase genes in *Arabidopsis*: tissue specificity and regulation by auxin, cytokinin, and nitrate. *Plant Journal* **37**, 128-138.

Miyawaki, K, Tarkowski, P, Matsumoto-Kitano, M, Kato, T, Sato, S, Tarkowska, D, Tabata, S, Sandberg, G, Kakimoto, T (2006) Roles of *Arabidopsis* ATP/ADP isopentenyltransferases and tRNA isopentenyltransferases in cytokinin biosynthesis. *Proceedings of the National Academy of Sciences* **103**, 16598-16603.

Mok, DW, Mok, MC (2001) Cytokinin metabolism and action. *Annual Review of Plant Biology* **52**, 89-118.

Morère-Le Paven, M-C, Viau, L, Hamon, A, Vandecasteele, C, Pellizzaro, A, Bourdin, C, Laffont, C, Lapied, B, Lepetit, M, Frugier, F (2011) Characterization of a dual-affinity nitrate transporter MtNRT1. 3 in the model legume *Medicago truncatula*. *Journal of Experimental Botany* **62**, 5595-5605.

Morvan-Bertrand, A, Boucaud, J, Le Saos, J, Prud'homme, M-P (2001) Roles of the fructans from leaf sheaths and from the elongating leaf bases in the regrowth following defoliation of *Lolium perenne* L. *Planta* **213**, 109-120.

Morvan-Bertrand, A, Boucaud, J, Prud'homme, M-P (1999) Influence of initial levels of carbohydrates, fructans, nitrogen, and soluble proteins on regrowth of *Lolium perenne* L. cv. Bravo following defoliation. *Journal of Experimental Botany* **50**, 1817-1826.

Mulvaney, R, Khan, S, Ellsworth, T (2009) Synthetic nitrogen fertilizers deplete soil nitrogen: a global dilemma for sustainable cereal production. *Journal of Environmental Quality* **38**, 2295-2314.

Novák, J, Černý, M, Pavlů, J, Zemánková, J, Skalák, J, Plačková, L, Brzobohatý, B (2015) Roles of proteome dynamics and cytokinin signaling in root to hypocotyl ratio changes induced by shading roots of *Arabidopsis* seedlings. *Plant and Cell Physiology* **26**, 217-228

Novoplansky, A (2002) Developmental plasticity in plants: implications of non-cognitive behavior. *Evolutionary Ecology* **16**, 177-188.

Nunes-Nesi, A, Fernie, AR, Stitt, M (2010) Metabolic and signaling aspects underpinning the regulation of plant carbon nitrogen interactions. *Molecular Plant (Oxford University Press/USA)* **3**,

Okamoto, M, Kumar, A, Li, W, Wang, Y, Siddiqi, MY, Crawford, NM, Glass, AD (2006) High-affinity nitrate transport in roots of *Arabidopsis* depends on expression of the NAR2-like gene AtNRT3. 1. *Plant Physiology* **140**, 1036-1046.

Okamoto, M, Vidmar, JJ, Glass, AD (2003) Regulation of NRT1 and NRT2 gene families of *Arabidopsis thaliana*: responses to nitrate provision. *Plant and Cell Physiology* **44**, 304-317.

Orsel, M, Chopin, F, Leleu, O, Smith, SJ, Krapp, A, Daniel-Vedele, F, Miller, AJ (2006) Characterization of a two-component high-affinity nitrate uptake system in *Arabidopsis*. Physiology and protein-protein interaction. *Plant Physiology* **142**, 1304-1317.

Ourry, A, Bigot, J, Boucaud, J (1989) Protein mobilization from stubble and roots, and proteolytic activities during post-clipping re-growth of perennial ryegrass. *Journal of Plant Physiology* **134**, 298-303.

Palenchar, PM, Kouranov, A, Lejay, LV, Coruzzi, GM (2004) Genome-wide patterns of carbon and nitrogen regulation of gene expression validate the combined carbon and nitrogen (CN)-signaling hypothesis in plants. *Genome Biol* **5**, R91.

Paul, M, Driscoll, S (1997) Sugar repression of photosynthesis: the role of carbohydrates in signalling nitrogen deficiency through source: sink imbalance. *Plant, Cell & Environment* **20**, 110-116.

Péret, B, De Rybel, B, Casimiro, I, Benková, E, Swarup, R, Laplaze, L, Beeckman, T, Bennett, MJ (2009) *Arabidopsis* lateral root development: an emerging story. *Trends in plant science* **14**, 399-408.

Postma, JA, Dathe, A, Lynch, JP (2014) The optimal lateral root branching density for maize depends on nitrogen and phosphorus availability. *Plant Physiology* **166**, 590-602.

Pound, MP, French, AP, Atkinson, JA, Wells, DM, Bennett, MJ, Pridmore, T (2013) RootNav: navigating images of complex root architectures. *Plant physiology* **162**, 1802-1814.

Qiao, C, Liu, L, Hu, S, Compton, JE, Greaver, TL, Li, Q (2015) How inhibiting nitrification affects nitrogen cycle and reduces environmental impacts of anthropogenic nitrogen input. *Global Change Biology* **21**, 1249-1257.

Ramesh, SA, Tyerman, SD, Xu, B, Bose, J, Kaur, S, Conn, V, Domingos, P, Ullah, S, Wege, S, Shabala, S (2015) GABA signalling modulates plant growth by directly regulating the activity of plant-specific anion transporters. *Nature Communications* **6**, 82-93.

Remans, T, Nacry, P, Pervent, M, Filleur, S, Diatloff, E, Mounier, E, Tillard, P, Forde, BG, Gojon, A (2006) The *Arabidopsis* NRT1. 1 transporter participates in the signaling pathway triggering root colonization of nitrate-rich patches. *Proceedings of the National Academy of Sciences* **103**, 19206-19211.

Richards, J, 1993. Physiology of plants recovering from defoliation. In 'Grassland for our world'.(Ed. MJ Bakes) pp. 85-94. SIR Publishing: Wellington, New Zealand,

Rideout, JW, Raper Jr, CD (1994) Diurnal changes in net uptake rate of nitrate are associated with changes in estimated export of carbohydrates to roots. *International Journal of Plant Sciences* 173-179.

Robaglia, C, Thomas, M, Meyer, C (2012) Sensing nutrient and energy status by SnRK1 and TOR kinases. *Current Opinion in Plant Biology* **15**, 301-307.

Roche, J, Love, J, Guo, Q, Song, J, Cao, M, Fraser, K, Huege, J, Jones, C, Novák, O, Turnbull, MH (2016) Metabolic changes and associated cytokinin signals in response to nitrate assimilation in roots and shoots of *Lolium perenne*. *Physiologia Plantarum*, **4**, 497-511.

Rolland, F, Baena-Gonzalez, E, Sheen, J (2006) Sugar sensing and signaling in plants: conserved and novel mechanisms. *Annu. Rev. Plant Biol.* **57**, 675-709.

Romanov, GA, Lomin, SN, Schmülling, T (2006) Biochemical characteristics and ligand-binding properties of *Arabidopsis* cytokinin receptor AHK3 compared to CRE1/AHK4 as revealed by a direct binding assay. *Journal of Experimental Botany* **57**, 4051-4058.

Romera FJ, Alcantara E, de la Guardia MD (1999) Ethylene production by Fe-deficient roots and its involvement in the regulation of Fe-deficiency stress responses by strategy I plants. *Annals of Botany* **83**, 51-55.

Rosas, U, Cibrian-Jaramillo, A, Ristova, D, Banta, JA, Gifford, ML, Fan, AH, Zhou, RW, Kim, GJ, Krouk, G, Birnbaum, KD (2013) Integration of responses within and across *Arabidopsis* natural accessions uncovers loci controlling root systems architecture. *Proceedings of the National Academy of Sciences* **110**, 15133-15138.

Rossi, L, McDonagh, J, McEvoy, M, O'Donovan, M, Lee, J, Chapman, D, Edwards, G (2014) 'Implications of species and management interactions for ranking perennial ryegrass (*Lolium perenne* L.) cultivars: a progress report from two hemispheres, *Proceedings of the 6th Australasian Dairy Science Symposium*. 2014

Ruffel, S, Freixes, S, Balzergue, S, Tillard, P, Jeudy, C, Martin-Magniette, ML, van der Merwe, MJ, Kakar, K, Gouzy, J, Fernie, AR (2008) Systemic signaling of the plant

nitrogen status triggers specific transcriptome responses depending on the nitrogen source in *Medicago truncatula*. *Plant Physiology* **146**, 2020-2035.

Ruffel, S, Gojon, A, Lejay, L (2014) Signal interactions in the regulation of root nitrate uptake. *Journal of Experimental Botany* **65**, 5509-5517.

Ruffel, S, Krouk, G, Ristova, D, Shasha, D, Birnbaum, KD, Coruzzi, GM (2011) Nitrogen economics of root foraging: transitive closure of the nitrate–cytokinin relay and distinct systemic signaling for N supply vs. demand. *Proceedings of the National Academy of Sciences* **108**, 18524-18529.

Sairanen, I, Novák, O, Pěnčík, A, Ikeda, Y, Jones, B, Sandberg, G, Ljung, K (2012) Soluble carbohydrates regulate auxin biosynthesis via PIF proteins in *Arabidopsis*. *The Plant Cell* **24**, 4907-4916.

Sakakibara, H (2006) Cytokinins: activity, biosynthesis, and translocation. *Annu. Rev. Plant Biol.* **57**, 431-449.

Sakakibara, H, Takei, K, Hirose, N (2006) Interactions between nitrogen and cytokinin in the regulation of metabolism and development. *Trends in Plant Science* **11**, 440-448.

Santi, S, Locci, G, Monte, R, Pinton, R, Varanini, Z (2003) Induction of nitrate uptake in maize roots: expression of a putative high-affinity nitrate transporter and plasma membrane H^+-ATPase isoforms. *Journal of Experimental Botany* **54**, 1851-1864.

Santner, A, Estelle, M (2009) Recent advances and emerging trends in plant hormone signalling. *Nature* **459**, 1071-1078.

Scheible, W-R, Morcuende, R, Czechowski, T, Fritz, C, Osuna, D, Palacios-Rojas, N, Schindelasch, D, Thimm, O, Udvardi, MK, Stitt, M (2004) Genome-wide reprogramming of primary and secondary metabolism, protein synthesis, cellular growth processes, and the regulatory infrastructure of *Arabidopsis* in response to nitrogen. *Plant Physiology* **136**, 2483-2499.

Scheible, WR, Lauerer, M, Schulze, ED, Caboche, M, Stitt, M (1997) Accumulation of nitrate in the shoot acts as a signal to regulate shoot-root allocation in tobacco. *The Plant Journal* **11**, 671-691.

Schmelz, EA, Alborn, HT, Engelberth, J, Tumlinson, JH (2003) Nitrogen deficiency increases volicitin-induced volatile emission, jasmonic acid accumulation, and ethylene sensitivity in maize. *Plant Physiology* **133**, 295-306.

Schmidt, S, Raven, JA, Paungfoo-Lonhienne, C (2013) Goldacre Review: The mixotrophic nature of photosynthetic plants. *Functional Plant Biology* **40**, 425-438.

Schmittgen, TD, Livak, KJ (2008) Analyzing real-time PCR data by the comparative CT method. *Nature Protocols* **3**, 1101-1108.

Sheen, J, Zhou, L, Jang, J-C (1999) Sugars as signaling molecules. *Current Opinion in Plant Biology* **2**, 410-418.

Shin, R, Schachtman, DP (2004) Hydrogen peroxide mediates plant root cell response to nutrient deprivation. *Proceedings of the National Academy of Sciences of the United States of America* **101**, 8827-8832.

Shtratnikova, VY, Kudryakova, N, Kudoyarova, G, Korobova, A, Akhiyarova, G, Danilova, M, Kusnetsov, V, Kulaeva, O (2015) Effects of nitrate and ammonium on growth of *Arabidopsis thaliana* plants transformed with the ARR5:: GUS construct and a role for cytokinins in suppression of disturbances induced by the presence of ammonium. *Russian Journal of Plant Physiology* **62**, 741-752.

Siddiqi, MY, Glass, AD, Ruth, TJ, Rufty, TW (1990) Studies of the uptake of nitrate in barley I. Kinetics of $^{13}NO_3^-$ influx. *Plant Physiology* **93**, 1426-1432.

Signora, L, De Smet, I, Foyer, CH, Zhang, H (2001) ABA plays a central role in mediating the regulatory effects of nitrate on root branching in *Arabidopsis*. *The Plant Journal* **28**, 655-662.

Sims, IM, Pollock, CJ, Horgan, R (1992) Structural analysis of oligomeric fructans from excised leaves of *Lolium temulentum*. *Phytochemistry* **31**, 2989-2992.

Sivaguru, M, Pike, S, Gassmann, W, Baskin, TI (2003) Aluminum rapidly depolymerizes cortical microtubules and depolarizes the plasma membrane: evidence that these responses are mediated by a glutamate receptor. *Plant and Cell Physiology* **44**, 667-675.

Smirnoff, N, Stewart, G (1985) Nitrate assimilation and translocation by higher plants: comparative physiology and ecological consequences. *Physiologia Plantarum* **64**, 133-140.

Song, J, Jiang, L, Jameson, PE (2012) Co-ordinate regulation of cytokinin gene family members during flag leaf and reproductive development in wheat. *BMC plant biology* **12**, 1-16.

Song, J, Jiang, L, Jameson, PE (2015) Expression patterns of *Brassica napus* genes implicate IPT, CKX, sucrose transporter, cell wall invertase and amino acid permease gene family members in leaf, flower, silique and seed development. *Journal of Experimental Botany* **66**, 5067-5082

Spíchal, L, Werner, T, Popa, I, Riefler, M, Schmülling, T, Strnad, M (2009) The purine derivative PI-55 blocks cytokinin action via receptor inhibition. *FEBS Journal* **276**, 244-253.

Stitt, M, Krapp, A (1999) The interaction between elevated carbon dioxide and nitrogen nutrition: the physiological and molecular background. *Plant, Cell & Environment* **22**, 583-621.

Sutton, MA, Howard, CM, Erisman, JW, Billen, G, Bleeker, A, Grennfelt, P, Van Grinsven, H, Grizzetti, B (2011) The European nitrogen assessment: sources, effects and policy perspectives. *Cambridge University Press*, Cambridge.

Suzuki, A, Knaff, DB (2005) Glutamate synthase: structural, mechanistic and regulatory properties, and role in the amino acid metabolism. *Photosynthesis Research* **83**, 191-217.

Svačinová, J, Novák, O, Plačková, L, Lenobel, R, Holík, J, Strnad, M, Doležal, K (2012) A new approach for cytokinin isolation from *Arabidopsis* tissues using miniaturized purification: pipette tip solid-phase extraction. *Plant Methods* **8**, 1.

Takei, K, Sakakibara, H, Sugiyama, T (2001a) Identification of genes encoding adenylate isopentenyltransferase, a cytokinin biosynthesis enzyme, in *Arabidopsis thaliana*. *Journal of Biological Chemistry* **276**, 26405-26410.

Takei, K, Sakakibara, H, Taniguchi, M, Sugiyama, T (2001b) Nitrogen-Dependent Accumulation of Cytokinins in Root and theTranslocation to Leaf: Implication of Cytokinin Species that Induces GeneExpression of Maize ResponseRegulator. *Plant and Cell Physiology* **42**, 85-93.

Takei, K, Ueda, N, Aoki, K, Kuromori, T, Hirayama, T, Shinozaki, K, Yamaya, T, Sakakibara, H (2004a) AtIPT3 is a key determinant of nitrate-dependent cytokinin biosynthesis in *Arabidopsis*. *Plant and Cell Physiology* **45**, 1053-1062.

Takei, K, Yamaya, T, Sakakibara, H (2004b) Arabidopsis CYP735A1 and CYP735A2 encode cytokinin hydroxylases that catalyze the biosynthesis of trans-zeatin. *Journal of Biological Chemistry* **279**, 41866-41872.

Taub, DR, Wang, X (2008) Why are nitrogen concentrations in plant tissues lower under elevated CO_2? A critical examination of the hypotheses. *Journal of Integrative Plant Biology* **50**, 1365-1374.

Terasaka, K, Blakeslee, JJ, Titapiwatanakun, B, Peer, WA, Bandyopadhyay, A, Makam, SN, Lee, OR, Richards, EL, Murphy, AS, Sato, F (2005) PGP4, an ATP binding cassette

P-glycoprotein, catalyzes auxin transport in Arabidopsis thaliana roots. *The Plant Cell* **17**, 2922-2939.

Tian, Q, Chen, F, Liu, J, Zhang, F, Mi, G (2008) Inhibition of maize root growth by high nitrate supply is correlated with reduced IAA levels in roots. *Journal of Plant Physiology* **165**, 942-951.

Tian, QY, Sun, P, Zhang, WH (2009) Ethylene is involved in nitrate-dependent root growth and branching in Arabidopsis thaliana. *New Phytologist* **184**, 918-931.

Tsay, Y-F, Chiu, C-C, Tsai, C-B, Ho, C-H, Hsu, P-K (2007) Nitrate transporters and peptide transporters. *FEBS Letters* **581**, 2290-2300.

Tsay, Y-F, Ho, C-H, Chen, H-Y, Lin, S-H (2011) Integration of nitrogen and potassium signaling. *Annual Review of Plant Biology* **62**, 207-226.

Tsay, Y-F, Schroeder, JI, Feldmann, KA, Crawford, NM (1993) The herbicide sensitivity gene CHL1 of *Arabidopsis* encodes a nitrate-inducible nitrate transporter. *Cell* **72**, 705-713.

Turner, LB, Cairns, AJ, Armstead, IP, Ashton, J, Skøt, K, Whittaker, D, Humphreys, MO (2006) Dissecting the regulation of fructan metabolism in perennial ryegrass (*Lolium perenne*) with quantitative trait locus mapping. *New Phytologist* **169**, 45-58.

Van den Ende, W, De Coninck, B, Van Laere, A (2004) Plant fructan exohydrolases: a role in signaling and defense? *Trends in Plant Science* **9**, 523-528.

Van Vuuren, M, Robinson, D, Griffiths, B (1996) Nutrient inflow and root proliferation during the exploitation of a temporally and spatially discrete source of nitrogen in soil. *Plant and Soil* **178**, 185-192.

Veach, YK, Martin, RC, Mok, DW, Malbeck, J, Vankova, R, Mok, MC (2003) O-glucosylation of cis-zeatin in maize. Characterization of genes, enzymes, and endogenous cytokinins. *Plant Physiology* **131**, 1374-1380.

Vidmar, JJ, Zhuo, D, Siddiqi, MY, Schjoerring, JK, Touraine, B, Glass, AD (2000) Regulation of high-affinity nitrate transporter genes and high-affinity nitrate influx by nitrogen pools in roots of barley. *Plant Physiology* **123**, 307-318.

Vitousek, PM, Naylor, R, Crews, T, David, M, Drinkwater, L, Holland, E, Johnes, P, Katzenberger, J, Martinelli, L, Matson, P (2009) Nutrient imbalances in agricultural development. *Science* **324**, 1519.

Vyroubalová, Š, Václavíková, K, Turečková, V, Novák, O, Šmehilová, M, Hluska, T, Ohnoutková, L, Frébort, I, Galuszka, P (2009) Characterization of new maize genes

putatively involved in cytokinin metabolism and their expression during osmotic stress in relation to cytokinin levels. *Plant Physiology* **151**, 433-447.

Walch-Liu, P, Filleur, S, Gan, Y, Forde, BG (2005) Signaling mechanisms integrating root and shoot responses to changes in the nitrogen supply. *Photosynthesis Research* **83**, 239-250.

Walch-Liu, P, Forde, BG (2007) l-Glutamate as a novel modifier of root growth and branching: what's the sensor? *Plant Signaling & Behavior* **2**, 284-286.

Walch-Liu, P, Ivanov, II, Filleur, S, Gan, Y, Remans, T, Forde, BG (2006a) Nitrogen regulation of root branching. *Annals of Botany* **97**, 875-881.

Walch-Liu, P, Liu, L-H, Remans, T, Tester, M, Forde, BG (2006b) Evidence that L-glutamate can act as an exogenous signal to modulate root growth and branching in *Arabidopsis thaliana*. *Plant and Cell Physiology* **47**, 1045-1057.

Walch-Liu, P, Forde, BG (2008) Nitrate signalling mediated by the NRT1. 1 nitrate transporter antagonises l-glutamate-induced changes in root architecture. *The Plant Journal* **54**, 820-828.

Wan, Y, Jasik, J, Wang, L, Hao, H, Volkmann, D, Menzel, D, Mancuso, S, Baluška, F, Lin, J (2012) The signal transducer NPH3 integrates the phototropin1 photosensor with PIN2-based polar auxin transport in Arabidopsis root phototropism. *The Plant Cell* **24**, 551-565.

Wang, L, Ruan, Y-L (2016) Shoot-root carbon allocation, sugar signalling and their coupling with nitrogen uptake and assimilation. *Functional Plant Biology* **43**, 105-113.

Wang, X, Bian, Y, Cheng, K, Zou, H, Sun, SS-M, He, J-X (2012a) A comprehensive differential proteomic study of nitrate deprivation in Arabidopsis reveals complex regulatory networks of plant nitrogen responses. *Journal of Proteome Research* **11**, 2301-2315.

Wang, Y-Y, Hsu, P-K, Tsay, Y-F (2012b) Uptake, allocation and signaling of nitrate. *Trends in Plant Science* **17**, 458-467.

Wang, Y-Y, Tsay, Y-F (2011a) *Arabidopsis* nitrate transporter NRT1. 9 is important in phloem nitrate transport. *The Plant Cell Online* **23**, 1945-1957.

Wang, Y-Y, Tsay, Y-F (2011b) *Arabidopsis* nitrate transporter NRT1. 9 is important in phloem nitrate transport. *The Plant Cell* **23**, 1945-1957.

Werner, T, Holst, K, Pörs, Y, Guivarc'h, A, Mustroph, A, Chriqui, D, Grimm, B, Schmülling, T (2008) Cytokinin deficiency causes distinct changes of sink and source parameters in tobacco shoots and roots. *Journal of Experimental Botany* **59**, 2659-2672.

Werner, T, Motyka, V, Laucou, V, Smets, R, Van Onckelen, H, Schmülling, T (2003) Cytokinin-deficient transgenic *Arabidopsis* plants show multiple developmental alterations indicating opposite functions of cytokinins in the regulation of shoot and root meristem activity. *The Plant Cell* **15**, 2532-2550.

Wu, M-F, Tian, Q, Reed, JW (2006) Arabidopsis microRNA167 controls patterns of ARF6 and ARF8 expression, and regulates both female and male reproduction. *Development* **133**, 4211-4218.

Wuebbles, DJ (2009) Nitrous oxide: no laughing matter. *Science* **326**, 56-57.

Xu, G, Fan, X, Miller, AJ (2012) Plant nitrogen assimilation and use efficiency. *Annual Review of Plant Biology* **63**, 153-182.

Xu, J, Li, H-D, Chen, L-Q, Wang, Y, Liu, L-L, He, L, Wu, W-H (2006) A Protein kinase, interacting with two calcineurin B-like proteins, regulates K^+ transporter AKT1 in *Arabidopsis*. *Cell* **125**, 1347-1360.

Xu, W, Ding, G, Yokawa, K, Baluška, F, Li, Q-F, Liu, Y, Shi, W, Liang, J, Zhang, J (2013) An improved agar-plate method for studying root growth and response of *Arabidopsis thaliana*. *Scientific reports* **3**, 1273.

Yang, X, Lee, S, So, Jh, Dharmasiri, S, Dharmasiri, N, Ge, L, Jensen, C, Hangarter, R, Hobbie, L, Estelle, M (2004) The IAA1 protein is encoded by AXR5 and is a substrate of SCFTIR1. *The Plant Journal* **40**, 772-782.

Yokawa, K, Kagenishi, T, Baluška, F (2013) Root photomorphogenesis in laboratory-maintained *Arabidopsis* seedlings. *Trends in Plant Science* **18**, 117-119.

Yokawa, K, Kagenishi, T, Kawano, T, Mancuso, S, Baluška, F (2011) Illumination of *Arabidopsis* roots induces immediate burst of ROS production. *Plant Signaling & Behavior* **6**, 1460-1464.

Yonekura-Sakakibara, K, Kojima, M, Yamaya, T, Sakakibara, H (2004) Molecular characterization of cytokinin-responsive histidine kinases in maize. *Plant Physiology* **134**, 1654-1661.

Yong, Z, Kotur, Z, Glass, AD (2010) Characterization of an intact two-component high-affinity nitrate transporter from *Arabidopsis* roots. *The Plant Journal* **63**, 739-748.

York, LM, Silberbush, M, Lynch, JP (2016) Spatiotemporal variation of nitrate uptake kinetics within the maize (*Zea mays* L.) root system is associated with greater nitrate uptake and interactions with architectural phenes. *Journal of Experimental Botany* **67**, 3763-3775.

Zhang, H, Forde, BG (1998) An *Arabidopsis* MADS box gene that controls nutrient-induced changes in root architecture. *Science* **279**, 407-409.

Zhang, H, Forde, BG (2000) Regulation of *Arabidopsis* root development by nitrate availability. *Journal of Experimental Botany* **51**, 51-59.

Zhang, H, Jennings, A, Barlow, PW, Forde, BG (1999) Dual pathways for regulation of root branching by nitrate. *Proceedings of the National Academy of Sciences* **96**, 6529-6534.

Zhang, H, Rong, H, Pilbeam, D (2007) Signalling mechanisms underlying the morphological responses of the root system to nitrogen in *Arabidopsis thaliana. Journal of Experimental Botany* **58**, 2329-2338.

Zheng, D, Han, X, An, Y, Guo, H, Xia, X, Yin, W (2013) The nitrate transporter NRT2. 1 functions in the ethylene response to nitrate deficiency in *Arabidopsis*. *Plant, Cell & Environment*, **7**, 2328-2337.

Zhuo, D, Okamoto, M, Vidmar, JJ, Glass, AD (1999) Regulation of a putative high-affinity nitrate transporter (Nrt2; 1At) in roots of*Arabidopsis thaliana*. *The Plant Journal* **17**, 563-568.

Appendix 1-Supporting information for Chapter 2

Protocol for oligosaccharide profiling

Perennial ryegrass samples were harvested and immediately flash frozen in liquid nitrogen. Ground and freeze-dried plant materials (25 mg) were weighed and placed into 2 mL Eppendorf tubes for fructan extraction. After addition of 750 mL of boiling milliQ water, samples were vortexed for 5 s, placed on a heating block at 90 °C for 15 min, and then cooled down to room temperature and centrifuged at 14000 rpm for 10 min. The supernatants were transferred to filter tubes, centrifuged at 14000 rpm for 2 min and transferred to LC vials. Extracts were analyzed using an Agilent 1290 Infinity LC System (Agilent Technologies, Waldbronn, Germany) coupled to an Agilent 6550 Accurate-Mass QTOF LC-MS system with a dual Agilent Jet Stream source operating in negative mode. The QTOF was tuned for a mass range of 70-1700 m/z. A 2 µL aliquot of the sample was injected onto an Acquity UPLC HSS T3 C_{18} column (2.1 x 50 mm, 1.8 µm) combined with a 2.1 mm x 5 mm, 1.8 µm VanGuard precolumn (Waters Corporation, Milford, MA, USA) held at 40 °C. Compounds were eluted using a linear gradient consisting of 0.1 to 10% solvents (0.1% FA, 75/25 ACN/IPA) over 2 min. Mass spectrometry grade formic acid was purchased from Sigma-Aldrich (St Louis, MO, USA) and HPLC grade acetonitrile from Fisher Scientific (Fair Lawn, NJ, USA). Data was collected in centroid mode with an acquisition rate of 4 scans/s and 1975 transients/spectrum. Analytical data were exported as NetCDF files and processed and analyzed using in-house-scripts in MATLAB 7.14.739 (R2012a) (Mathworks, Natick, MA).

Table S1. Primer sequences

F, forward; R, reverse

Primers	Sequence	GenBank Accession No.
Lp1-FEHF	AAGGTGCCAAACATGTCCTC	AY693396.5
Lp1-FEHR	TGCGACGTCATCTGAAGAAC	
Lp6-FEHF	AGATAGTGTTTCAGATGATGGCGTG	KY554803
Lp6-FEHR	CATGCTCCATGCCCTGAGTTG	
LpNRT1.1F	CGTACATCGGVCAGCTMGACTTCT	KY554804
LpNRT1.1R	YTGATGTCGTCGGCGAGCCAG	
LpNRT1.2F	TCAGCAGCATTGGTGGAGAGTAAC	KY554805
LpNRT1.2R	GCACAAGAGAMAGGATRAACGAAY	
LpNRT1.3F	CCTCCTCTTCACCTCCCTCAACGAG	KY554806
LpNRT1.3R	AACTGCGGCACCAGCCAGAAC	
LpNRT1.4F	GGACCATCTACGCGCAGATGAT	KY554807
LpNRT1.4R	ACGAGGCCGATGCCGATCTTCTC	
LpNRT1.5F	CCWYMGCCCTGCTGCTSTTC	KY554808
LpNRT1.5R	AACCTGAAGCCTTYGGTGTGCAGAAG	
LpNRT2.1aF	CACCTCTCGTGGATCTCCTTCTT	KY554809
LpNRT2.1aR	GCGGCGAGCATGACGAGGAAG	
LpNRT2.1bF	GCTGGTGGTAACGTGGGTGCAG	KY554810
LpNRT2.1bR	AGCGGGAGTTCTCKGCRAACTTTTG	
LpNRT2.5F	CTGCCGCTCATCCGGGACAC	KY554811
LpNRT2.5R	MGKYGATGATGGASGAGCAGTACAC	
LpNRT2.7F	CATCCCCTGCGCCCTGCTCATC	KY554812
LpNRT2.7R	GCGGCCACGTTYTCCATGATGAG	
LpNARF	CGAGCACAAGGCSAAGWCCW	KY554813
LpNARR	AGCGGGAGTTCTCTGCGAACT	

LpNR1F	CCGTCCATGGCGGTTCCAATC	KY554814
LpNR1R	CCGGAGCCGTACTCGTC	
LpNRbF	CCTCACCGCCATCGTCGA	KY554815
LpNRbR	CAGGCCGACGAAGGAG	
LpNiRF	AGAGCAGCCACGCCGAC	KY554816
LpNiRR	ACACRAAGATGTGCTTG	
LpCKX4F	CTGAACCTTCTWATCCCAAGAAGC	KY554817
LpCKX4R	CAGGAGGCGTCCTTCGGTTTCA	
LpCKX6F	AGTTTGCGGTTCATGATTACCAGCAC	KY554818
LpCKX6R	CGCCCACGGAGAGGTAGAGGTAG	
***LpRR2*F**	CCAGTTCGTCTAGCTTTCAGAGTTCC	KU136271
***LpRR2*R**	GCCTTCACATCTGTCCACTAAATCCG	
***LpRR3*F**	ATCGTCGGAGCTGAAGCAGATTC	KU136272
***LpRR3*R**	CTGACAGGCTTGAGCAGGAACTC	
LpRR6F	GCATCCTCCGCAGCTCCAAGT	KU136273
LpRR6R	CGGGCATCCAGTAGTCGGTGAT	
***LpRR10*F**	CCAACCAGCACCCATTCTCAGTC	KU136275
***LpRR10*R**	GCCGCCAGTGATACACCATTTGA	
***LpRR12a*F**	GCAGGATTCTAGTATATCCCAGCAGTGT	KU136276
***LpRR12a*R**	TGCCAGAAGAACGAGTTCCACATTTG	
***LpRR12b*F**	GTTCCACAAGCGAAGATTGATTTCCTC	KU136277
***LpRR12b*R**	AAGCCCCGAGCGAGTAGAAGTC	

Table S 1-S6 Cytokinin concentrations in low (LN) and high (HN) roots and leaf sheaths 48 h after defoliation. Values are means ±SEM (n=5, pools of five plants each).*denotes significantly different means between intact plants (gray bars) and defoliated plants (black bars), or between defoliated plants (black bars) and defoliated plants supplemented with 1% glucose (white bars) or 1% mannitol (hatched bars) (* *P<0.05*, ** *P<0.01*, ***$P<0.001$).

e	Conditions	State	tZ		tZOG		tZR		tZROG		tZ7G		tZ9G	
	LN-0.05	NO CUT-T48	1.52 ± 0.28		0.11 ± 0.02		0.79 ± 0.24		0.35 ± 0.06		0.17 ± 0.02		25.38 ± 5.5	
ble	LN-0.05	CUT-T48	1.60 ± 0.54		0.15 ± 0.04		0.78 ± 0.22		0.37 ± 0.07		0.19 ± 0.04		34.71 ± 10.	
	HN-5	NO CUT-T48	4.81 ± 1.06		0.88 ± 0.17		2.91 ± 0.87		2.62 ± 0.75		0.40 ± 0.03		93.03 ± 25.	
	HN-5	CUT-T48	**2.75 ± 0.75**	*	0.62 ± 0.16		**1.01 ± 0.22**	**	1.96 ± 0.58		0.45 ± 0.04		**64.34 ± 11.**	
	LN-0.05	NO CUT-T48	1.06 ± 0.30		0.22 ± 0.02		0.51 ± 0.13		0.28 ± 0.09		0.33 ± 0.13		38.54 ± 8.0	
ot	LN-0.05	CUT-T48	1.67 ± 0.48		0.21 ± 0.03		0.53 ± 0.14		0.17 ± 0.04		**0.69 ± 0.24**	*	28.53 ± 4.3	
	HN-5	NO CUT-T48	2.49 ± 0.45		0.66 ± 0.16		1.61 ± 0.43		0.90 ± 0.13		0.67 ± 0.15		98.39 ± 26.	
	HN-5	CUT-T48	3.59 ± 1.17		0.57 ± 0.07		1.01 ± 0.31		**0.64 ± 0.14**	*	**0.41 ± 0.14**	*	109.67 ± 11.	
	Glucose-0.1%		1.94 ± 0.68		0.74 ± 0.16		1.54 ± 0.45		1.48 ± 0.37		0.38 ± 0.09		105.25 ± 21.	
ble	Mannitol-0.1%		2.05 ± 0.72		0.59 ± 0.12		1.24 ± 0.43		1.80 ± 0.49		0.38 ± 0.07		104.57 ± 28.	
	Glucose-1%		1.89 ± 0.65		**0.79 ± 0.15**	**	1.07 ± 0.26		**2.03 ± 0.31**	*	0.47 ± 0.08		89.94 ± 15.	
	Mannitol-1%		1.60 ± 0.59		0.44 ± 0.06		0.72 ± 0.26		1.54 ± 0.12		0.37 ± 0.08		75.96 ± 12.	
	Glucose-0.1%		**2.80 ± 0.45**	*	**0.99 ± 0.19**	**	1.00 ± 0.24		**0.38 ± 0.13**	**	0.14 ± 0.02		106.20 ± 22.	
ot	Mannitol-0.1%		1.94 ± 0.57		0.56 ± 0.14		1.21 ± 0.36		0.86 ± 0.19		0.12 ± 0.02		99.24 ± 23.	
	Glucose-1%		2.30 ± 0.61		0.59 ± 0.09		0.85 ± 0.20		0.64 ± 0.20		**0.13 ± 0.03**	**	74.38 ± 10.	
	Mannitol-1%		2.04 ± 0.43		0.55 ± 0.11		1.30 ± 0.34		0.90 ± 0.24		0.31 ± 0.07		84.82 ± 16.	

e	*Conditions*	*State*	*cZ*		*cZOG*		*cZR*		*cZROG*		*cZRMP*		*cZ9G*	
	LN-0.05	NO CUT-T48	14.86 ± 4.16		25.19 ± 3.82		128.36 ± 24.08		127.06 ± 13.08		2.28 ± 0.59		0.30 ± 0.08	
›ble	LN-0.05	CUT-T48	15.73 ± 4.00		34.00 ± 6.66		169.15 ± 29.96		**161.26 ± 23.44**	*	2.49 ± 0.33		0.37 ± 0.10	
	HN-5	NO CUT-T48	59.85 ± 16.11		49.79 ± 13.80		396.21 ± 111.88		125.00 ± 25.69		9.12 ± 2.08		0.39 ± 0.13	
	HN-5	CUT-T48	**105.29 ± 11.41**	**	**77.37 ± 18.73**	*	324.48 ± 103.01		127.60 ± 26.88		**4.00 ± 1.22**	**	0.51 ± 0.15	
	LN-0.05	NO CUT-T48	4.14 ± 0.80		40.04 ± 4.21		18.81 ± 5.35		116.18 ± 20.30		1.79 ± 0.25		0.62 ± 0.05	
›ot	LN-0.05	CUT-T48	3.84 ± 0.87		**59.83 ± 11.24**	*	**10.02 ± 3.12**	*	**82.58 ± 18.29**	*	1.91 ± 0.54		0.54 ± 0.09	
	HN-5	NO CUT-T48	21.03 ± 5.18		44.99 ± 7.93		63.62 ± 14.53		152.14 ± 31.52		4.75 ± 1.26		0.86 ± 0.15	
	HN-5	CUT-T48	28.46 ± 7.83		49.47 ± 7.44		70.47 ± 17.28		190.07 ± 46.22		3.21 ± 0.90		1.56 ± 0.41	
	Glucose-0.1%		**46.82 ± 15.57**	**	85.26 ± 19.43		311.56 ± 102.14		172.57 ± 34.41		**8.48 ± 1.43**	**	0.50 ± 0.03	
›ble	Mannitol-0.1%		12.44 ± 2.75		66.33 ± 20.37		346.00 ± 106.31		238.29 ± 62.33		22.32 ± 5.73		0.47 ± 0.10	
	Glucose-1%		**40.33 ± 12.24**	**	87.56 ± 19.05		378.53 ± 110.67		168.86 ± 41.90		21.22 ± 5.99		0.51 ± 0.07	
	Mannitol-1%		17.10 ± 4.03		68.68 ± 13.61		321.97 ± 113.11		176.31 ± 27.24		23.29 ± 5.30		0.68 ± 0.15	
	Glucose-0.1%		7.51 ± 1.92		43.33 ± 7.46		**12.31 ± 3.61**	*	**110.38 ± 29.15**	***	**3.61 ± 0.67**	*	0.98 ± 0.24	
›ot	Mannitol-0.1%		9.56 ± 1.56		39.75 ± 10.28		28.31 ± 9.36		237.33 ± 33.41		5.85 ± 1.30		1.02 ± 0.27	
	Glucose-1%		6.92 ± 1.61		41.64 ± 5.18		28.79 ± 7.49		170.46 ± 38.68		4.48 ± 0.79		0.73 ± 0.18	
	Mannitol-1%		8.54 ± 1.69		33.11 ± 5.88		38.79 ± 11.33		225.95 ± 48.15		4.51 ± 1.23		0.99 ± 0.23	

e	*Conditions*	*State*	*Total DHZ-types*	*DHZ*	*DHZOG*	*DHZR*	*DHZRMP*	*DHZ7G*	*DHZ9G*
	LN-0.05	NO CUT-T48	3.5 ± 0.6	0.20 ± 0.07	0.036 ± 0.00	2.24 ± 0.47	1.00 ± 0.13	0.11 ± 0.02	0.04 ± 0.01
ɔble	LN-0.05	CUT-T48	4.4 ± 0.5	0.16 ± 0.04	**0.044 ± 0.01** *	2.87 ± 0.57	1.18 ± 0.23	0.17 ± 0.05	0.03 ± 0.01
	HN-5	NO CUT-T48	13.3 ± 2.3	0.78 ± 0.26	0.21 ± 0.04	7.51 ± 1.54	4.44 ± 0.99	0.43 ± 0.08	0.13 ± 0.04
	HN-5	CUT-T48	10.7 ± 1.1	0.86 ± 0.24	0.22 ± 0.06	5.85 ± 1.36	3.30 ± 0.82	0.32 ± 0.09	0.14 ± 0.04
	LN-0.05	NO CUT-T48	1.2 ± 0.2	0.19 ± 0.03	0.02 ± 0.00	0.44 ± 0.13	0.27 ± 0.06	0.19 ± 0.06	0.08 ± 0.02
ɔot	LN-0.05	CUT-T48	0.9 ± 0.2	0.25 ± 0.05	0.01 ± 0.00	0.31 ± 0.09	**0.14 ± 0.04** *	0.17 ± 0.05	0.06 ± 0.01
	HN-5	NO CUT-T48	3.6 ± 0.9	0.51 ± 0.13	0.05 ± 0.01	1.67 ± 0.47	0.90 ± 0.28	0.39 ± 0.11	0.13 ± 0.03
	HN-5	CUT-T48	4.1 ± 0.5	0.79 ± 0.24	0.04 ± 0.01	1.86 ± 0.34	0.81 ± 0.22	0.40 ± 0.09	0.19 ± 0.07
		Glucose-0.1%	8.6 ± 1.2	0.55 ± 0.12	0.27 ± 0.05	3.48 ± 1.00	3.88 ± 0.91	0.41 ± 0.12	0.15 ± 0.05
ɔble		Mannitol-0.1%	9.4 ± 1.2	0.36 ± 0.11	0.20 ± 0.06	3.61 ± 0.90	4.72 ± 0.99	0.42 ± 0.14	0.10 ± 0.03
		Glucose-1%	**14.0 ± 1.7** *	0.47 ± 0.13	**0.32 ± 0.08** *	6.17 ± 1.29	6.47 ± 1.26	0.42 ± 0.10	0.15 ± 0.01
		Mannitol-1%	10.8 ± 2.0	0.39 ± 0.05	0.21 ± 0.04	4.45 ± 1.24	5.28 ± 1.02	0.30 ± 0.07	0.17 ± 0.05
		Glucose-0.1%	**2.4 ± 0.4** *	0.33 ± 0.12	0.09 ± 0.02	**0.46 ± 0.14** **	**0.98 ± 0.28** *	0.39 ± 0.07	0.15 ± 0.03
ɔot		Mannitol-0.1%	4.1 ± 1.2	0.31 ± 0.10	0.08 ± 0.02	1.06 ± 0.32	2.15 ± 0.71	0.33 ± 0.09	0.14 ± 0.04
		Glucose-1%	3.0 ± 0.5	0.34 ± 0.05	**0.08 ± 0.02** *	**0.85 ± 0.27** *	1.30 ± 0.36	0.28 ± 0.07	0.13 ± 0.03
		Mannitol-1%	3.6 ± 0.5	0.31 ± 0.03	0.05 ± 0.01	1.38 ± 0.36	1.43 ± 0.24	0.26 ± 0.05	0.13 ± 0.03

Tissue	*Conditions*	*State*	*Total iP-types*	*iP*	*iPR*	*iP7G*	*iP9G*
Stubble	LN-0.05	NO CUT-T48	17.4 ± 3.4	1.82 ± 0.36	11.62 ± 3.13	1.10 ± 0.38	2.83 ± 0.54
	LN-0.05	CUT-T48	22.2 ± 2.9	1.84 ± 0.30	**16.47 ± 2.43** *	0.77 ± 0.27	3.08 ± 0.45
	HN-5	NO CUT-T48	12.5 ± 2.1	2.27 ± 0.46	5.52 ± 1.20	1.17 ± 0.42	4.18 ± 0.96
	HN-5	CUT-T48	13.3 ± 1.9	2.17 ± 0.36	5.33 ± 1.13	0.89 ± 0.10	4.91 ± 0.73
Root	LN-0.05	NO CUT-T48	9.9 ± 1.8	2.28 ± 0.61	4.61 ± 1.18	0.33 ± 0.10	2.86 ± 0.58
	LN-0.05	CUT-T48	9.0 ± 1.5	2.30 ± 0.50	4.23 ± 1.33	0.20 ± 0.07	2.27 ± 0.65
	HN-5	NO CUT-T48	20.6 ± 1.6	3.91 ± 0.75	10.67 ± 0.86	0.27 ± 0.07	5.80 ± 0.63
	HN-5	CUT-T48	**16.6 ± 3.0** *	**2.56 ± 0.30** *	**5.48 ± 1.10** ***	0.16 ± 0.02	**8.53 ± 2.12** *
Stubble	Glucose-0.1%		28.0 ± 4.4	3.11 ± 0.78	19.13 ± 5.06	0.48 ± 0.12	6.09 ± 1.69
	Mannitol-0.1%		26.0 ± 3.5	2.63 ± 0.59	16.67 ± 3.84	0.95 ± 0.31	5.74 ± 1.19
	Glucose-1%		**30.5 ± 5.6** *	3.06 ± 0.66	**22.42 ± 6.07** *	0.44 ± 0.13	4.57 ± 1.14
	Mannitol-1%		19.6 ± 5.0	2.31 ± 0.21	11.75 ± 3.66	0.42 ± 0.09	5.07 ± 1.46
Root	Glucose-0.1%		20.3 ± 4.8	3.42 ± 0.99	7.55 ± 1.62	< *LOD*	9.38 ± 2.46
	Mannitol-0.1%		22.1 ± 3.0	2.75 ± 0.32	10.34 ± 2.97	< *LOD*	9.05 ± 1.23
	Glucose-1%		15.5 ± 1.0	2.49 ± 0.61	8.19 ± 0.73	< *LOD*	4.78 ± 0.86
	Mannitol-1%		17.7 ± 2.9	2.45 ± 0.43	8.49 ± 2.29	< *LOD*	6.77 ± 1.51

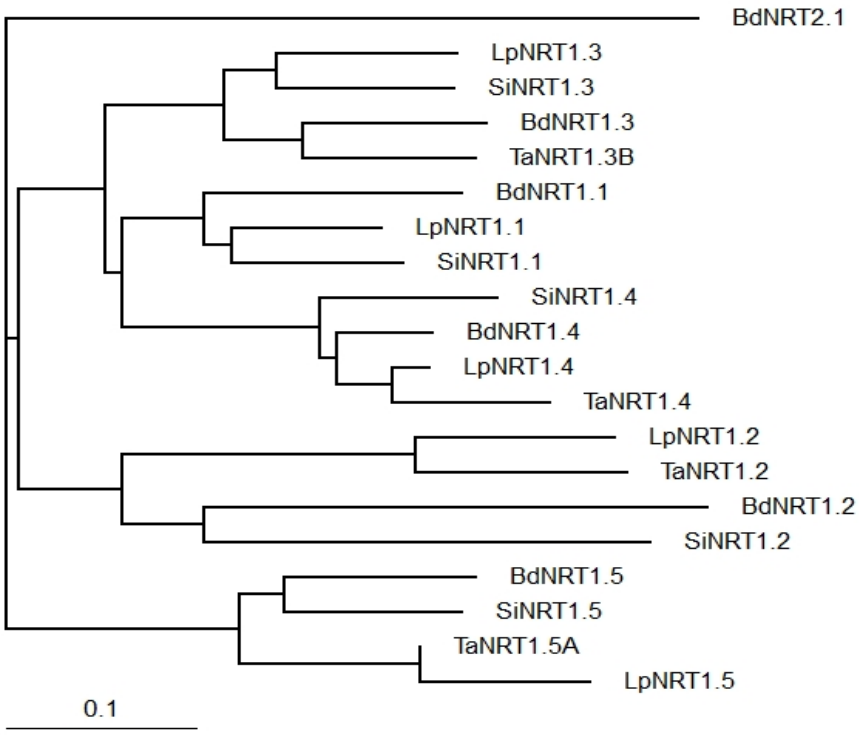
BdNRT2.1
LpNRT1.3
SiNRT1.3
BdNRT1.3
TaNRT1.3B
BdNRT1.1
LpNRT1.1
SiNRT1.1
SiNRT1.4
BdNRT1.4
LpNRT1.4
TaNRT1.4
LpNRT1.2
TaNRT1.2
BdNRT1.2
SiNRT1.2
BdNRT1.5
SiNRT1.5
TaNRT1.5A
LpNRT1.5
0.1

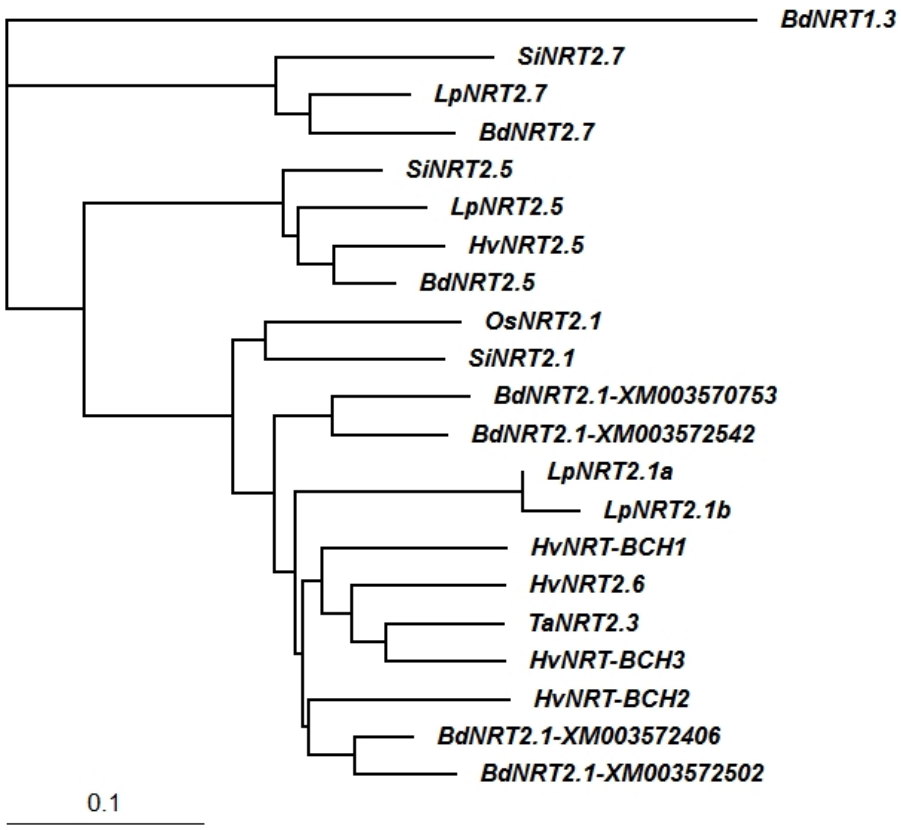
BdNRT1.3
SiNRT2.7
LpNRT2.7
BdNRT2.7
SiNRT2.5
LpNRT2.5
HvNRT2.5
BdNRT2.5
OsNRT2.1
SiNRT2.1
BdNRT2.1-XM003570753
BdNRT2.1-XM003572542
LpNRT2.1a
LpNRT2.1b
HvNRT-BCH1
HvNRT2.6
TaNRT2.3
HvNRT-BCH3
HvNRT-BCH2
BdNRT2.1-XM003572406
BdNRT2.1-XM003572502
0.1

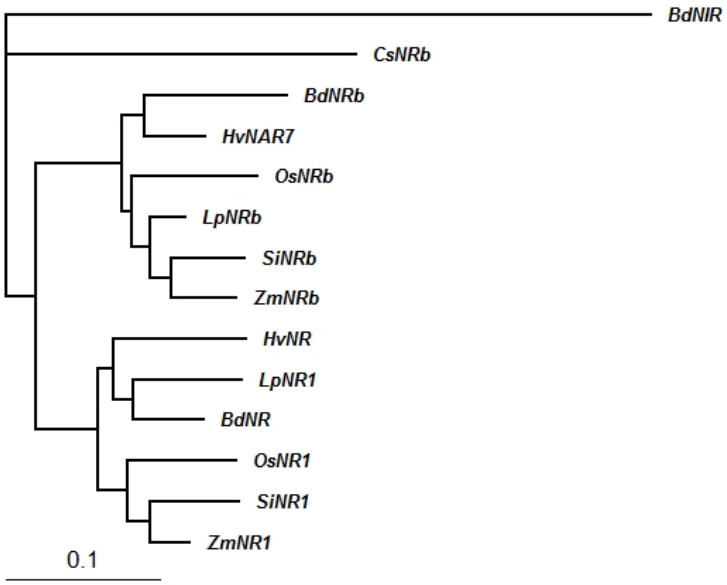

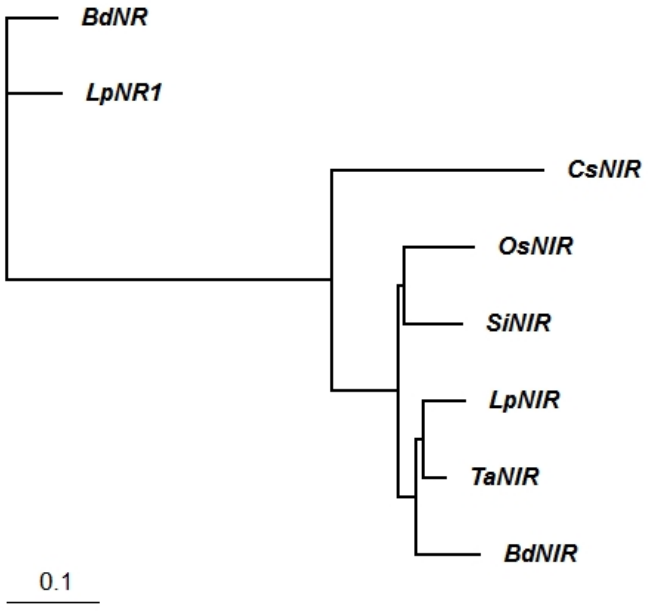

Fig S 1. **Phylogeny of *LpNRT* , *LpNR*, *LpNiR* gene family**

Neighbor-joining (NJ) phylogenetic trees of the newly identified sequences and their orthologues were created using ClustalX2 software with 1000 bootstrap replicates. Phylogenetic tree was visualised with TreeView X software. The tree was rooted with an out group sequence, *NRT2.1*, in *Brachypodium distachyon* Bd. *Brachypodium distachyon* Bd, *Lolium perenne* Lp, *Oryza Brachyantha* Ob, *Oryza sativa* Os, *Seteria italica* Si, *Triticum aestivum* Ta, *Triticum urartu* Tu, *Zea mays* Zm.

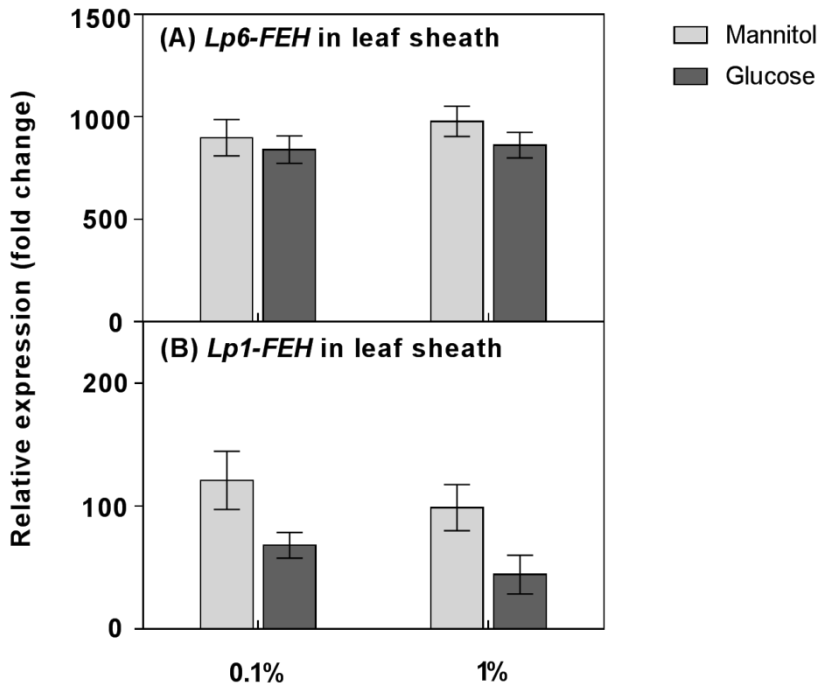

Fig S 2. *Lp6-FEH* and *Lp1-FEH* expression in *L. perenne* leaf sheaths with 6 h of supplemental glucose. Plants were grown in HN conditions and supplied with 0.1% or 1% glucose 42 h after defoliation. Each data point is normalized against reference genes *eEF-1α* and *GAPDH*. Values are means ±SEM (n=3, pools of five plants each)

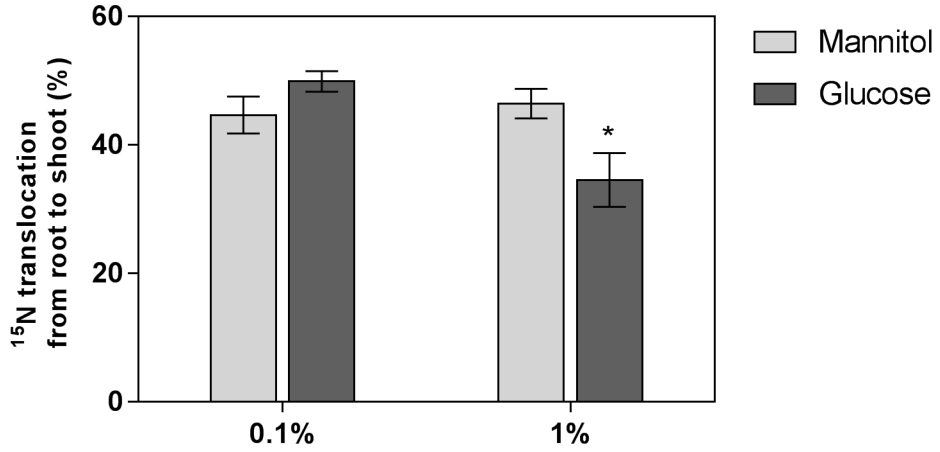

Fig S 3. Effects of glucose addition on N allocation to leaf sheaths in *L. perenne* grown in 5 mM NO_3^-, 48 h after defoliation. Values are means ±SEM (n=5, pools of five plants each). *denotes significantly different means between mannitol (gray bars) and glucose (black bars) treatment (* $P<0.05$).

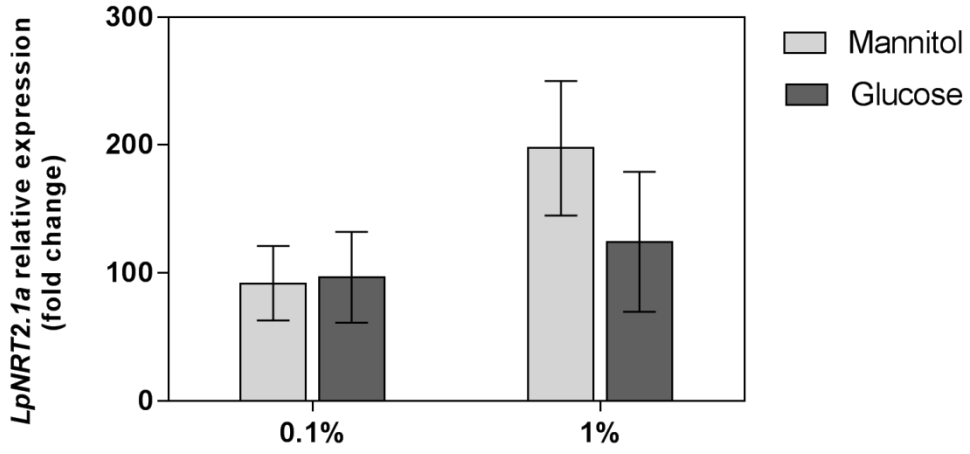

Fig S 4. Effects of 0.1% and 1% glucose addition on putative *LpNRT2.1a* gene expression in *L. perenne* roots grown in 5 mM NO_3^-, 48 h after defoliation. Each data point is normalized against reference genes *eEF-1α* and *GAPDH*. Values are means ±SEM (n=3, pools of five plants each).

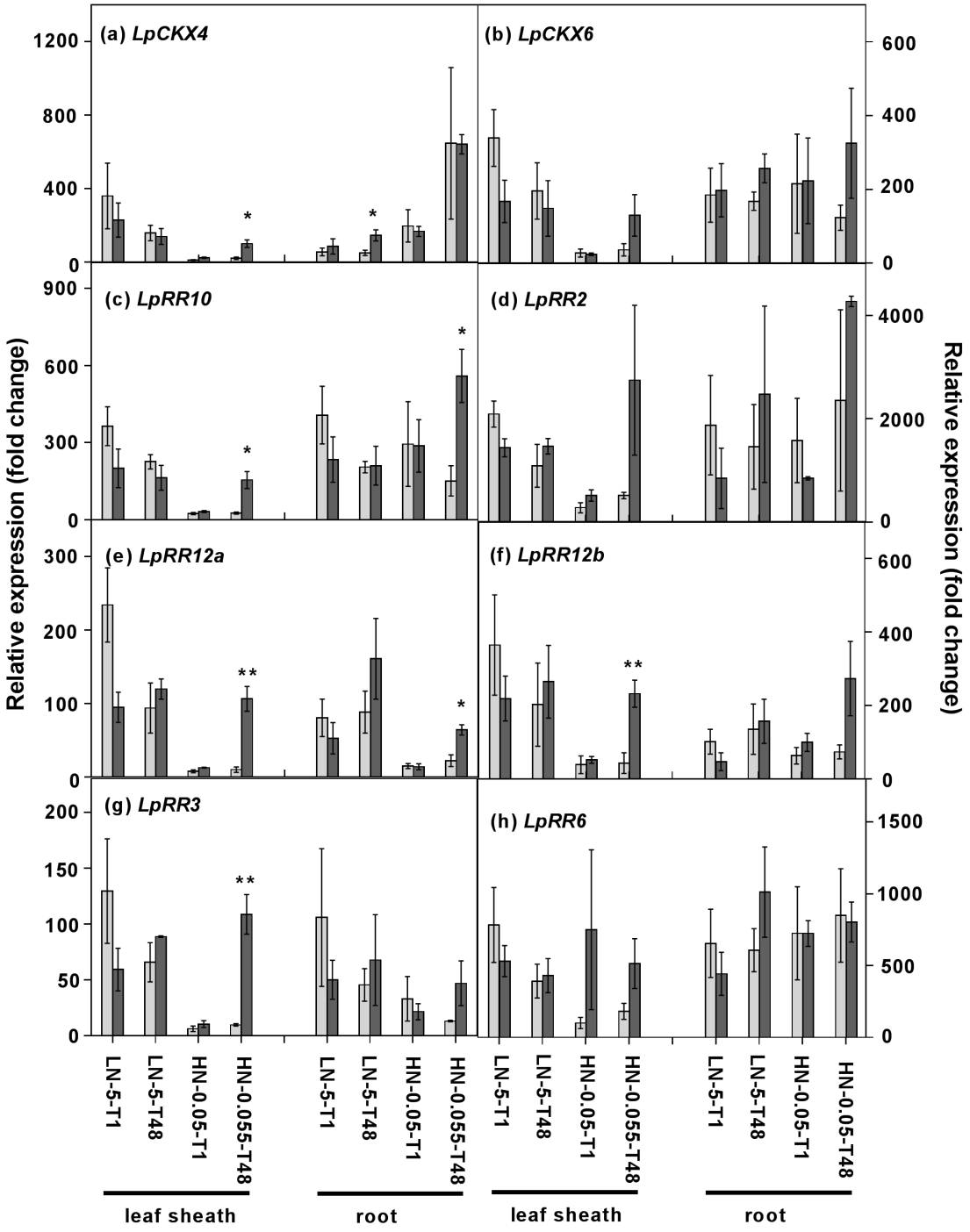

Fig S 5. Expression of putative *LpCKX* and *LpR* in *L. perenne.* Plants grown at either 0.05 mM (LN) or 5 mM (HN) NO_3^-, were defoliated (or left intact) and then incubated 5 mM or 0.05 mM NO_3^- for 1 h. Each data point is normalized against reference genes *eEF-1α* and *GAPDH*. Values are means ±SEM (n=3, pools of five plants each). *denotes significantly different means between intact plants (gray bars) and defoliated plants (black bars) (* *P<0.05*, ** *P<0.01*).

Appendix 2-Supporting information for Chapter 3

***L. perenne* growth in germination paper system and technical difficulties**

L. *perenne* seeds were surface sterilized for 5 min in 75% (v/v) ethanol, followed by 15 min in 5 mL of 0.5% SDS (v/v). Sterilized seeds were planted in filter papers soaked with ddH_2O in petri dishes. After germination for 5 d, the uniform seedlings were selected and transferred to germination papers soaked with Hoagland medium containing different nitrate concentrations. During the treatments, roots were grown in darkness by wrapping containers in aluminium foil. Some preliminary success was achieved in obtaining root system images (see Fig. S6). However, the paper system was not able to be successfully adopted with any degree of consistency due to seed contamination and because the liquid medium soaked into the upper part of germination papers easily dried out. Given these circumstances, and in the time available, a decision was made to focus this analysis on *B. napus*.

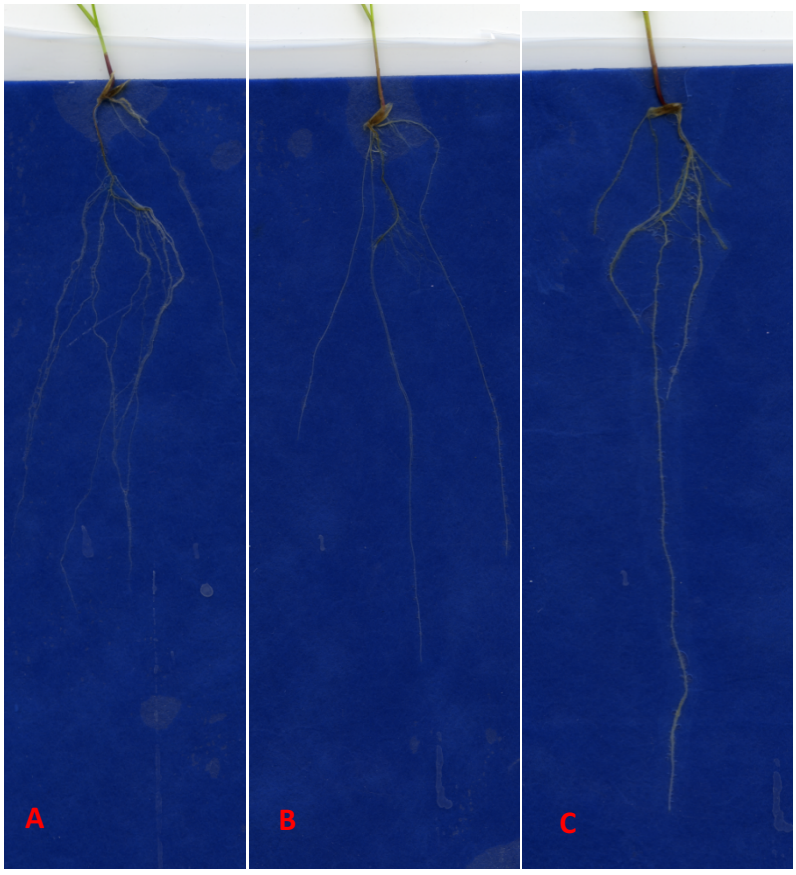

Fig S6 *L. perenne* seedlings show differences in root system architecture on various nitrate conditions. Representative examples of 19-day-old seedlings on Hoagland medium containing 0.1 mM nitrate (A), 1 mM nitrate (B), and 10 mM nitrate (C).

Appendix 3-Supporting information for Chapter 4

Table S7. **Primer sequences**

F, forward; R, reverse

Primers	Sequence
BnNRT1.1F	TCTAGGGTTTTMTCTACTCATCCCACAATAC
BnNRT1.1R	CAGCKATCCAYGGATGAGCTTTATC
BnNRT1.5F	CACTCACTGTGATGGCTCAAGCTC
BnNRT1.5R	TTGGAATCCAACCAGGCATGTGATC
BnNRT1.8F	TCAGTACATGATGATAGGTGCATCAGAAG
BnNRT1.8R	AGCACAAACCAGGTAAACCACAAAATC
BnNRT2.1F	TGGATMTCTTTCTCCACATGTTTTGTCTC
BnNRT2.1R	TCCCATCACSAGCCTAGAGAAGATAC
BnPHO1aF	GGCCAACCAAGTCGATACAATTCCTG
BnPHO1aR	GTAACACGCAGTTGACTCTAAATGTCTCAG
BnPHO1bF	TGAAGTCGACACCATTCCAGGCATC
BnPHO1bR	ACGCAGTTGACTCAATATGTCTAAGCAATG

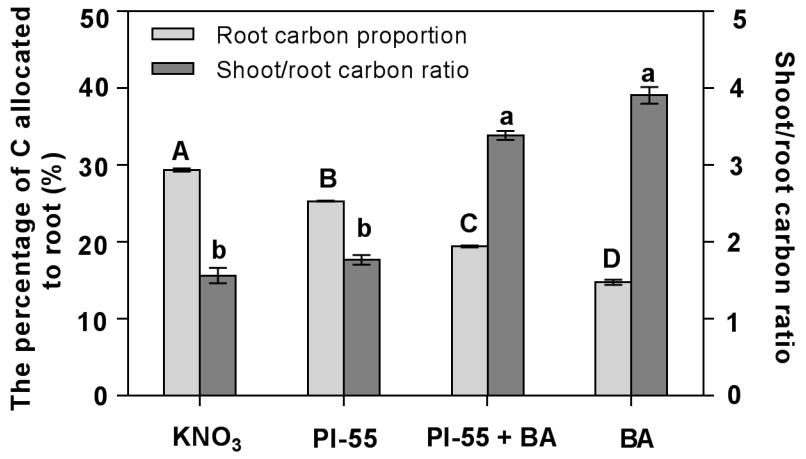

Fig S 7 The effects of PI-55 and BAP on C allocation in *B.napus* during 96 h of growth on phytogel plates with a homogeneous supply of 1 mM KNO_3. Percentage of C allocation to roots is referred to as the percentage of whole plant C allocated to roots. Vertical bars indicate mean ± SE of 30 plates with two seedlings per plate. Bars with different upper and lower case letters denote means that are significantly different within the measurements of C allocation to roots and shoot/root carbon ratio, respectively (P<0.05).

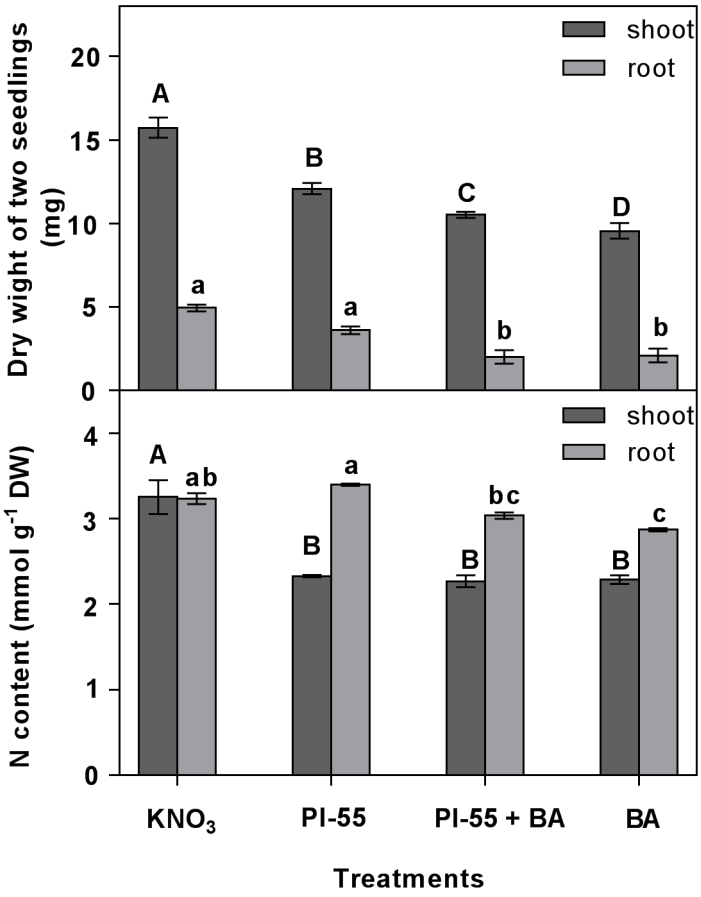

Fig S 8. The effects of PI-55 and BAP on dry weight and N content of shoots and roots in *B. napus* during 96 h of growth on phytogel plates with a homogeneous supply of 1 mM KNO_3. Percentage of C allocation to roots is referred to as the percentage of whole plant C allocated to roots. Vertical bars indicate mean ± SE of 30 plates with two seedlings per plate. Bars with different upper case letters denote means that are significantly different within the measurements of dry weight and N content in shoots, respectively (P<0.05). Bars with different lower case letters denote means that are significantly different within the measurements of dry weight and N content in roots, respectively (P<0.05).